

Chapter 1

ELEMENTS OF GROUP 1

Peter Hubberstey

1.1	INTRODUCTION.....	2
1.2	THE ELEMENTS.....	2
1.2.1	General Properties.....	3
1.2.2	The Alkali Metals as Solvent Media.....	4
1.2.3	Metallic Solutions.....	14
1.2.4	Intermetallic Compounds.....	16
1.3	SIMPLE COMPOUNDS OF THE ALKALI METALS.....	17
1.3.1	Ion Pairs.....	17
1.3.2	Theoretical Treatment of Small Moieties.....	19
1.3.3	Binary Compounds.....	28
1.3.4	Ternary Pnictides.....	32
1.3.5	Ternary Oxides and Chalcogenides.....	32
1.3.6	Ternary Halides.....	34
1.4	COMPOUNDS OF THE ALKALI METALS CONTAINING ORGANIC MOLECULES OR COMPLEX IONS.....	40
1.4.1	Complexes of Acyclic Lipophilic Ionophores.....	40
1.4.2	Crown Complexes.....	43
1.4.3	Complexes of Lariat Ethers.....	52
1.4.4	Complexes of Macrocyclic Polyethers of Novel Design.....	55
1.4.5	Cryptates and Related Complexes.....	60
1.4.6	Complexes of Macrocyclic Polyimine and Related Ligands.....	61
1.4.7	Salts of Carboxylic and Thiocarboxylic Acids...	64
1.4.8	Heterobimetallic Complexes containing Alkali Metals.....	66
1.4.9	Lithium Derivatives.....	70
1.4.10	Sodium Derivatives.....	84
1.4.11	Potassium, Rubidium and Caesium Derivatives....	87
	REFERENCES.....	90

1.1 INTRODUCTION

The format of the first two Chapters of this review is similar to that adopted previously.¹ The chemistry of both the Group 1 and Group 2 elements is considered in sections which reflect subjects of topical interest and significance; certain aspects of their chemistry, particularly the formation of crown and related complexes, are so similar that they are reported once only, in the relevant section of the present Chapter.

The material chosen for inclusion in the review is selective, only those papers in which some unique aspect of the inorganic chemistry of these two groups of metals is described being abstracted; those papers in which their organometallic chemistry is discussed are omitted since they are reviewed in detail elsewhere. The remarkable upsurge in interest in the coordination chemistry of lithium, first noted in the 1983 review² has been maintained throughout 1984. To permit appropriate coverage of this exciting, rapidly expanding field, other topics including molten salts have, regretfully, had to be omitted from the present review.

Preliminary communications reporting that activated carbon supported alkali metals catalyse both the methanation of CO by H₂ (T>750K)³ and the reduction of NO_x (x = 1,2) by C or CO (T>500K)⁴ have been published. The activity of the catalysts, prepared by pore volume impregnation of an activated carbon with an aqueous solution of an alkali metal carbonate followed by slow evaporation of the water at 323K and drying at 400K, increases with increasing atomic number:



Attempts to poison the catalysts by addition of H₂S (for the methanation process)³ or Et₄Pb (for the NO_x reduction process)⁴ were unsuccessful.

1.2 THE ELEMENTS

The application of the lighter alkali metals, particularly lithium and sodium, in nuclear energy and high energy battery technologies continues to stimulate interest in the chemistry of these metals. Mindful of their industrial significance, Addison⁵ has written a book reviewing the chemistry of the liquid

alkali metals; chapters covering aspects of the manipulation, purification and analysis of the liquids, the solubility, solvation and reactivity of solutes dissolved therein, the reactions of the liquids with non-metals, water, hydrocarbons and halogen-containing compounds, and the corrosion of transition metals including stainless steel containment materials, by the liquid metals, are included.⁵ The proceedings of two conferences devoted, in part, to the specific roles of liquid alkali metals in nuclear reactor technology^{6,7} and of one conference devoted exclusively to current applications of lithium in science, medicine and technology⁸ have been published during 1984. Since the majority of the papers published in these proceedings are technologically oriented, they are of only peripheral interest to the average inorganic chemist and will not be considered in detail; the specialist reader is referred to the appropriate proceedings.⁶⁻⁸ There are however a number of papers of more general interest; these have been abstracted and are reviewed, as appropriate, in the following sub-sections.

The development of battery systems using alkali metal, particularly lithium, electrodes has resulted in a large number of papers in the Journal of the Electrochemical Society. Again, owing to the mainly technological nature of these papers they are not reviewed here, the specialist reader being referred to the appropriate volume of the Journal.⁹

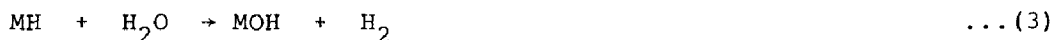
1.2.1 General Properties

An XPS study of lithium surfaces exposed to low levels of gaseous reactants has been undertaken.¹⁰ Molecular oxygen and carbon monoxide yield Li_2O and Li_2O plus a material tentatively identified as Li_2C_2 , respectively, under all exposure conditions. Water vapour always gives Li_2O and a species tentatively identified as LiOH ; the ratio of the products varies with coverage, however, Li_2O being favoured at submonolayer levels and LiOH at higher exposures. Carbon dioxide and sulphur dioxide produce different products depending on coverage; whereas for submonolayer coverages Li_2O plus Li_2C_2 and Li_2O plus Li_2S are formed, for greater exposures, Li_2CO_3 plus a $\text{Li}_2\text{O} \cdot \text{CO}_2$ adduct and Li_2SO_3 , respectively, are formed.¹⁰

The kinetics of the reaction of molecular hydrogen or nitrogen with liquid lithium¹¹ may be explained by chemisorption of

reactant followed by either conversion of reactant to product and solubilisation of product or solubilisation of reactant followed by conversion to product in the bulk liquid. The reactions proceed at a constant rate with apparent activation energies of $69.9 \text{ kJ.mol}(\text{H}_2)^{-1}$ and $45.2 \text{ kJ.mol}(\text{N}_2)^{-1}$ until the bulk liquid is saturated. Subsequently, the reaction rate is controlled by mass transport through the surface product layer.¹¹

Novel high speed photographic methods have been used to study the reaction resulting on injection of a thread of liquid sodium or NaK alloy into liquid water ($293 < T/K < 333$).¹² The metal reacts rapidly ($K \cdot 10^{-3} \text{ moles s}^{-1} \text{mm}^{-2}$) but incompletely (~15%) at the nozzle; the thread then breaks into globules which are carried away in a semi-protective bubble of hydrogen subsequent reaction being much slower ($K \cdot 10^{-5} \text{ mole s}^{-1} \text{mm}^{-2}$). The reaction produces hydrogen both directly and via MH as an intermediate:



1.2.2 The Alkali Metals as Solvent Media

The solution chemistry of both metals and non-metals has been extensively studied during the past year. For lithium as solvent non-metallic solutes predominate, whereas for sodium, both types of solute appear. For potassium, rubidium and caesium a limited number of papers have been published on the chemistry of dissolved oxygen.

The solubility of Ni in liquid lithium ($503 < T/K < 873$) has been determined¹³ by chemical analysis (atomic absorption spectroscopy) of samples filtered from equilibrated specimens held in nickel crucibles. The data, which are described by the relationship:

$$\log_{10} (C_{\text{Li}}^{\text{Ni}}/\text{wppm}) = 6.5392 - 2845/T \quad \dots(4)$$

complement earlier data.

The results of several attempts to determine the solubilities of the transition metals, V,¹⁴ Cr,¹⁵ Fe,¹³ Co,¹⁵ Ni^{13,15} and Mo¹⁴ in liquid sodium have been published. With the exception of Co and Mo the results were scattered and temperature relationships could not be established. The solubility ranges observed for all solutes are summarised in Table 1 together with the quoted $\log_{10}(C_{Na}^M/\text{wppm})$ vs $(T/K)^{-1}$ relationships. The Co solubility was determined¹⁴ by radiochemical analysis of samples obtained by equilibration in sealed nickel crucibles internally plated with cobalt. Analysis of the sodium for impurities showed it to

Table 1. Solubility ranges for V, Cr, Fe and Ni in liquid sodium

Solute (M)	Solubility	C_{Na}^M/wppm	Temperature Range/K	A*	B*	Ref
	Range	Average				
Vanadium	0.01 - 0.15	0.05	557 - 751	-	-	14
Chromium	0.89 - 18.8	4.04	673 - 923	-	-	15
Iron	0.18 - 3.03	1.26	773 - 963	-	-	13
Cobalt	0.002 - 0.123	0.034	673 - 973	0.101	1493	15
Nickel	0.16 - 18.7	4.28	673 - 948	-	-	15
Nickel	0.09 - 0.30	0.16	773 - 963	-	-	13
Molybdenum	0.04 - 0.48	0.23	628 - 978	2.738	2200	14

* These constants refer to the solubility expression

$$\log_{10}(C_{Na}^M/\text{wppm}) = A - B(T/K)^{-1}$$

† wppm is equivalent to $\mu\text{gM/gNa}$.

contain 10-20 wppm oxygen. The Mo solubility was determined¹³ by classical chemical analysis of samples obtained by equilibration in tantalum crucibles containing molybdenum foil and magnesium powder. The magnesium was added to ensure oxygen-free sodium.

As for several previous determinations of transition metal solubilities in liquid sodium the Cr¹⁴ and Fe¹⁵ solubility data appeared to be influenced by non-metallic contaminants, especially oxygen. In independent studies, two groups of authors have attempted to elucidate the role of oxygen in this context; they both consider the formation of ternary oxides to be of paramount importance. From a comparison of experimental and

theoretically derived Fe solubility data Awasthi and Sundaresan,¹⁶ have shown that, at high oxygen activities, the predominant species is Na_4FeO_3 and that the enhanced solubility of iron can be explained by the initial formation of FeO followed by its conversion to Na_4FeO_3 . By deriving a thermochemical expression for the solubility of ternary oxides in sodium, Grundy¹⁷ has calculated data for NaOH, Na_2CO_3 , Na_2FeO_2 , Na_4FeO_3 , NaCrO_2 , $\text{Na}_2\text{Si}_2\text{O}_5$, Na_2SiO_3 and Na_3PO_4 as a function of both temperature and third component activities.

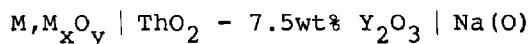
The chemical status of Sr and Ba in reactor sodium has been assessed both theoretically and practically.¹⁸ Thermodynamically based calculations indicate that MO formation is favoured over MH_2 , MBr or MI formation. A fifth potential product, M_2N , cannot be included in this analysis owing to a dearth of appropriate thermochemical data. Its formation has been noted, however, in experimental studies of the reaction of both Na-Sr and Na-Ba solutions with nitrogen. The process occurs via a consecutive solution-precipitation mechanism, the extent of the solution process being dependent on the alkaline earth metal content of the solution. At saturation, N:Sr and N:Ba ratios of ~0.05:1 and ~0.25:1, respectively, are consistently obtained. The difference is attributed to the greater effect Ba has on reducing nitrogen activities in liquid sodium.¹⁸

As the technological potential of liquid lithium is being realised analytical methods for assessment of non-metallic impurity inventories are being perfected. Two papers^{19,20} outlining chemical methods for the determination of carbon, nitrogen and oxygen, and in one case,²⁰ hydrogen and silicon, have been presented. The application of the foil equilibration technique to the estimation of carbon and nitrogen has also been established.²¹ Activity-concentration relationships were derived from literature thermodynamic data for both non-metals in the foil material (304 SS) and in liquid lithium. Using these relationships, chemical analysis of foils after immersion in liquid lithium gave carbon and nitrogen concentrations in the liquid metal which showed significant correlation with values obtained by direct chemical analysis.²¹

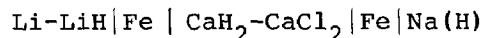
Neither chemical nor foil equilibration methods are continuous. Experience in liquid sodium has shown that diffusion and/or electrochemical sensors can be used to monitor

hydrogen, carbon and oxygen activities (see later). DeKeyser et al²² have started a programme to consider the application of these sensors to liquid lithium systems. The hydrogen diffusion sensor was found to operate successfully except at very low hydrogen activities and low temperatures ($T < 673K$); preliminary experiments with the oxygen electrochemical sensor were encouraging, the electrolyte material ($ThO_2-7.5wt\% Y_2O_3$) being found to be compatible with a liquid lithium environment.²²

A large number of papers reporting the considerable effort applied during recent years to the development and testing of these sensors for use in liquid sodium systems were presented at the third international conference on "Liquid Metal Engineering and Technology".⁷ Only one sensor, the electrochemical type, is available for oxygen.²³⁻²⁹ It is very well established, being based on the cell:

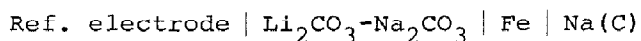


A variety of metal-metal oxide couples have been proposed, the most popular being In-In₂O₃. Recent developments to this sensor have been of detail rather than of principle. When treated carefully, it is a very effective sensor. When subjected to thermal shock, however, its operating lifetime is reduced considerably.²³ Both electrochemical^{24,30} and diffusion^{23,24,30,31} hydrogen sensors have been designed. The former is based on the cell:



and the latter on the diffusion of hydrogen through a nickel^{23,24,30,31} or iron²⁴ membrane. A flow of argon sweeps the inner surface of the membrane, the hydrogen partial pressure in the sweep gas being determined by a variety of methods including thermal conductivity,^{24,30,31} and mass spectrometric analysis.²³ Comparative experiments have shown that the diffusion sensor, particularly that with a nickel membrane, is more reliable than the electrochemical sensor, the reproducibility of the calibration curves being much better. Carbon sensors also fall into the two categories of electrochemical type^{23-25,32} and diffusion^{24,28,32,33} type. The former is based on emf changes

associated with carbon activity changes manifest in the cell:



the reference electrode varying from CO/CO₂ gas mixtures,^{23,25} through pure graphite³² to Fe₃C.²⁴ The latter^{24,28,32,33} depends on the diffusion of carbon through a pure iron membrane with a previously oxidised inner surface. After oxidation at this FeO surface layer the CO/CO₂ so formed is swept to a flame ionisation detector by a continuous flow of argon. The diffusion sensor is generally considered to be much more robust than the electrochemical sensor and to have a much longer working life.

After careful calibration of an electrochemical oxygen sensor, by both metered gas addition and cold trap equilibration (433 < T/K < 773) Smith and Simm³⁴ have estimated an expression for oxygen solubilities in liquid sodium:

$$\log_{10} (C_{\text{Na}}^{\text{O}}/\text{wppm}) = 5.52 - 1900(T/K)^{-1} \quad \dots(5)$$

Their data³⁴ and those of Nafe²⁶ for the concentration dependence of oxygen activity in liquid sodium both suggest that negative deviations from Henry's Law occur in these solutions particularly at concentrations close to saturation. Ivanovskii et al³⁵ have noted similar behaviour for potassium-oxygen (from electrochemical oxygen sensor measurements) and caesium-oxygen solutions (from vapour pressure measurements). It is suggested³⁵ that the observed deviations can be rationalised in terms of a heterophase oxygen state model composed of oxygen containing molecular-type particles and crystal like inclusions. For the metallic solvent, this disperse system is apparently single phased.

Hubberstey et al^{36,37} have reported the results of detailed X-ray diffraction and electrical resistivity studies of aspects of the behaviour of dilute solutions of silicon,³⁶ nitrogen³⁷ and hydrogen³⁷ in liquid lithium ($x_{\text{Li}} > 0.96$; T = 675, 750K). Silicon is reported to be chemically reactive towards particulate nickel (but not iron or chromium) and towards dissolved nitrogen (but not hydrogen or oxygen). Whereas the reaction with particulate nickel follows a heterogeneous mechanism in which insoluble Ni₂Si is formed at the nickel-solution interface following attack by

dissolved silicon, that with dissolved nitrogen is a simple homogeneous solution reaction resulting in formation of insoluble Li_5SiN_3 . Neither nitrogen nor hydrogen was found to react with either lead or tin.³⁷ The presence of lead in lithium ($x_{\text{Li}} = 0.99$; $675 \leq T/\text{K} \leq 735$) was, however, observed to increase the solubility of hydrogen relative to that in the pure alkali metal. The enhanced solubilities are attributed to a decreased hydrogen activity in the ternary solutions relative to the binary solutions. Hubberstey³⁸ has also reviewed the chemistry of dissolved nitrogen in liquid lithium, noting that it adopts the corrosive role filled by oxygen in liquid sodium systems.

The extraction of hydrogen from impure lithium by yttrium has been analysed thermochemically by consideration of the Li-Y-O-H , Li-Y-N-H and Li-Y-O-N systems.³⁹ It is concluded that the ternary oxide LiYO_2 will be formed on the surface of yttrium in impure lithium thus influencing the ability of the yttrium to extract hydrogen. It is suggested that ternary oxide formation may be reduced at high hydrogen and/or low oxygen levels.³⁹

Two independent studies of the reaction of hydrogen with carbon in the presence of alkali metals have been undertaken; whereas Barker et al⁴⁰ have shown, using mass spectroscopic methods ($T = 823\text{K}$) that the product in liquid lithium is C_2H_4 , Borgstedt and Pillai,⁴¹ using gas chromatographic methods ($723 < T/\text{K} < 823$) claim that in liquid sodium the reaction product is CH_4 .

X-ray powder diffraction analysis of the products (isolated by filtration) of the reaction ($T = 673\text{K}$) between liquid sodium and a pump lubricating oil has shown the presence of NaH , Na_2S and residual sodium.⁴² These materials form the minority of the product, the majority being a black, amorphous, material with a C:H molar ratio of 5:2. Comparison of d.s.c. and i.r. data for this material with those for the thermal decomposition product ($T = 608\text{K}$) of NaHC_2 showed many similarities. Despite considerable effort, the chemical identity of this product is still uncertain although it is thought to contain ($-\text{C}\equiv\text{C}-$) fragments bonded to alkyl groups.⁴²

Solutions of non-metals in liquid alkali metals are known to corrode containment materials. The most deleterious impurities are nitrogen in lithium and oxygen in sodium; carbon transfer is also a problem in both lithium and sodium systems. A perspective of the corrosive behaviour of lithium and sodium has

been written.⁴³ It is noted that although corrosion in sodium has been extensively studied, corrosion data for lithium are fragmentary and hence our understanding of corrosion processes in lithium lags far behind that for sodium. Striking similarities in the overall mass transfer processes for the two solvents in austenitic stainless steels is observed; preferential depletion of nickel and chromium leads to the development of a ferritic surface layer and a constant corrosion rate (with time). The corrosion processes do show, however, basic differences in their chemistry, the principal products being nitrogen containing species in lithium and oxygen containing species in sodium.⁴³ The corrosive behaviour of lithium has also been compared to that of liquid $\text{Li}_{17}\text{Pb}_{83}$, an alternative coolant/tritium breeder for the fusion reactor.⁴⁴ The mechanisms and kinetics of corrosion processes in the two liquids are examined and their influence on the degradation of structural material is discussed.

Well subscribed sessions devoted to the subject of corrosion in liquid metal systems were organised at both the "Fusion Reactor Materials"⁶ and "Liquid Metal Engineering and Technology"⁷ conferences. Sodium,⁴⁵⁻⁵⁶ lithium⁵⁷⁻⁶³ and $\text{Li}_{17}\text{Pb}_{83}$ ⁶⁴⁻⁶⁶ were considered as solvents; surface depletion phenomena, ferrite layer production, grain boundary penetration and carburization/decarburization processes were studied for austenitic, ferritic and speciality stainless steels. The data reported for sodium⁴⁵⁻⁵⁶ simply corroborate and extend previously reported information. Those presented for lithium⁵⁷⁻⁶³ confirm the point, made earlier in the review of corrosion phenomena in lithium and sodium solutions,⁴³ that corrosion of austenitic steels in flowing lithium mirrors that in flowing sodium. Thus a surface loss of nickel and chromium results in a ferromagnetic corrosion layer of distorted bcc structure. The underlying austenitic matrix is depleted in carbon and nitrogen and lithium penetrates into the grain boundaries probably forming Li_9CrN_5 . Evidence for lithium penetration has been obtained using secondary imaging mass spectrometry (SIMS) and metallographic techniques.⁴⁰ The potential of Auger electron spectroscopy (AES) as a technique for analysis and detection of lithium compounds on surfaces has been pointed out.⁶⁷ Interpretation of the spectra is at an embryonic stage but it does appear that they can be used to derive important bonding information.

Results presented for liquid $\text{Li}_{17}\text{Pb}_{83}$ ⁶⁴⁻⁶⁶ indicate that corrosion rates for both austenitic and ferritic steels are 10x greater than in pure lithium. The influence of time, temperature and steel composition on corrosion behaviour is the same in $\text{Li}_{17}\text{Pb}_{83}$ as in lithium. Surface analysis (EDAX, XRD) of austenitic steels after exposure to $\text{Li}_{17}\text{Pb}_{83}$ indicated nickel depletion and formation of a ferritic layer which easily spalls from the specimen surface.

The chemical reactivity of $\text{Li}_{17}\text{Pb}_{83}$ towards hydrogen isotopes,⁶⁸⁻⁷⁰ nitrogen^{66,71} and oxygen⁶⁶ has been ascertained, often as part of a study of the entire Li-Pb system.⁶⁸⁻⁷¹ Independent studies of the equilibrium pressure of hydrogen,⁶⁸ deuterium⁶⁹ and tritium,⁶⁹ p_{X_2} , as a function of hydrogen isotope concentration, x_{X} , have shown that Sieverts relationship:

$$p_{\text{X}_2}^{\frac{1}{2}} = K_{\text{S}} \cdot x_{\text{X}} \quad \dots (6)$$

where K_{S} is the Sieverts constant, is valid throughout the entire Li-Pb system at low concentrations of all three hydrogen isotopes; it becomes invalid, however, as the hydrogen isotope concentration approaches saturation. The variation of K_{S} with increasing lead content in the Li-Pb- H_2 system⁶⁸ exhibited three features of interest: (i) a 10^5 -fold increase; (ii) an inflexion point at $x_{\text{Pb}} \sim 0.3$, presumably caused by the formation of partially ionic bonds; and (iii) a steady decrease in temperature coefficient resulting in a reversal at $x_{\text{Pb}} \sim 0.6$. The solubilities of hydrogen, deuterium and tritium have been derived as a function of composition and temperature using thermodynamic data for the binary systems.⁷⁰ The calculated values are considerably lower than those determined experimentally; a ternary Li-Pb-H interaction term is postulated to achieve agreement between experimental and calculated results.

Lithium-rich Li-Pb alloys react with nitrogen or Li_3N ($900 < T/K < 950$) until the lithium activity in the alloy equals that in equilibrium with Li_3N (i.e. at a composition close to $x_{\text{Li}} = 0.215$).⁷¹ Thus alloys richer in lithium than $\text{Li}_{21.5}\text{Pb}_{78.5}$ are converted to this composition by reaction with nitrogen or Li_3N whereas alloys richer in lead are inert. These alloys, although inert to austenitic steels in the absence of nitrogen, will in its presence corrode the steel to give Li_9CrN_5 and the alloy $\text{Li}_{62}\text{Pb}_{38}$ ($T = 879\text{K}$). This limit

defines the thermodynamic stability of Li_9CrN_5 for which a value of $\Delta G_f^\circ(\text{Li}_9\text{CrN}_5, c, 879\text{K}) = -328 \text{ kJ.mol}^{-1}$ is calculated.⁷¹

Unlike nitrogen which is inert to $\text{Li}_{17}\text{Pb}_{83}$,^{66,71} oxygen reacts with it to form Li_2O ($T > 673\text{K}$) which in the presence of air is hydrolysed to LiOH and ultimately $\text{LiOH.H}_2\text{O}$; complete reaction of the lithium content of the alloy is observed.⁶⁶

The large deviations from ideality observed in Li-Pb solution thermodynamics have been explained by postulating the existence of LiPb molecules in solution and strong surface tension effects around dissolved impurity species.⁷² The equilibrium constant for LiPb formation obeys the equation:

$$\ln K_{\text{eq}} = -1.44 + 7000 (T/\text{K})^{-1} \quad \dots (7)$$

Formulations which derive from these assumptions are used to calculate solubility data for hydrogen, nitrogen and oxygen in liquid $\text{Li}_{17}\text{Pb}_{83}$:

$$\ln(x_{\text{H}}/\text{mol.fr}) = 6.53 - 8370 (T/\text{K})^{-1} \quad \dots (8)$$

$$\ln(x_{\text{N}}/\text{mol.fr}) = 3.05 - 5770 (T/\text{K})^{-1} \quad \dots (9)$$

$$\ln(x_{\text{O}}/\text{mol.fr}) = -1.39 - 5480 (T/\text{K})^{-1} \quad \dots (10)$$

The values obtained for cold trap solubilities ($T = 508\text{K}$), $x_{\text{H}} = 4.8 \times 10^{-5}$, $x_{\text{N}} = 2.5 \times 10^{-4}$ and $x_{\text{O}} = 5.1 \times 10^{-6}$ are much lower than those observed in pure lithium. Sieverts constants for hydrogen and nitrogen in lead-rich Li-Pb solutions, calculated using the formulations, agree with experimentally derived constants.⁷²

The reactions of metal oxides with liquid lithium have been reviewed by Barker.⁷³ Of the alkali metals, lithium is the most powerful reducing agent owing to the very high free energy of formation of Li_2O ($\Delta G_f^\circ(\text{Li}_2\text{O}, c, 1000\text{K}) = -442 \text{ kJ.mol}^{-1}$; cf. $\Delta G_f^\circ(\text{Na}_2\text{O}, c, 1000\text{K}) = -277 \text{ kJ.mol}^{-1}$, $\Delta G_f^\circ(\text{K}_2\text{O}, c, 1000\text{K}) = -211 \text{ kJ.mol}^{-1}$, $\Delta G_f^\circ(\text{Rb}_2\text{O}, c, 1000\text{K}) = -186 \text{ kJ.mol}^{-1}$, $\Delta G_f^\circ(\text{Cs}_2\text{O}, c, 1000\text{K}) = -155 \text{ kJ.mol}^{-1}$). Consequently, the majority of metal oxides are reduced by liquid lithium forming Li_2O and metal. In the presence of impurity nitrogen or carbon, some transition metals react further to form binary or ternary nitrides, binary carbides

and even carbonitrides. Only ThO_2 has been found to be stable in liquid lithium. In the presence of impurity nitrogen, however, even ThO_2 reacts to form either ThN or Li_2ThN_2 . Intermediate behaviour is exhibited by CeO_2 which undergoes partial reduction in liquid lithium forming the ternary product LiCeO_2 . Again in the presence of nitrogen, binary or ternary nitride formation (CeN or Li_2CeN_2) occurs.⁷³

Compatibility studies⁷⁴ of sintered specimens of AlN containing metal oxide (1% as a sintering aid) with liquid lithium containing nitrogen (~ 850 wppm N) at 873K indicate that the AlN ceramic is basically unreactive. Specimens containing CaO or Cr_2O_3 deteriorated slightly, however, owing to loss of calcium and chromium.⁷⁴

Chemical interactions between liquid sodium and sintered specimens of UO_2 , $\text{UO}_2\text{-PuO}_2$ and $\text{UO}_2\text{-PuO}_2$ doped with various cations to simulate the presence of fission products have been studied under both low ($773 < T/K < 1073$)⁷⁵ and high ($1323 < T/K < 1873$)⁷⁶ temperature regimes. Similar behaviour was observed at all temperatures; pure sodium and stoichiometric UO_2 are compatible whereas sodium reacts with $\text{UO}_2\text{-PuO}_2$ to form a reduced oxide phase and $\text{Na}_3\text{U}_{1-x}\text{Pu}_x\text{O}_4$. At low temperatures,⁷⁵ the threshold plutonium valency for reaction to occur decreased with increase in temperature; at 973 and 1073K it was 3.46(3) and 3.41(2), respectively. The addition of fission product cations to $\text{UO}_2\text{-PuO}_2$ resulted in increased changes in volume and increased reaction rates. Some of the specimens containing these cations were found to break up on reaction with sodium. At high temperatures,⁷⁶ for which kinetic data were not obtained, pronounced grain growth was observed during reaction of all the oxides with liquid sodium at 1873K.

Compatibility studies⁷⁷ of commercially available ceramics based on basalt and MgO with liquid sodium ($673 < T/K < 1173$) have shown that whereas MgO is inert the basalt based ceramics exhibit complete loss of integrity, presumably owing to ternary oxide formation.⁷⁷

Two reports describing the solution chemistry of liquid rubidium have been abstracted.^{78,79} Confirmation that the rubidium-oxygen phase diagram ($0.00 < x_{\text{O}} < 0.25$) is similar to that of the caesium-oxygen system has been achieved from the results of a preliminary thermal analysis study.⁷⁸ Evidence for the

existence of Rb_7O and Rb_4O , which are thought to decompose in peritectic reactions at 262 and 293K respectively, is presented. Addition of oxygen to rubidium results in a depression of the freezing point (312K) to 259K at the eutectic composition ($x_{\text{O}} = 0.095$).⁷⁸

Reaction of liquid rubidium with chromium oxides ($T = 773\text{K}$) leads, depending on the oxygen inventory in the liquid metal to Rb_4CrO_4 and Rb_3CrO_4 ;⁷⁹ the products were identified by chemical analysis and by analogy of their XRD patterns with those of Cs_4CrO_4 and Cs_3CrO_4 . Similarly, reaction with iron oxides ($T = 773\text{K}$) leads to two products. Although that found at lower oxygen activities was identified by single crystal XRD studies as $\text{Rb}_6\text{Fe}_2\text{O}_6$ that found at higher oxygen activities was not identified; analytical data suggested a Rb:Fe stoichiometry similar to that in $\text{Rb}_2\text{Fe}_2\text{O}_6$.⁷⁹

1.2.3 Metallic Solutions

Chemical short range order in liquid phase binary metallic solutions continues to arouse the interest of both experimentalists and theoreticians. Neutron diffraction studies have been completed for Li-Sn,⁸⁰ Li-Pb⁸¹ and Li-Ag^{81,82} solutions. Whereas van der Lugt et al⁸⁰ have studied Li-Sn solutions as a function of composition, Ruppertsberg et al^{81,82} have investigated lithium, $\text{Li}_{80}\text{Pb}_{20}$, $\text{Li}_{90}\text{Ag}_{10}$ and $\text{Li}_{70}\text{Ag}_{30}$ as a function of temperature. The results provide evidence for appreciable ordering in the liquid probably accompanied by charge transfer from lithium to tin, lead or silver. The concentration dependence data⁸⁰ indicate that chemical short range order is maximised at $\text{Li}_{80}\text{Sn}_{20}$. The temperature dependence data^{81,82} suggest that the effect is pronounced at distances $< 400\text{pm}$; at larger distances the atoms are distributed randomly and the global structure of the solutions is similar to that of pure lithium. Ruppertsberg et al⁸¹ also conclude that although the amount of charge transfer in the Li-Pb and Li-Ag systems is similar, the electronic screening in $\text{Li}_{90}\text{Ag}_{10}$ and $\text{Li}_{70}\text{Ag}_{30}$ is significantly stronger than that in $\text{Li}_{80}\text{Pb}_{20}$.

Electrical resistivity data for dilute solutions of group IV elements (Si, Ge, Sn and Pb) in liquid lithium⁸³ have been interpreted within the context of chemical short range order, the relationship between the existence of ordering in liquid phase binary metallic solutions and the formation of a Zintl phase which

approximates to a normal valency compound in the solid state, being stressed.⁸³

Evidence for chemical short range order in dilute solutions of lithium in mercury has been derived from the presence of a minimum (at $x_{Li} \sim 0.05$) in the thermoelectric power isotherms. The minimum is attributed to higher order atom-atom correlation effects which are caused by charge transfer from lithium to mercury.

Three models for the interpretation of thermodynamic data for solutions which exhibit chemical short range order have been presented.⁸⁵⁻⁸⁸ Hafner et al^{85,86} have developed a simple model which has been applied successfully to liquid Li-Mg, Li-Pb and Li-Ag solutions,⁸⁵ good agreement being obtained for enthalpy and entropy of formation data as well as for structural data. The model has also been applied to the more complex Na-Sn and Na-Pb systems which exhibit two anomalies in the thermodynamic excess functions (at $\sim Na_{50}M_{50}$, $Na_{80}M_{20}$; $M = Sn, Pb$) usually associated with the formation of two different compounds. The model shows that the anomaly at $Na_{80}M_{20}$ arises from a preferred A-B interaction (of electronic origin) and that at $Na_{50}M_{50}$ from packing effects. The structural implications inherent in this interpretation have been corroborated by recent neutron diffraction studies,⁸⁹ reported in the 1983 review.⁹⁰

Enthalpy of mixing data for Na-Hg solutions have been successfully calculated by Khanna⁸⁷ using a semi-empirical model based on the simple hard-sphere theory.

Using equations derived by Kirkwood and Buff,⁹¹ Saboungi and Corbin⁸⁸ have shown that the sign and magnitude of the limiting slope of the activity coefficient, ϵ , for the less electro-positive component of binary metallic mixtures containing $x_M < 0.12$ ($M = Li, Na$) yield information on the attractions and repulsions between like and unlike atoms. A positive value for ϵ indicates repulsions between alkali metal atoms and attractions between solute and solvent. The magnitude of ϵ is indicative of the degree of ordering. The model has been applied to a number of Li-M ($M = Ga, In, Pb, Te$) and Na-M ($M = In, Sn, Pb, Bi, Te, Au, Cd$) systems (Table 2). With the exception of the Na-Au system, positive values of ϵ are obtained; the negative value of ϵ obtained for the Na-Au system requires confirmation. The zero values of ϵ for the tellurium systems, combined with very large

Table 2 Limiting slopes of the activity coefficients of the less electropositive member of dilute binary metallic mixtures ($x_M < 0.12$; M = Li, Na).⁸⁸

System	ϵ	T/K	System	ϵ	T/K
Li-Ga	1.4	800	Na-In	3.9	717
Li-In	0.4	800	Na-Sn	0.8	673
Li-Pb	1.7	932	Na-Pb	2.3	723
Li-Te	0.0	823	Na-Bi	2.2	673
			Na-Te	0.0	800
			Na-Cd	6.1	673
			Na-Au	-1.1	1500

negative values of limiting excess chemical potential may indicate the existence of covalent bonding in these systems.

1.2.4 Intermetallic Compounds

High pressure (4 GPa), high temperature ($873 < T/K < 973$) modifications of MSi and MGe (M = K, Rb, Cs) have been synthesised from the elements under argon.⁹² They adopt the tetragonal NaPb-type structure; pertinent crystallographic data are collected in Table 3. The crystal structure of CsIn₃ has been determined;⁹³ it is of the RbGa₃-type, tetragonal, space group $I\bar{4}m2$ with unit cell parameters, $a = 704.7$, $c = 1680.3$ pm.

Table 3 Crystallographic parameters of the high pressure (4 GPa), high temperature ($873 < T/K < 973$) modifications of MSi and MGe (M = K, Rb, Cs).⁹²

Compound	a/pm	c/pm	Compound	a/pm	c/pm	Compound	a/pm	c/pm
KSi	1057	1710	RbSi	1083	1758	CsSi	1123	1834
KGe	1069	1737	RbGe	1104	1787	CsGe	1138	1850

A theory to describe chemical bonding in intermetallic compounds has been developed.⁹⁴ The model, which involves the modified Bethe lattice, offers a general framework for discussing

stability, clustering tendency and valency in charge-transfer compounds. Its viability was demonstrated by application to the transition from simple ionic octet compounds to clustered configurations as observed in alkali metal-group IV metal systems.⁹⁴

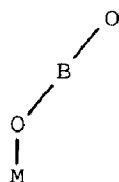
1.3 SIMPLE COMPOUNDS OF THE ALKALI METALS

Following the precedent set in the 1982 and 1983 reviews, subsections devoted to the chemistry of ion pairs containing alkali metal cations and to the theoretical treatment of small molecules, particularly those containing lithium, have been incorporated in this section to cater for the continuing interest in these fields; subsections devoted to the chemistry of binary and ternary derivatives of the alkali metals have also been retained. To avoid unnecessary duplication with other chapters of this review, the ternary compounds considered are restricted to those containing both an alkali metal and a transition metal.

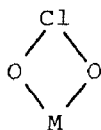
1.3.1 Ion pairs

The ion pairs $M[BO_2]$, ($M = Li-Cs$),⁹⁵ $M[AsO_3]$ ($M = K-Cs$),⁹⁶ $M[ClO_2]$ ($M = Li-Cs$),⁹⁵ $M[ClO_3]$ ($M = Li, Na, Rb$),⁹⁶ $M[ClO_4]$ ($M = Na-Cs$),⁹⁷ $M[ReO_4]$ ($M = Li-Rb$)⁹⁸ and $M[UF_6]$ ($M = Na-Cs$)⁹⁹ have been isolated in low temperature (nitrogen and/or argon) matrices by condensation from the vapour phase above the corresponding salts. Infra-red spectroscopic data, including those from $^{18}O/^{16}O$ isotopic substitution experiments reveal interesting structural information. Whereas $M[BO_2]$ ion pairs (1) have C_s symmetry with linear $[BO_2]^-$ groups and MOB bond angles between 100° ($Li[BO_2]$) and 127° ($Cs[BO_2]$), $M[ClO_2]$ ion pairs (2) have C_{2v} symmetry.⁹⁵ Differences also occur in the geometries of the $M[AsO_3]$ (3) and $M[ClO_3]$ (4) ion pairs. Whereas $[AsO_3]^-$ coordinates the metal in a bidentate fashion with C_{2v} symmetry, $[ClO_3]^-$ acts as a tridentate ligand forming a complex with C_{3v} symmetry.⁹⁶ The coordination geometry of the $M[ClO_3]$ ion pair also contrasts with that of the $M[ClO_4]$ ion pair (5) which adopts a C_{2v} bidentate interaction⁹⁷ similar to that of the $M[ReO_4]$ species.⁹⁸ The dimerisation of $M[ReO_4]$ ion pairs has also been studied spectroscopically in these matrices, a bridged structure of D_{2h} symmetry being suggested for the dimers, $\{M[ReO_4]\}_2$.⁹⁸

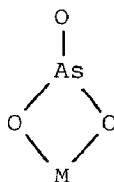
Infra-red data for MUF_6 ($M = K-Cs$) suggest a C_{3v} symmetry - a



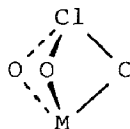
(1)



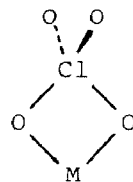
(2)



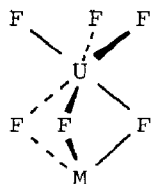
(3)



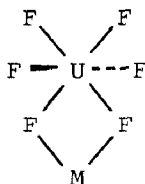
(4)



(5)



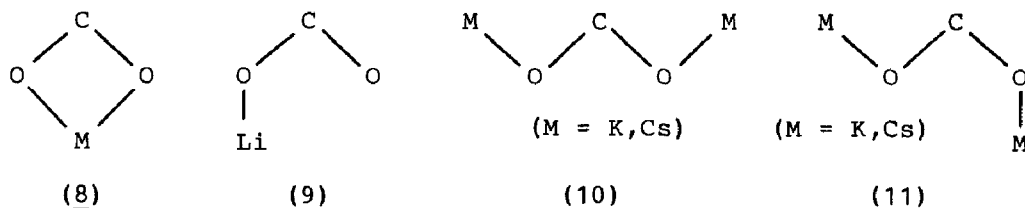
(6)



(7)

facial interaction (6) - for the species isolated in argon and a C_{2v} symmetry - an edge interaction (7) - for that trapped in nitrogen.⁹⁹ For $NaUF_6$, the spectra are complicated by decomposition reactions leading to UF_5 as one of the products; it is probable, however, that the isolated $NaUF_6$ species has a C_{2v} or lower symmetry in both matrices.⁹⁹

Ion pair formation by reaction of alkali metals with carbon dioxide has been studied spectroscopically by two groups. Teghil et al.⁹⁵ have investigated the $Li-CO_2$ reaction in argon matrices, while Margrave et al.¹⁰⁰ have characterised the products of the $M-CO_2$ ($M = Na, K, Cs$) reaction in argon, nitrogen and neat matrices. Reaction of Li with CO_2 leads to both C_{2v} (8) and C_s (9) isomers of $Li[CO_2]$; ⁹⁵ the C_s isomer photolytically rearranges to the C_{2v} structure after prolonged exposure to the i.r. source. The C_{2v} isomer of $Li[CO_2]$ has also been isolated in argon matrices by condensation from the vapour above lithium carbonate.⁹⁵ Very small amounts of $Na[CO_2]$ were produced when sodium was allowed to react with CO_2 in inert gas matrices; the product was found to have C_{2v} symmetry (8).¹⁰⁰ Similar $M[CO_2]$ ion pairs (8) were obtained when potassium or caesium were used as activating metals.¹⁰⁰ They were not the sole product, however, $M_2[CO_2]$ ion pairs of both C_{2v} (10) and C_s (11) symmetry also being formed, probably as a result of the reaction of the alkali metal dimer M_2 and CO_2 . Photolysis of the C_{2v} isomers of $M_2[CO_2]$ with the i.r. source caused their rearrangement to the C_s form.¹⁰⁰



Reaction of HCHO with alkali metal halide salt molecules in argon matrices,¹⁰¹ instead of yielding the anticipated halide transfer product, the $M[CH_2XO]$ ion pair, generally gave an unusual complex involving an ion-dipole interaction between the halide ion and the carbon centre of HCHO. For CsF, however, slight indication of a covalent interaction was noted.¹⁰¹

1.3.2 Theoretical Treatment of Small Moieties

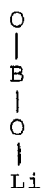
In a departure from previous practise, this subsection is divided into two parts. Firstly, theoretical studies of low molecular weight inorganic species containing lithium or sodium are considered; secondly, the theoretical and structural chemistry of selected organolithium compounds are discussed.

Ab initio SCF MO calculations of the electronic and geometrical structures and properties of lithium and sodium oxides and hydroxides,¹⁰² of lithium borate¹⁰³ and of lithium and sodium complexes of aziridine and ethylene oxide rings¹⁰⁴ have been undertaken. Calculated data for MO and MOH ($M = Li, Na$) molecules are collected in Table 4 where they are compared with analogous data for corresponding beryllium and magnesium derivatives.¹⁰² Calculations using various basis sets have shown that the $C_{\infty v}$ structure of $LiBO_2$ (12) is the equilibrium structure and that the alternative C_{2v} structure (13) is a saddle point on the potential energy surface of the molecule.¹⁰³ This conclusion contrasts slightly with the assertion, based on i.r. evidence, that the $M[BO_2]$ ($M = Li-Cs$) ion pair when isolated in cryogenic matrices adopts a C_s structure (1).⁹⁶ The calculated geometries of the alkali metal complexes of aziridine (14) and ethylene oxide (15) rings are as expected, the only difference being that whereas the Li^+ cation is positioned in the plane of the ethylene oxide ring (180°) the Na^+ cation is located marginally above it (169.3°).¹⁰⁴ Both aziridine and ethylene oxide exhibit a substantial Li^+ and Na^+ activity. Hence use of

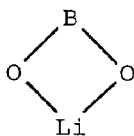
Table 4 Electronic and geometrical structures and properties of MO, MOH and (MOH)⁺ (M = Li, Na, Be, Mg) species.¹⁰²

Species	State	R _e (MO) pm	μ D	Species	State	R _e (MO) pm	R _e (OH) pm	μ D
LiO	² π	168.4	-7.02	LiOH	¹ Σ ⁺	157.1	94.3	-4.51
NaO	² π	206.2	-8.52	NaOH	¹ Σ ⁺	192.6	94.7	-6.71
BeO	¹ Σ ⁺	132.1	-7.43	BeOH	² Σ ⁺	139.9	93.4	0.85
MgO	¹ Σ ⁺	179.5	-8.44	MgOH	² Σ ⁺	177.4	94.1	-1.27
				(BeOH) ⁺	¹ Σ ⁺	134.0	94.4	-5.41
				(MgOH) ⁺	¹ Σ ⁺	170.9	94.5	-7.77

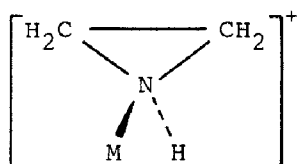
mitomycin (an aziridine-containing drug with anti-tumour activity) in conjunction with alkali metal salts may facilitate ring opening at neutral pH leading to enhanced drug activity.¹⁰⁴



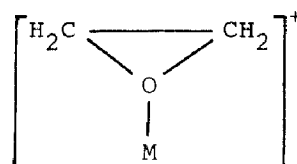
(12)



(13)

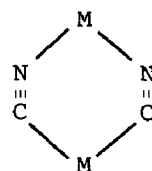
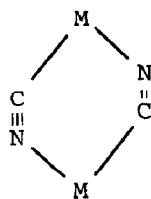
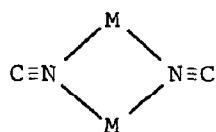


(14)



(15)

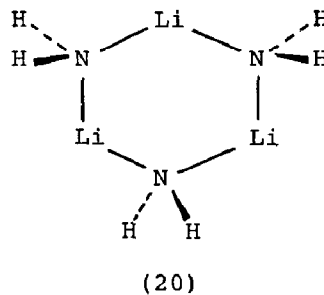
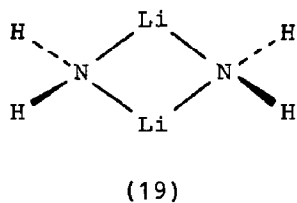
A considerable number of lithium containing dimers¹⁰⁵⁻¹⁰⁸ and in one instance trimers,¹⁰⁶ have been treated theoretically using ab initio and/or semiempirical MO methods. Interest in these species arises from the marked tendency of lithium compounds to oligomerise. The formation of aggregates in solution has long been recognised; an increasing awareness of their presence in the solid state has resulted from recent X-ray crystallographic studies (section 1.4.9). The shapes and energetics of many different isomers of (LiCN)₂ and (NaCN)₂ have been determined.¹⁰⁵ For both dimers, there are three different isomers of very similar stability. The energy difference between the lowest-energy structure, a four membered planar ring of alternating M (M = Li, Na) and N atoms of D_{2h} symmetry (16) and two different six-membered planar rings of C_{2h} (17) and C_{2v} (18) symmetries is ~20 kJ.mol⁻¹ for (LiCN)₂ but only ~5 kJ.mol⁻¹ for (NaCN)₂. Linear structures are substantially less stable.¹⁰⁵



	Li	Na		Li	Na		Li	Na
r(C...N)	117.5	117.3	r(C...N)	116.1	116.2	r(C...N)	116.1	116.2
r(M...N)	193.0	223.4	r(M...N)	193.1	223.2	r(M...N)	194.9	223.7
NM̂N	103.1	98.3	r(M...C)	209.0	235.4	r(M...C)	207.2	234.8
			ĈMN	108.2	101.9	NM̂N	117.5	108.5
(16)			M̂NC	118.2	121.3	M̂NC	116.9	121.8
				(17)		N̂CM	134.7	136.0
						ĈMC	99.2	95.8
							(18)	

distances/pm angles/°

The calculated structures and energies of LiNH_2 dimers and trimers are in agreement with XRD data;¹⁰⁶ thus $(\text{LiNH}_2)_2$ and $(\text{LiNH}_2)_3$ prefer symmetrical D_{2h} (19) and D_{3h} (20) geometries with hydrogen atoms perpendicular to the $(\text{LiN})_n$ rings. The



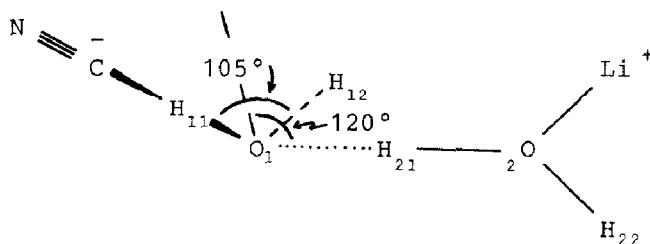
	$r(N...H)$	$r(N...Li)$	\hat{HNH}	\hat{HNLi}	\hat{NLiN}	\hat{LiNLi}
(19)	101.6	190.8	105.9	119.2	108.3	71.7
(20)	101.7	190.6	105.9	114.4	93.7	146.3

distances/pm angles/°

dimerisation energies of LiNH_2 have been compared with those of the other first row hydrides (LiBeH , LiBH_2 , LiCH_3 , LiOH) and lithium fluoride (LiF) by two independent groups;^{107,108} the two sets of data are very similar. The dimerisation energy of LiNH_2

is comparable with those of LiOH and LiF, almost double those of LiBH₂ and LiCH₃ and approximately four times greater than that of LiBeH. A significant conclusion reached by both groups is that the dimerisation energies are dominated by electrostatic interactions.^{107,108}

Theoretical analysis of the interaction of excited lithium atoms with molecular hydrogen,¹⁰⁹ of the hydrolysis of lithium cyanide¹¹⁰ and of the reaction of lithium alkoxyamides with organolithium compounds¹¹¹ have been undertaken. A mechanism has been proposed for the hydrolysis¹¹⁰ which involves (i) the approach of the hydrated ions Li⁺ and CN⁻, (ii) the formation of a hydrogen bonded intermediate (21), (iii) the coordinated proton transfer along the hydrogen bonds of the intermediate, and (iv) the dispersion of LiOH away from the hydrated neutral molecule, NCH.H₂O.

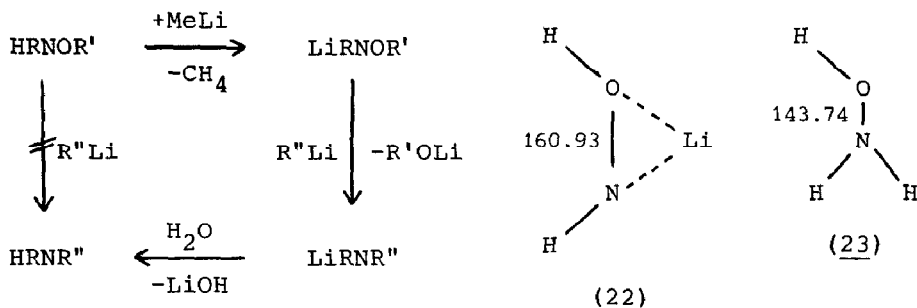


Distances/pm	(C...N)	(C...H ₁₁)	(H ₁₁ ...O ₁)	(O ₁ ...H ₁₂)
Initial geometry	116	176	96	96
Final geometry	116	107	∞	96

Distances/pm	(O ₁ ...H ₂₁)	(H ₂₁ ...O ₂)	(O ₂ ...H ₂₂)	(O ₂ ...Li)
Initial geometry	∞	96	96	184.2
Final geometry	96	∞	95.2	158.8

distances/pm angles/° (21)

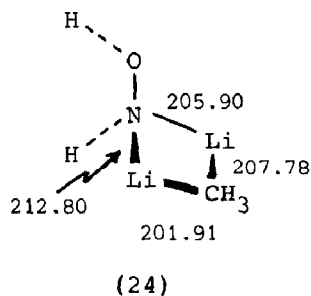
Semi-empirical (MNDO) MO investigations¹¹¹ of the reactions in Scheme 1 have shown that the lithium alkoxyamides LiRNOR' (22) react (in contrast to the alkoxyamines HRNOR' (23)) with organolithium compounds R''Li owing to (i) formation of an intermediate dimer (24), (ii) a long N-O bond in (22), and (iii) the high stability of LiNH⁺:



R = H, alkyl

Scheme 1

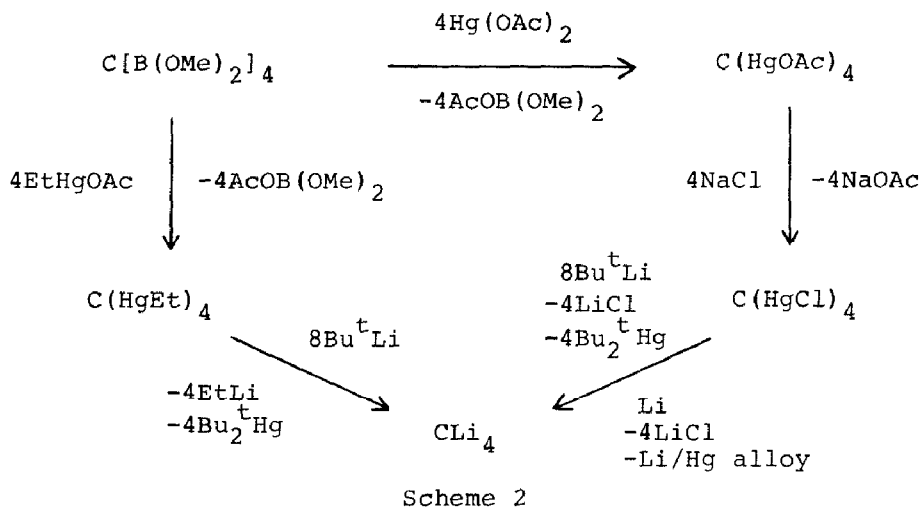
distances/pm



Continuing their studies of hypervalent molecules, Schleyer and Pople,¹¹² using ab initio SCF MO theory, have shown that ONa_3 (D_{3h}) and ONa_4 (T_d) are highly stable as isolated molecules towards all possible dissociation reactions (eg. loss of Na or Na_2). Further examples of hypermetalation are provided by HONa_2 (C_{2v}) and HONa_3 (C_{3v}). The ninth and tenth valence electrons in these hypervalent molecules are involved in metal-metal rather than in oxygen-metal bonding; the central oxygen atoms are content with the usual complement of eight electrons and do not have an expanded valence shell. Hypermetalation is predicted to be a general phenomenon involving all alkali metals in combination with many, if not most, of the other elements in the Periodic Table.¹¹²

New developments in the chemistry of polylithium compounds have been reviewed by Lagow et al.¹¹³ Two novel synthetic routes to CLi_4 (Scheme 2) have been reported by Maercker and Theis.¹¹⁴ Reaction of $\text{C}(\text{HgEt})_4$ or $\text{C}(\text{HgCl})_4$ with Bu^tLi in cyclopentane yields almost exclusively CLi_4 ; lithium dust in ether on reaction with $\text{C}(\text{HgCl})_4$ leads to not only CLi_4 but also $\text{Li}_2\text{C}=\text{CLi}_2$ and Li_3CCLi_3 presumably owing to the radical reaction mechanism.¹¹⁴

Lagow et al have reported the synthesis of various isotopic forms of dilithiomethane ($(\text{CH}_2^6\text{Li}_2)_n$ and $(\text{CD}_2\text{Li}_2)_n$)¹¹⁵ and of mono- and bis(trimethylsilyl)dilithiomethane¹¹⁶ by reaction of lithium



vapour with the corresponding dichloroderivatives. Preliminary XRD and solid phase ^{13}C -nmr studies of the isotopically substituted dilithiomethanes indicate a triclinic structure with a single highly symmetrical carbon environment.¹¹⁵ The trimethylsilyl derivatives of dilithiomethane were characterised simply by hydrolysis using D_2O in a vacuum line.¹¹⁶ The bonding in dilithiomethane has been elucidated by Streitwieser et al¹¹⁷ from an ab initio SCF MO study at the 6-31** level. Singlet CH_2Li_2 structures are basically C^-Li^+ in character with a small amount of three-centre bonding. Three-centre bonding is less important for triplet CH_2Li_2 structures which have significant Li-Li bonding instead.¹¹⁷

Schleyer et al¹¹⁸ have predicted the structures and stabilities of the organolithium and organosodium compounds MCH_2X ($\text{M} = \text{Li}, \text{Na}$; $\text{X} = \text{CH}_3, \text{NH}_2, \text{OH}, \text{F}, \text{SiH}_3, \text{PH}_2, \text{SH}, \text{Cl}$) by ab initio calculations. Comparisons are made with the corresponding free anions. The energetic results are summarised pictorially in Figure 1. The first row LiCH_2X ($\text{X} = \text{NH}_2, \text{OH}, \text{F}$) species are more stable than the corresponding anions due to lithium bridging. Sodium displays a diminished tendency to bridge resulting in an absence of such extra stabilisation for the corresponding sodium compounds. The second-row systems behave differently. The MCH_2Cl species are stabilised to the same extent as the free anions. However the presence of the metals in MCH_2X ($\text{X} = \text{SH}, \text{SiH}_3$ and especially PH_2) cancels much of the α -substituent stabilising effects in the corresponding anions resulting in much less stable species.

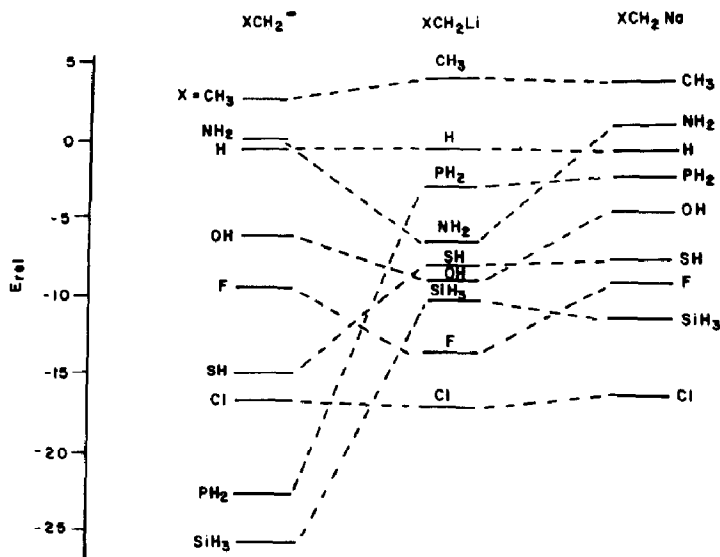
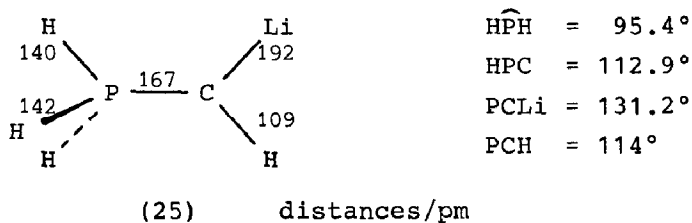


Figure 1. Comparison of stabilisation energies of substituted methyl anions and their corresponding organosodium and organolithium compounds (reproduced by permission from J. Am. Chem. Soc., 106(1984)6467).

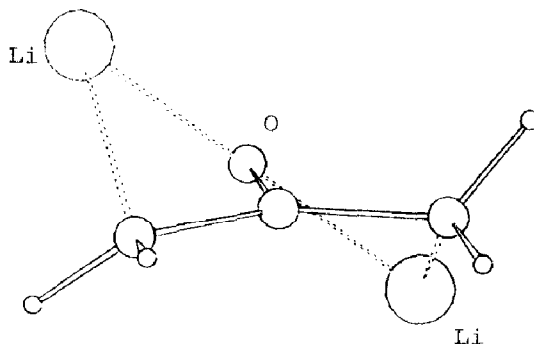
Ab initio SCF MO studies of (α -lithiomethylene)phosphorane and the corresponding anion have also been completed. Geometries, optimised at the 3-21G+(*) level, exhibit but marginal differences.¹¹⁹ It is concluded that the lithium derivative (25) is best described as an ion pair, the chemistry of which is largely that of the corresponding anion.¹¹⁹



The production of the lithiated pentacoordinate carbocations $[\text{CH}_n\text{Li}_{5-n}]^+$ ($0 \leq n \leq 3$) by flash vapourization and electron impact of polylithium organic molecules has been reported by Lagow et al.¹²⁰

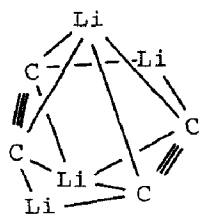
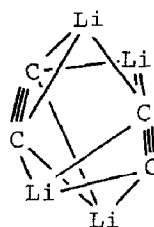
The 3-21G optimised structure of 1,3-dilithioacetone (26) has

C_2 symmetry.¹²¹ The two lithium cations bridge the oxygen and α -carbon atoms above and below the molecular plane of the dianion; some twisting of the CH_2 groups occurs as a result. This conformation is more favourable electrostatically than the alternative with both lithium atoms on the same side of the dianion moiety.¹²¹



(26)

The C_4Li_4 potential surface has been examined theoretically using ab initio SCF MO methods.¹²² Of the twelve structures considered, the most stable is a novel D_{2h} tetralithiodiacetylene (27) which lies $309.2 \text{ kJ.mol}^{-1}$ below two molecules of dilithioacetylene and $\sim 21 \text{ kJ.mol}^{-1}$ above the corresponding D_{2d} tetralithiodiacetylene structure (28).¹²²

(27) D_{2h} (28) D_{2d}

Schleyer et al.¹²³ have determined the crystal and molecular structure of $[\{ o-C_6H_4(CHPh)_2 \} \{ Li(tmeda) \}_2]$ (29) by single crystal X-ray diffraction methods. The two lithium atoms (Figure 2) prefer quite different locations in contrast to the symmetrical C_{2v} double bridging exhibited by other 1,4-dilithium compounds such as $[\{ o-C_6H_4(CHSiMe_3)_2 \} \{ Li(tmeda) \}_2]$ (30) and $[\{ C_{12}H_8 \} \{ Li(tmeda) \}_2]$ (31). Model MNDO calculations¹²⁴ have

shown, however, that symmetrical C_{2v} double bridging is not favoured in (29) since charge delocalisation in the dianion, hybridisation, and orbital orientation effects are more important than quadrupole-like electrostatic interactions. Thus, unlike SiMe_3 substituents, which stabilise carbanions very effectively and redistribute the electrons in part by polarisation,

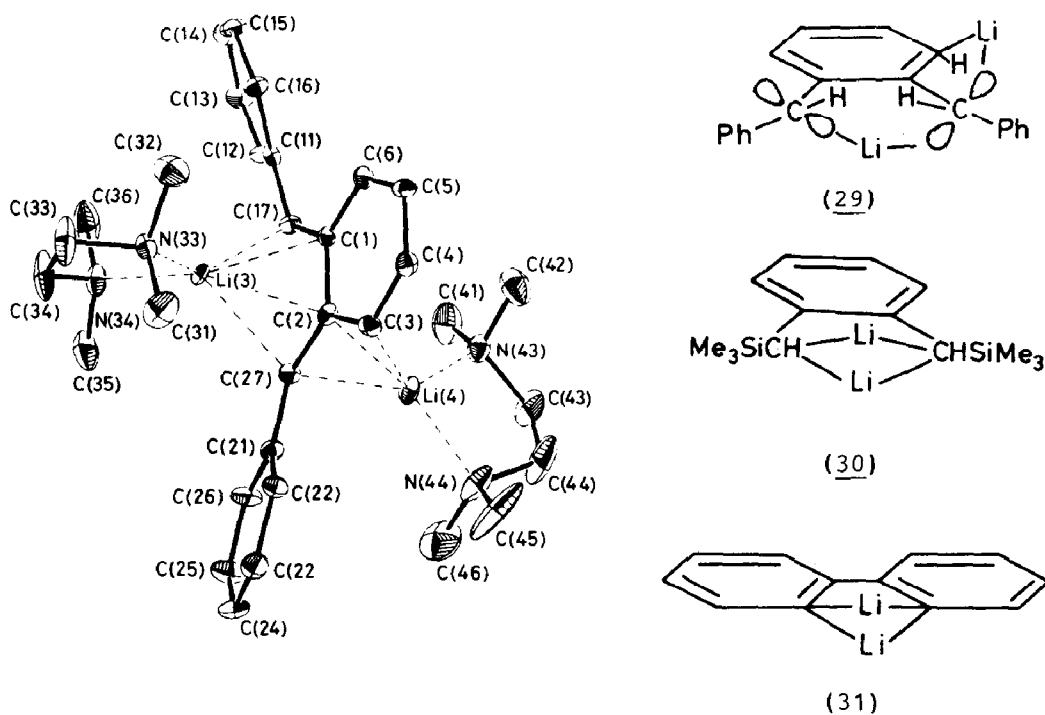


Figure 2. Molecular structure of $[\{\text{o-C}_6\text{H}_4(\text{CHPh})_2\}\{\text{Li}(\text{tmeda})\}_2]$ and simplified structural formulae for $[\{\text{o-C}_6\text{H}_4(\text{CHPh})_2\}\{\text{Li}(\text{tmeda})\}_2]$ (29), $[\{\text{o-C}_6\text{H}_4(\text{CHSiMe}_3)_2\}\{\text{Li}(\text{tmeda})\}_2]$ (30) and $[\{\text{C}_{12}\text{H}_8\}\{\text{Li}(\text{tmeda})\}_2]$ (31) (reproduced by permission from J. Chem. Soc., Chem. Commun., (1984) 1493, 1495).

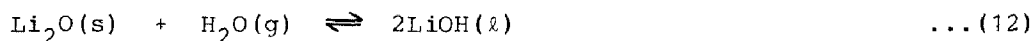
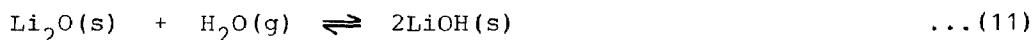
Ph substituents delocalise the charge into the aromatic ring preventing stabilisation of the two Li^+ ions by electrostatic interaction with the two $\alpha\text{-CH}_2$ groups in either C_{2v} or C_2 geometries. Thus only one Li^+ remains in a central position; the other prefers a benzyl-lithium-like location, the Huckel π -charges on the ring being greatest at the C(3) and C(6)

positions.¹²⁴

1.3.3 Binary Compounds

Once again there is a dearth of abstracted papers for this section; hence the data are considered en bloc rather than in separate subsections. As predicted in the 1982 review,¹²⁵ however, there has been a limited increase in interest in the chemistry of lithium containing ceramics owing to their potential application as tritium breeding materials in fusion reactors. Recent advances in this field were considered at, and published in the proceedings of, the third topical meeting on "Fusion Reactor Materials."⁶ In a 'state-of-the-art' review, Johnson and Hollenberg¹²⁶ concluded that Li_2O is the prime ceramic candidate for tritium breeder owing to its high breeding potential and good thermal characteristics. Its chemical properties are also attractive to the fusion reactor technologist except in the presence of water when the highly deleterious LiOH is produced.

Several groups¹²⁷⁻¹²⁹ have addressed the question of the chemistry of the Li_2O - LiOH - H_2O system. The adsorption of H_2O vapour from a helium gas stream onto solid Li_2O according to the equilibria:

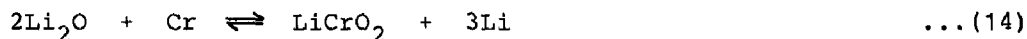
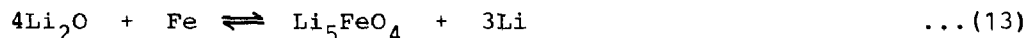


has been studied using isothermal dynamic adsorption methods.¹²⁷ The temperature dependence ($573 < T/\text{K} < 890$) of the partial pressure of H_2O vapour above the $\text{Li}_2\text{O}(\text{s})$ - $\text{LiOH}(\text{s}, \text{l})$ system has been measured in a sealed system;¹²⁸ the derived second law enthalpy and entropy data for equilibrium (11) are $\Delta H^\circ = -128.5(2.5) \text{ kJ.mol}^{-1}$ and $\Delta S^\circ = -123.4(4.2) \text{ JK}^{-1}\text{mol}^{-1}$, while those for equilibrium (12) are $\Delta H^\circ = -83.3(2.5) \text{ kJ.mol}^{-1}$ and $\Delta S^\circ = -61.9(3.3) \text{ JK}^{-1}\text{mol}^{-1}$. The melting point of LiOH was confirmed as 744K and its enthalpy of fusion as $22.6(1.7) \text{ kJ.mol}^{-1}$.¹²⁸ The activity coefficient of LiOH dissolved in solid Li_2O has also been determined for very dilute solutions using a thermobalance technique.¹²⁹

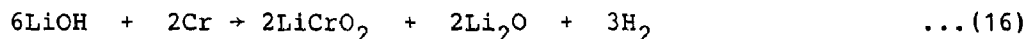
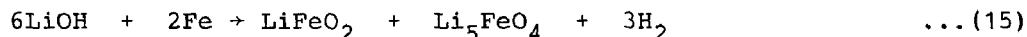
The solubility of deuterium in solid Li_2O has been determined¹³⁰ by measuring the adsorption of deuterium gas by single crystals of

Li_2O located in a fused silica tube; the results ($10 < p_{\text{D}_2}/\text{Pa} < 130$) suggest that $x_{\text{D}} \propto p_{\text{D}_2}$ indicating that D_2 molecules are the dissolved species.

Chemical compatibility studies between solid Li_2O ($873 < T/\text{K} < 1273$)¹³¹ or molten LiOH ($744 < T/\text{K} < 933$)¹³² and transition metals (Ti, V, Cr, Mn, Fe, Ni and various stainless steels) have been undertaken by Pulham et al. Pure Li_2O is inherently stable towards transition metals except when equilibria such as:



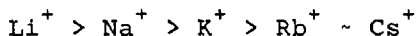
are disturbed by removal of lithium by vacuum or chemical means.¹³¹ Molten LiOH , however, corrodes transition metals according to the equations:



The corrosion rates, determined from the rate of evolution of hydrogen gas, indicate that Cr reacts most rapidly, and that the corrosion of steels increases with increasing Cr and decreasing Ni content, 316 stainless steel being the most reactive steel studied.¹³²

Other than those reporting on the chemistry of Li_2O and LiOH , the papers abstracted for this section do not portray a recurrent theme; they describe the results of diverse studies on varied compounds.

Evidence that alkali metal halide salts are not fully dissociated in aqueous solution has been obtained from fluoride ion selective electrode potentiometry studies of aqueous solutions of MF ($\text{M} = \text{Li}-\text{Cs}$) at $T = 298\text{K}$ and $I = 1.0\text{M}$;¹³³ extremely weak monofluoride (MF) complexes are formed, their stability constants decreasing in the order:



The ions, K^+ , K_2I^+ , K_3I_2^+ , I^- , KI_2^- and K_2I_3^- have been

recorded in the saturated vapour over KI; in the presence of KOH, however, the ions observed were K^+ , K_2I^+ , $K_2(OH)^+$, I^- , KI_2^- , $(OH)^-$, $K(OH)_2^-$, K^- and K_2I^- .¹³⁴ The enthalpies of formation (kJ.mol^{-1}) of the ions K_2I^+ [233(8)], $K_3I_2^+$ [-35(15)], KI_2^- [-483(8)], $K_2I_3^-$ [-760(15)] and K_2I^- [-244(11)], the electron affinities (kJ.mol^{-1}) of KI_2 [386(20)] and K_2I [135(20)] and the ionisation enthalpy (kJ.mol^{-1}) of K_2I [347(20)] have been estimated.¹³⁴

The LiF-LiOH and LiF-LiH phase diagrams have been constructed from the results of dta, XRD and ac-impedance studies.¹³⁵ Whereas the former system is a simple eutectic one with eutectic parameters, $T = 705\text{K}$, $x_{\text{LiOH}} = 0.85$, the latter system exhibits, at sufficiently high temperatures ($T > 823\text{K}$), a continuous series of solid solutions throughout the composition range. At lower temperatures ($T < 823\text{K}$) a miscibility gap, which extends over the composition range $0.60 < x_{\text{LiH}} < 0.90$ at $T = 298\text{K}$, is observed.¹³⁵

Structural studies have been completed on a small number of novel interalkali metal compounds; pertinent crystallographic parameters for KLiS ,¹³⁶ RbLiBr_2 ,¹³⁷ CsLiBr_2 ,¹³⁷ $\text{Cs}_2\text{Na}_2\text{Cl}_3 \cdot \text{H}_2\text{O}$ ¹³⁸ and $\text{Cs}_{0.57}(\text{Na}, \text{H}_2\text{O})_{0.43}\text{Cl}$ ¹³⁸ are collected in Table 5. The sulphide¹³⁶ and bromides¹³⁷ were prepared by thermal treatment of equimolar mixtures of the appropriate binary compounds; the chlorides¹³⁸ were crystallised from the $\text{CsCl-NaCl-H}_2\text{O}$ system. The structure of $\text{CsNa}_2\text{Cl}_3 \cdot 2\text{H}_2\text{O}$ consists of a slightly distorted cubic CsCl framework in which $2/3$ of the Cs atoms are replaced by H_2O molecules and Na atoms are inserted into the Cl_4 face centres between pairs of H_2O molecules to form coiled $(\text{Na} \cdot \text{H}_2\text{O})_n$ chains. This structural principle also accounts for the unusual solid solution series $\text{Cs}_{1-x}(\text{Na} \cdot \text{H}_2\text{O})_x\text{Cl}$ ($0 < x < 0.43$) in which H_2O molecules replace Cs atoms and $(\text{Na} \cdot \text{H}_2\text{O})_n$ chains are looped or coiled at random in the cubic structure.¹³⁸

A variety of techniques have been used for structural elucidation of Li_3N ,¹³⁹ NaN_3 ,¹⁴⁰ $[\text{Li}(\text{tmeda})]_3\text{P}_7$,¹⁴¹ $\text{Na}_2\text{S} \cdot 5\text{H}_2\text{O}$ ¹⁴² and $\text{MOH} \cdot \text{H}_2\text{O}$ ($M = \text{K}, \text{Rb}$).¹⁴³ The electron density distribution in Li_3N has been investigated using Compton scattering techniques;¹³⁹ the results are interpreted within an ionic model. A temperature dependent ($12 < T/\text{K} < 293$) diffraction study of NaN_3 has shown¹⁴⁰ that the low temperature (monoclinic, C2/m) phase results from a discontinuous shear in the (010) plane of the high temperature (rhombohedral, $\text{R}\bar{3}\text{m}$) structure. The magnitude of the shear increases from 0.5° at the transition temperature of 292.2K to a value of 5.3° at 12K .¹⁴⁰

Table 5. Crystallographic parameters for a number of interalkali metal compounds.

	symmetry	space group	a/pm	b/pm	c/pm	$\beta/^\circ$	ref.
KLiS	tetragonal	P4/nmm*	431.8	-	696.2	-	136
RbLiBr ₂	orthorhombic	Comm	1512.0	436.4	765.4	-	137
CsLiBr ₂	tetragonal	-	518.7	-	992.4		137
CsNa ₂ Cl ₃ ·2H ₂ O	monoclinic	I2/c	1362.4	583.2	1070.5	91.26	138
Cs _{0.57} (Na, H ₂ O) _{0.43} Cl	cubic	-	412.3				138

* alternative $P\bar{4}m2$.

Crystalline $[\text{Li}(\text{tmeda})]_3\text{P}_7$, formed by reaction of white phosphorus with $\text{LiCH}_2\text{PPh}_2(\text{tmeda})$, has been studied by XRD analysis.¹⁴¹ It comprises an isolated, ionic complex with approximately $3m$ (C_{3v}) symmetry. The Li atoms are each coordinated in a distorted tetrahedron to the two nitrogen atoms of one tmeda molecule, $r(\text{Li}\dots\text{N})_{\text{av}} = 207.1\text{pm}$, and to two twofold bonded phosphorus atoms of the heptaphosphane (3) moiety, $r(\text{Li}\dots\text{P})_{\text{av}} = 255.5\text{pm}$; the threefold bonded phosphorus atoms of the latter unit do not participate in the coordination of the Li atoms, which is typical of solvent-free polyphosphides.¹⁴¹ This paper is only one of many, submitted primarily by Baudler or von Schnering, on the chemistry of alkali metal polyphosphides; the others, however, concentrate on the polyphosphide unit and hence are considered in detail in Chapter 5 of this review.

The crystal and molecular structures of $\text{Na}_2\text{S}\cdot 5\text{H}_2\text{O}$ have been redetermined with greater precision to define the hydrogen bonding.¹⁴² It contains two crystallographically distinct Na atoms located in NaO_6 distorted octahedral (D_{4h}), $r(\text{Na}(1)\dots\text{O}(1)) = 246.3\text{pm}$, $r(\text{Na}(1)\dots\text{O}(2)) = 236.1\text{pm}$ and NaO_4S square based pyramidal (C_{4v}) coordination spheres, $r(\text{Na}(2)\dots\text{O}(2)) = 239.7\text{pm}$, $r(\text{Na}(2)\dots\text{S}) = 288.7\text{pm}$. A vibrational (i.r. and Raman) study has also been undertaken.¹⁴²

Recrystallisation of $\text{MOH}\cdot\text{H}_2\text{O}$ ($M = \text{K}, \text{Rb}$) from supercritical ammonia afforded crystals suitable for structure determination.¹⁴³ Their closely related structures, ($\text{RbOH}\cdot\text{H}_2\text{O}$ has more symmetry) contain metal cations in distorted octahedral coordination spheres generated by four H_2O molecules $r(\text{K}\dots\text{O}) = 278.8\text{--}293.9$, $r(\text{Rb}\dots\text{O}) = 292.8, 304.0\text{pm}$, and two OH^- anions, $r(\text{K}\dots\text{O}) = 283.9, 284.7$, $r(\text{Rb}\dots\text{O}) = 299.6\text{pm}$; they are compared with the structures of PbFCl and $\gamma\text{-AlO}(\text{OH})$.¹⁴³

1.3.4 Ternary Pnictides

Schuster et al.^{144,145} have provided the only papers abstracted for this subsection. They have synthesised and structurally characterised a large number of phosphides, arsenides, stibnides and bismuthides; the compounds synthesised are listed in Table 6 together with representative crystallographic data.

1.3.5 Ternary Oxides and Chalcogenides

The apparent loss of interest in the chemistry of ternary oxides

Table 6. Ternary pnictides synthesised by Schuster et al.^{144,145}

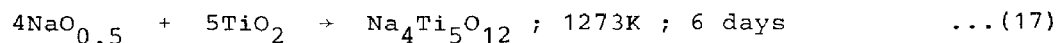
CaAl ₂ Si ₂ - structure type tetragonal P $\bar{3}$ m1 a = 425.1, c = 690.6pm*			
Li ₃ LaP ₂	Li ₃ NdAs ₂	Li ₃ LaSb ₂	Li ₃ LaBi ₂
		Li ₃ YSb ₂	Li ₃ YBi ₂
ThCr ₂ Si ₂ - structure type tetragonal I4/mmm a = 380.8, c = 1297.2pm*			
KFe ₂ P ₂	KCo ₂ P ₂	RbFe ₂ As ₂	RbCo ₂ As ₂
KRu ₂ P ₂	RbCo ₂ P ₂	KRu ₂ As ₂	RbRh ₂ As ₂
RbRu ₂ P ₂	RbRh ₂ P ₂	RbRu ₂ As ₂	KIr ₂ As ₂
	KIr ₂ P ₂		RbIr ₂ As ₂
	RbIr ₂ P ₂		
K ₂ PdP ₂ - structure type orthorhombic Cmc a = 645.4, b = 1371.6, c = 560.2pm*			
K ₂ NiP ₂	Rb ₂ PdP ₂	K ₂ NiAs ₂	Rb ₂ PdAs ₂
Rb ₂ NiP ₂	Rb ₂ PtP ₂	Rb ₂ NiAs ₂	Rb ₂ PtAs ₂

* The crystallographic parameters refer to Li₃LaP₂, KFe₂P₂ and K₂NiP₂.

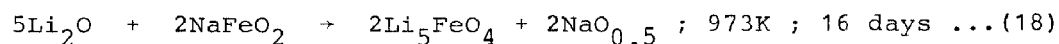
and chalcogenides continues; as for the 1983 review¹⁴⁶ the number of papers abstracted for this subsection is again exceeded by the number devoted to ternary halides. A significant development, however, is the publication, by Hoppe et al, of crystallographic data (Table 7) for several oxides containing two alkali metals, viz KLi₃TiO₄,¹⁴⁷ K₂NaFeO₃,¹⁴⁸ KNa₂CuO₂,¹⁴⁹ KNaZnO₂¹⁵⁰ and K₃NaTh₂O₆.¹⁵¹ These materials were synthesised by high temperature reaction of either three binary oxides or two ternary oxides. For example, mixtures of KO_{0.48}, NaO_{0.5} and Cu₂O, sealed at 913K for 30 days, afford KNa₂CuO₂ while mixtures of K₂ZnO₂ and Na₂ZnO₂ at 873K for 14 days yield KNaZnO₂. Unit cell parameters for these materials are listed in Table 7 together with

corresponding data for those regular ternary oxides which have been synthesised and structurally characterised.¹⁵²⁻¹⁶¹

Preparation of the ternary oxides was generally achieved in high temperature reactions involving either combination of binary oxides:



or exchange between binary and ternary oxides:



β - NaVO_3 , however, was prepared by topotactic dehydration of synthetic $\text{NaVO}_3 \cdot 2\text{H}_2\text{O}$.¹⁵³ With the exception of $\text{NaNb}_7\text{O}_{18}$ ¹⁵⁴ and LiCoO_2 ,¹⁵⁸ structural analysis of the ternary oxides was achieved using single crystal XRD data. For $\text{NaNb}_7\text{O}_{18}$,¹⁵⁴ a combination of high resolution electron microscopy and powder XRD methods, and for LiCoO_2 ¹⁵⁸ powder neutron diffraction techniques were used. The results of the latter study confirm the earlier XRD structure, showing it to be a completely ordered rock salt arrangement with alternating planes of Li and Co atoms.¹⁵⁸

A novel potassium trivanadate, $\text{K}_{1+x}\text{V}_3\text{O}_8$ has been produced¹⁶² by rapid quenching of high temperature melts ($T = 1023\text{K}$) containing K_2CO_3 and V_2O_5 in the approximate molar ratio 1:3. It is metastable and isomorphous with lithium and sodium trivanadates (γ -phase). No further details are quoted.¹⁶²

The vibrational spectra ($33 < \bar{\nu} / \text{cm}^{-1} < 4000$) of isotopically substituted $\text{Li}_2\text{Ti}_3\text{O}_7$ have been measured;¹⁶³ the observed wavenumber shifts confirm that the structure contains both tetrahedrally and octahedrally coordinated Li atoms.

The only report of a novel ternary sulphide to be abstracted for this review is that of $\text{Na}_2\text{Co}_2\text{S}_5$ which was prepared by reaction of Co powder and Na_2CO_3 with dry H_2S at 1000K ;¹⁶⁴ the crystallographic parameters of this material, which is sensitive to both air and moisture, are included in Table 7.

1.3.6 Ternary Halides

Discussion in this section is restricted to the chemistry of anhydrous ternary halides; solvated species are not considered.

Phase relationships in the KCl-NiCl_2 ,¹⁶⁵ MCl-PdCl_2 ($\text{M} = \text{Rb}$,

Table 7. Crystallographic parameters for diverse ternary oxides and sulphides.

Compound	Symmetry	Space Group	a/pm	b/pm	c/pm	$\beta/^\circ$	Ref.
KLi_3TiO_4	triclinic	$\text{P}\bar{1}$	1040.0 (100.4°)	757.0 (110.1°)	592.5 (90.6°)	-	147
K_2NaFeO_3	orthorhombic	Cmma	1101.2	619.7	670.6	-	148
KNa_2CuO_2	tetragonal	I4mm	432.7	-	1089.1	-	149
KNaZnO_2	monoclinic	$\text{P}2_1/\text{c}$	582.4	970.0	551.3	103.7	150
$\text{K}_3\text{NaTh}_2\text{O}_6$	monoclinic	$\text{C}2/\text{c}$	629.6	1089.9	1259.8	99.7	151
$\text{Na}_4\text{Ti}_5\text{O}_{12}$	monoclinic	$\text{C}2/\text{m}$	2654.4	295.2	632.2	95.8	152
$\beta\text{-NaVO}_3$	orthorhombic	Pnma	1414.7	365.0	536.4	-	153
$\text{NaNb}_7\text{O}_{18}$	orthorhombic	Immm	1428.4	2622.4	384.1	-	154
Na_5MnO_4	orthorhombic	$\text{P}2_1/\text{mn}$	582.2	776.9	600.5	-	155
Li_5ReO_6	monoclinic	$\text{C}2/\text{m}$	506.8	873.2	502.9	110.2	156
Na_5ReO_6	monoclinic	$\text{C}2/\text{m}$	568.8	973.1	560.7	111.0	156
Li_5FeO_4	orthorhombic	Pbca	921.8	921.3	915.9	-	157
LiCoO_2	rhombohedral	$\text{R}\bar{3}\text{m}$	281.5	-	1405	-	158
Li_2IrO_3	orthorhombic	-	513.0	886	971	-	159
Li_8IrO_6	hexagonal	-	541	-	1494	-	159
Li_2CuO_2	orthorhombic	Immm	365.4	285.9	937.4	-	160
LiCeO_2	monoclinic	$\text{P}12_1/\text{c}1$	582.4	616.6	579.3	102.5°	161
$\text{Na}_5\text{Co}_2\text{S}_5$	tetragonal	I4mm	915.0	-	622.2	-	164

Cs), ¹⁶⁶ MBr-TaBr₃ (M = Na-Cs), ¹⁶⁷ CsBr-DyBr₃, ¹⁶⁸ MBr-HoBr₃, ¹⁶⁹ and CsBr-HoBr₃ ^{168,169} systems have been investigated using dta, tga, and/or XRD methods. The compounds formed in these systems are listed in Table 8 together with their thermal properties. Two significant features arise from these studies. Firstly, the results for the KCl-NiCl₂ system ¹⁶⁵ contrast with those of an earlier study ¹⁷⁰ which indicated the formation of K₂NiCl₄ as well as KNiCl₃. Secondly, the two sets of results for the CsBr-HoBr₃ system differ. Whereas Podorozhnyi and Safonov ¹⁶⁸ claim the formation of Cs₃HoBr₆ and Cs₃Ho₂Br₉, Dudareva et al ¹⁶⁹ conclude that Cs₃HoBr₆ and CsHo₂Br₇ are produced. Furthermore, they disagree in the detail of the thermal properties of Cs₃HoBr₆.

A significant proportion of commitment in this field lies in the

Table 8. Thermal properties of the ternary halides formed in the KCl-NiCl_2 , MCl-PdCl_2 , MBr-TaBr_5 , CsBr-DyBr_3 , MBr-HoBr_3 and CsBr-HoBr_3 systems.

KCl-NiCl_2 ¹⁶⁵		CsBr-TaBr_6 ¹⁶⁷	
KNiCl_3 d. peritectic 948K		CsTaBr_6 $\beta \rightarrow \alpha$ trans. 675K	
		m.p. 798K	
RbCl-PdCl_2 ¹⁶⁶		CsBr-DyBr_3 ¹⁶⁸	
Rb_2PdCl_4 m.p. 799K		Cs_3DyBr_6 $\beta \rightarrow \alpha$ trans. 710K	
RbPd_3Cl_7 d. peritectic 613K		m.p. 1063K	
CsCl-PdCl_2 ¹⁶⁶		$\text{Cs}_3\text{Dy}_2\text{Br}_9$ d. peritectic 908K	
Cs_2PdCl_4 m.p. 759K			
CsPd_3Cl_7 d. peritectic 634K		LiBr-HoBr_3 ¹⁶⁹	
NaBr-TaBr_5 ¹⁶⁷		$\text{LiHo}_9\text{Br}_{28}$ $\epsilon \rightarrow \delta$ trans. 473K	
NaTaBr_6 $\beta \rightarrow \alpha$ trans. 573K		$\delta \rightarrow \gamma$ trans. 469K	
d. peritectic 679K		$\gamma \rightarrow \beta$ trans. 648K	
		d. peritectic 781K	
KBr-TaBr_5 ¹⁶⁷		NaBr-HoBr_3 ¹⁶⁹	
KTaBr_6 $\beta \rightarrow \alpha$ trans. 443K		Na_3HoBr_6 d. peritectic 753K	
d. peritectic 723K		Na_2HoBr_5 $\beta \rightarrow \alpha$ trans. 499K	
$\text{K}_2\text{Ta}_3\text{Br}_{17}$ d. peritectic 543K		d. peritectic 651K	
RbBr-TaBr_5 ¹⁶⁷		CsBr-HoBr_3 ¹⁶⁹	
RbTaBr_6 $\beta \rightarrow \alpha$ trans. 603K		Cs_3HoBr_6 $\beta \rightarrow \alpha$ trans. 749K	
m.p. 677K		m.p. 1045K	
		CsHo_2Br_7 d. peritectic 537K	
		CsBr-HoBr_3 ¹⁶⁸	
		Cs_3HoBr_6 $\beta \rightarrow \alpha$ trans. 736K	
		m.p. 1101K	
		$\text{Cs}_3\text{Ho}_2\text{Br}_9$ d. peritectic 918K	

Abbreviations:

m.p. - melts congruently

d. peritectic - decomposes in a peritectic reaction

$\beta \rightarrow \alpha$ trans. - polymorphic transformation

synthesis, preferably as single crystals, of ternary halides for structural elucidation. Those compounds which have been characterised at ambient temperature^{166,171-179} are listed in Table 9 together with salient crystallographic parameters; those compounds which exhibit polymorphism and have been studied as a function of temperature^{180,181} are listed in Table 10 together with pertinent thermal and crystallographic parameters.

Polymorphism has also been studied in Li_2UBr_6 , for which structural data are absent; techniques used include electrical conductivity, differential thermal and differential enthalpic analyses.¹⁸² Two thermal effects ($\Delta H_{\text{trans}} = 1.70(40)$ and $0.35(15) \text{ kJ.mol}^{-1}$ at $505(2)$ and $740(2)\text{K}$, respectively) were observed before melting ($\Delta H_{\text{m}} = 48(2) \text{ kJ.mol}^{-1}$ at $781(2)\text{K}$). The data are discussed by comparison with those of Na_2UBr_6 for which more reliable structural data are available.

A variety of synthetic routes have been employed for the preparation of these ternary halides. The majority are variants of classical solid state methods. Meyer,¹⁷⁶ for example, has obtained LiGdCl_4 by reaction of GdCl_3 with liquid lithium, by synproportionation of GdCl_3 and LiCl and by thermal decomposition of $(\text{NH}_4)_2\text{LiGdCl}_6$. Hoppe et al¹⁸³ have also reported an alternative preparation of MLnF_3 ($\text{M} = \text{K-Cs}$; $\text{Ln} = \text{Eu, Yb}$) which involves reduction of MLnF_4 by liquid alkali metal, it being more effective than the normal method which involves LnF_3 as substrate.

X-ray diffraction studies have been completed on the interstitial compounds Rb_xCrF_3 ($x = 0.18, 0.20, 0.225, 0.25, 0.275, 0.30$),¹⁸⁴ Li_xYCl ($x = 0.2$),¹⁸⁵ Li_xGdCl ($x = 0.5$)¹⁸⁵ and $\text{K}_x\text{Zr}_6\text{I}_{14}$ ($x = 0.46, 1.0$). For Rb_xCrF_3 ,¹⁸⁴ a hexagonal bronze like system spans the range $0.18 \leq x \leq 0.29$. An orthorhombic sublattice ($a \sim 1270$, $b \sim 740$, $c \sim 740\text{pm}$) was identified in every sample. Modulated structures, designated $\alpha(x)$, resulting from $1/2$, $2/3$ and $3/4$ -filled Rb^+ sites occur for $x = 0.167, 0.222$ and 0.250 . The $\alpha(0.167)$ unit cell has the same dimensions as the orthorhombic sublattice, but unlike the sublattice, which is primitive, the superstructure is body centered. The $\alpha(0.222)$ unit cell has the same a and b dimensions as the sublattice but it is base centered with $c(\text{super}) = (3/2)c(\text{sub})$. The $\alpha(0.250)$ phase has a primitive unit cell with dimensions $a(\text{super}) = 2a(\text{sub})$, $b(\text{super}) = 3b(\text{sub})$ and $c(\text{super}) = 2c(\text{sub})$. An undistorted

Table 9. Crystallographic parameters for a number of ternary halides.

Compound	Symmetry	Space Group	a/pm	b/pm	c/pm	$\beta/^\circ$	Ref
Na_3GdCl_6	rhombohedral	$R\bar{3}$	700.7	-	1879.1	-	171
Rb_2PdCl_4	tetragonal	$P4/\text{mmm}$	727	-	478	-	166
Cs_2PdCl_4	tetragonal	$P4/\text{mmm}$	753	-	465	-	166
Cs_2YbCl_4	tetragonal	$I4/\text{mmm}$	541.8	-	1727.6	-	172
K_2PtCl_6	cubic	$\text{Fm}\bar{3}\text{m}$	974.3	-	-	-	173
$\text{Cs}_6\text{Ni}_5\text{F}_{16}$	orthorhombic	Cmca	618.4	1455.5	2145.1	-	174
KCdCl_3	orthorhombic	Pnma	879.2	400.9	1459.7	-	175
LiGdCl_4	tetragonal	$I4_1/a$	645.8	-	1316.0	-	176
CsReF_6	rhombohedral	$R\bar{3}$	785.3	-	814.0	-	177
CsCu_2Cl_2	orthorhombic	Cmcm	950.8	1189.8	559.9	-	178
CsCu_2Br_2	orthorhombic	Cmcm	987.3	1235.5	581.8	-	178
$\text{KLn}_2\text{Cl}_7^*$	monoclinic	$P2_1/a$	1283.1	694.7	1277.4	89.90	179
$\text{RbLn}_2\text{Cl}_7^*$	orthorhombic	Pnma	1293.2	702.4	1278.7	-	179
$\text{CsLn}_2\text{Cl}_7^*$	orthorhombic	Pnma	1320.5	709.9	1295.2	-	179

* Ln = Sm-Yb, Y; the data quoted refer to the samarium compound.

hexagonal bronze phase was also observed in samples where $x = 0.20$, 0.225, 0.25 and 0.275.¹⁸⁴ Both $\text{Li}_{0.2}\text{YCl}$ ($a = 375.13$, $c = 2780.3\text{pm}$)¹⁸⁵ and $\text{Li}_{0.5}\text{GdCl}$ ($a = 381.5$, $c = 2783.2\text{pm}$)¹⁸⁵ occur in the ZrBr-type structure (rhombohedral, $R\bar{3}\text{m}$) with lithium evidently randomly distributed in trigonal antiprismatic interstices.

The phase $\text{KZr}_6\text{I}_{14}$ ¹⁸⁶ is the first example of an unprecedented structural configuration (Figure 3) in which a potassium atom is located in the centre of an octahedral zirconium cluster, $r(\text{K} \dots \text{Zr}) = 239.3$, 246.0pm ; iodine atoms bridge both the edges of the cluster $r(\text{Zr} \dots \text{I})_{\text{av}} = 289.8\text{pm}$ and between clusters $r(\text{Zr} \dots \text{I})_{\text{av}} = 312.4$, 340.8pm . The cluster (Figure 3) has C_{2h} symmetry resulting from a 2-fold axis, which passes through K and I(5), together with a mirror plane that contains K, I(4) and Zr(2).¹⁸⁶

The electron density distribution in K_2PtCl_6 has been determined from a detailed single crystal XRD study (Final R value = 0.009).¹⁷³ X-X synthesis shows a peak of $0.5(2) \times 10^{-6} \text{e pm}^{-3}$ in

Table 10. Polymorphism of K_3VF_6 ,¹⁸⁰ Cs_2CdBr_4 ¹⁸¹ and Cs_2HgBr_4 .¹⁸¹

Compound	Transition Temperature K*	Symmetry	Space Group	a/pm	b/pm	c/pm	$\beta/^\circ$
K_3VF_6	-	monoclinic		1210.2	1745.6	1200.7	92.6
	453	monoclinic		1714	1237	547.9	91.5
	483	tetragonal [†]		1370.8	-	875.2	-
Cs_2CdBr_4	-	triclinic	$P\bar{1}$	1020.0 (90.0)	778.8 (90.0)	1389.8 (90.0)	-
	158	monoclinic	$P2_1/n$	1020.1	785.6	1394.9	90.0
	237	incommensurate phase					
	252	orthorhombic	Pnma	1022.8	793.1	1396.6	-
Cs_2HgBr_4	-	triclinic	$P\bar{1}$	1010 (90.0)	1540 (90.0)	1380 (90.0)	-
	85	triclinic	$P\bar{1}$	1014.8 (90.0)	775.4 (90.0)	1383.7 (90.0)	-
	167	monoclinic	$P2_1/n$	1016.2	781.3	1379.6	90.0
	232	incommensurate phase					
	245	orthorhombic	Pnma	1024.8	792.7	1390.1	-

* This temperature is the lower limit of existence of the associated phase.

[†] This phase can be stabilised at room temperature by incorporation of trace quantities of Na^+ .

the (111) direction at 50pm from the Pt nucleus which is tentatively attributed to the non-bonding 5d electrons in t_{2g} orbitals.¹⁷³

Transfer of electronic excitation energy has been studied¹⁸⁷ in crystals of the antiferromagnetic compounds $RbMnCl_3$, $CsMnCl_3$, $CsMnBr_3$ and Rb_2MnCl_4 .

Finally, the standard enthalpies of formation ($\Delta H_f^\circ(298K, c, x)$) of K_2NiF_6 ($-1963 \text{ kJ.mol}^{-1}$), K_2PdF_6 ($-2040 \text{ kJ.mol}^{-1}$) and K_2PtF_6 ($-2055 \text{ kJ.mol}^{-1}$) have been determined by solution calorimetry.¹⁸⁸

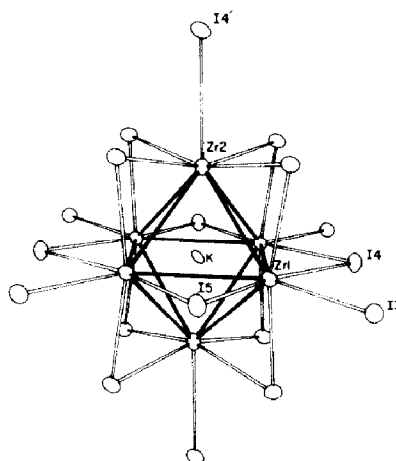


Figure 3. The molecular structure of the $\text{KZr}_6\text{I}_{14}$ cluster with all exo iodines (reproduced by permission from J. Am. Chem. Soc., 106(1984)4618).

1.4 COMPOUNDS OF THE ALKALI METALS CONTAINING ORGANIC MOLECULES OR COMPLEX IONS

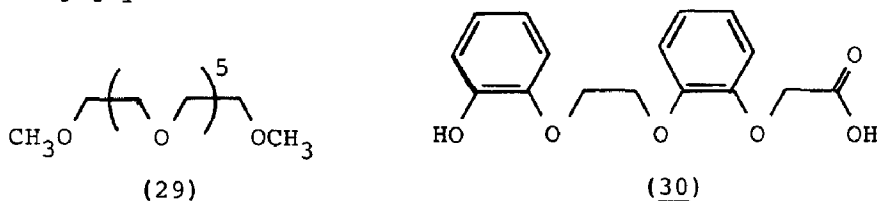
The format adopted for this section is similar to that used for the 1983 Review.¹⁸⁹ Thus the text is simplified by incorporation of subdivisions for specialised topics of current interest and significance; these include complexes of acyclic and macrocyclic lipophilic ionophores, salts of carboxylic and thiocarboxylic acids, and heterobimetallic complexes. The subdivision previously included for derivatives of nucleotides and related species has been omitted owing to a marked reduction in pertinent data. Those which have been abstracted are considered in the subdivisions for the individual alkali metals. Of these, that for lithium is very extensive, reflecting recent developments in the chemistry of lithium-containing oligomers.

1.4.1 Complexes of Acyclic Lipophilic Ionophores

Complex formation between lithium and lipophilic ionophores, including acyclic oligoethers, crowns and cryptands has been reviewed by Pacey.¹⁹⁰ Emphasis is put on the production of chromogenic derivatives which act as colorimetric reagents for alkali metals; their formation involves the addition of a chromophore to a monoanion or azo-type linkage on the ionophore.¹⁹⁰

Competition reactions between linear oligoethers or crowns anchored to solvent swollen microporous polystyrene resins and soluble ligands for lithium or sodium picrate in toluene at 298K have been studied;¹⁹¹ the results are used to generate a scale of relative ligand affinities for linear oligoethers and oligoamines, crowns, cryptates and other cation binding ligands. The linear oligoethers have much lower cation affinities than the corresponding macrocyclic polyethers; for example, glyme 7 has an affinity for sodium picrate lower than that of B18C6 by a factor of 265.¹⁹¹

Single crystal XRD studies have been completed on three complexes containing acyclic oligoethers; viz the barium thiocyanate complex of (29),¹⁹² the sodium salt of (30)¹⁹³ and the potassium acid salt of (30).¹⁹⁴ The structure of the former is the first of a complex between an unsubstituted oligoglyme and an alkaline earth metal cation to be determined.¹⁹²



The open chain oligoether approximates to one turn of a helix, thus facilitating coordination of the cation to all seven ether oxygen atoms (287.9-294.1pm) and to the nitrogen atoms of the two anions located on the same side of the helix (282.5, 284.2pm).

Despite the apparent similarity of the latter two salts, they exhibit markedly different structural chemistry; whereas the sodium salt shows a tetrameric association,¹⁹³ the potassium acid salt contains monomeric units joined by hydrogen bonding in a step-polymer formation.¹⁹⁴ The molecular structure of the sodium salt (Figure 4a)¹⁹³ shows alternating oxygen and sodium atoms at the corners of a fairly regular cube which is at the centre of an Na_4L_4 tetramer. The symmetry of the cube is such that there are two crystallographically distinct Na atoms which have similar pentagonal bipyramidal coordination spheres (Figure 4a). Each Na atom is coordinated by the carboxylate oxygen atoms of three ligands (located at the corners of the cube) and also by three ether oxygen atoms from one of these ligands. The seventh coordination position is filled by the

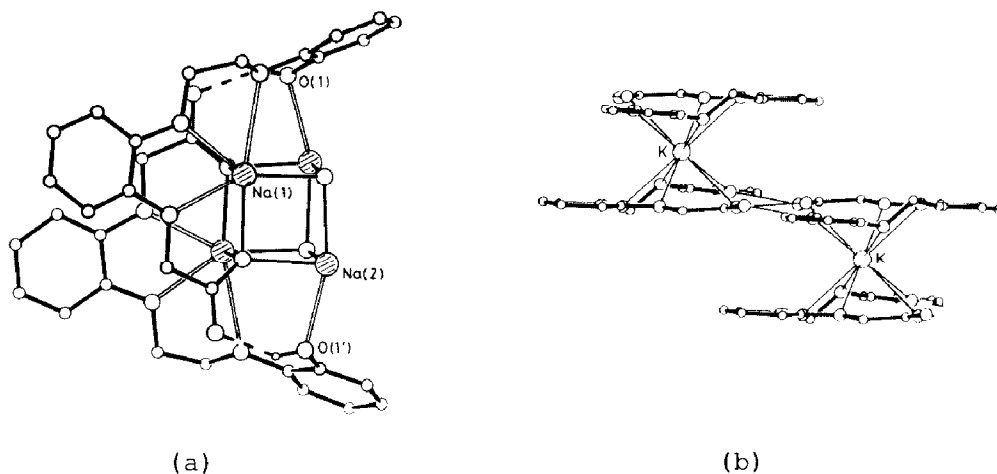
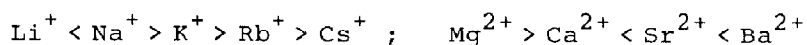


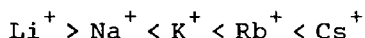
Figure 4. Aspects of the molecular structure of (a) the sodium salt of (30) showing the sodium-oxygen cube and two ligands, related by two-fold symmetry, and the saddle-shape of the hydrogen bonded dimer unit, and (b) the potassium acid salt of (30) showing the linking of hydrogen bonded anions through coordinated potassium cations (reproduced by permission from (a) J. Chem. Soc., Chem. Commun., (1984)408 and (b) J. Chem. Soc., Dalton Trans., (1984)1187).

phenolic oxygen atom of the fourth ligand. For each Na atom, one equatorial Na-O bond is significantly longer, $r(\text{Na}(1) \dots \text{O}) = 285$, $r(\text{Na}(2) \dots \text{O}) = 270\text{pm}$, than the others, $r(\text{Na} \dots \text{O}) = 232\text{--}251\text{pm}$. The molecular structure of the potassium acid salt (Figure 4b) shows it to be composed of K atoms sandwiched between planar hydrogen bonded acid salt anions. Thus each K atom is irregularly coordinated by eight oxygen atoms, four (three ether and one phenolic) from each of two ligands, (271–287pm) with two somewhat more remote carboxylate oxygen atoms (319pm) completing the 10-fold coordination sphere.

Cox et al^{195,196} have reported stability constant data for complexes of the anionic ionophores monensin and lasalocid with M^+ ($\text{M} = \text{Li}\text{--}\text{Cs}$) and M^{2+} ($\text{M} = \text{Mg}\text{--}\text{Ba}$) ions, measured in both protic and polar aprotic solvents. The monensin complexes are very stable.^{195,196} They exhibit the same stability sequences:



in all solvents except dmsO for which Ca^{2+} appears at a maximum. The lasalocid complexes are less stable.¹⁹⁵ They exhibit the same stability sequence as the monensin complexes for M^{2+} ions in all solvents (dmsO was not studied) but no consistent trends were discernable for M^{+} ions. Cox et al¹⁹⁶ have also reported kinetic data for the formation and dissociation of the monensin complexes of M^{+} ions in ethanol. Whereas the dissociation rate constants are sensitive to cation size, their variation:



reflecting the stability sequence noted above, the formation rate constants increase monotonically with increasing cation size.

Fuhrhop and Liman¹⁹⁷ have synthesised the monopyromellitic ester of monensin. Unlike monensin, which prefers a cyclic conformation, the ester adopts a stretched conformation owing to the presence of the negative charges at both ends of the molecule. Incorporation of the ester into monolayer membranes during sonication resulted in the formation of channels (Figure 5a) through which alkali metal ions could proceed. Incorporation into bilayer membranes, however, did not result in channel formation, the ester being too short to cross the bilayer lipid membrane (Figure 5b).¹⁹⁷

1.4.2 Crown complexes

In view of the continuing significance of alkali and alkaline earth metal complexes of crown and related macrocyclic ligands, this topic has again been divided into three subsections in which complexes formed by (i) 'classical' crown compounds and their substituted derivatives, (ii) lariat ethers, and (iii) novel macrocyclic ligands of unusual design are considered.

Holton et al¹⁹⁸ have measured the nmr spectra of the alkalide anions, Na^{-} and Rb^{-} , present in solutions of sodium and rubidium in 12C4. Cation resonances were not detected, presumably due to broadening of the absorption. These M-12C4 (M = Na, Rb) solutions are shown to represent a convenient stable source of high concentrations of alkalide anions. It is proposed that, in view of recent evidence for alkalide anions, the reducing power of metal-amine and metal-hexamethylphosphoramide solutions may be attributable to these anions rather than to the solvated

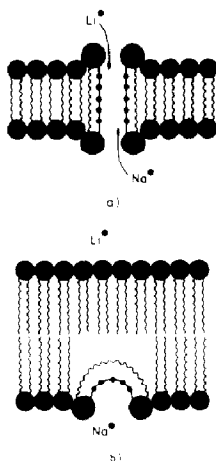
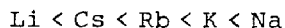


Figure 5. Models of (a) an ~2000pm monolayer membrane prepared by sonication of a symmetric α,ω -bifunctional amphiphile (●~~~~●) in the presence of the monopyromellitic ester of monensin (●~~~~●), and (b) an ~4000pm bilayer membrane similarly prepared by sonication of a monofunctional amphiphile (●~~~~) in the presence of the monensin derivative (reproduced by permission from J. Am. Chem. Soc., 106(1984)4643).

electron.¹⁹⁸

Solvent extraction of alkali metal salts (picrates,¹⁹⁹⁻²⁰² phenolates,²⁰¹ and o-nitrophenolates²⁰¹) by 15C5,^{199,200} 18C6,^{199,201} DB18C6^{201,202} and DCH18C6²⁰¹ has been studied in $\text{H}_2\text{O}-\text{CHCl}_3$,¹⁹⁹ $\text{H}_2\text{O}-\text{CH}_2\text{Cl}_2$,²⁰¹ $\text{H}_2\text{O}-\text{C}_6\text{H}_6$ ²⁰⁰ and $\text{H}_2\text{O}-\text{C}_6\text{H}_5\text{NO}_2$ ²⁰² solvent systems. The results for the $\text{H}_2\text{O}-\text{C}_6\text{H}_5\text{NO}_2$ system²⁰² were used to calculate stability constant data for 1:1 complexes of M^+ ($\text{M} = \text{Li}-\text{Cs}$) with DB18C6 in $\text{C}_6\text{H}_5\text{NO}_2$ saturated with water. The stability of the complexes increases in the sequence:



Stability constants have also been determined conductometrically for 1:1 complexes of M^+ ($\text{M} = \text{Na}-\text{Cs}$) with B18C6 in a variety of solvents (CH_3OH , CH_3CN , dmf and dmsO)²⁰³ and of M^+ ($\text{M} = \text{Na}, \text{K}$) with DB18C6 or DCH18C6 in aqueous isopropyl alcohol.²⁰⁴ In general, the selectivity of B18C6 for the alkali metals is governed primarily by the size-fit concept. It varies in the sequence:

Na < K > Rb > Cs

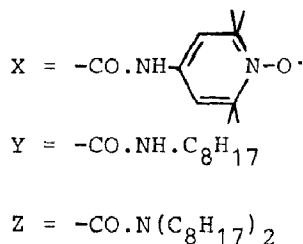
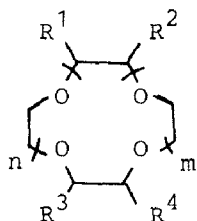
and is independent of solvent.²⁰³ A clearly defined K^+/Cs^+ selectivity is also observed for DB18C6 in aqueous isopropyl alcohol. The selectivity is dependent, however, on the dielectric constant of the solutions, decreasing with increasing alcohol content.²⁰⁴

A number of novel alkyl- and aryl-substituted crown ether derivatives have been synthesised and their complexing ability towards alkali and/or alkaline earth metal cations assessed;²⁰⁵⁻²¹⁰ they are listed in Table 11. The complexing abilities of alkyl and aryl substituted 12C4, 15C5 and 18C6 (31) have been assessed by consideration of the transport of alkali metal picrates ($M = Li, Na, K$) across a bulk $CHCl_3$ membrane.²⁰⁵ As the substituents render the crown ethers more lipophilic the complexes become more soluble in $CHCl_3$. For Na^+ and K^+ this leads to a reduction in transport; for Li^+ , however, transport is improved although the overall rate is much less than that for Na^+ or K^+ .²⁰⁵ The analogous dodecyl substituted 18C6 (32) has been coated onto insoluble supports through hydrophobic interactions.²⁰⁶ The resultant material provides a relatively cheap stationary phase for efficient chromatographic separation of alkali metal cations. Comparative studies have been undertaken with decyl substituted C221.²⁰⁶

The use of epr methods to study the effect of K^+ ion binding on the geometrical properties of syn- and antichiral dinitroxide substituted 18C6 (33,34) and of tetranitroxide substituted 18C6 (35) has been described.²⁰⁷

The complexation of M^+ ($M = Li-Cs$) and M^{2+} ($M = Mg-Ba$) ions by crown ether carboxylic acids (36-39) in aqueous methanol solution has been studied both spectroscopically (i.r. and nmr) and potentiometrically.²⁰⁸ Complexation is governed by electrostatic interactions between the cation and carboxylate residues; hence discrimination among cations on the basis of ionic radius is poor. The syn- and antichiral isomers (38,39) exhibit differing complexation behaviour, the antichiral isomer giving the stronger complexes.²⁰⁸ The extraction and transport of M^{2+} ($M = Mg-Ba$) from a basic to an acidic solution across an artificial membrane by crown ether carboxylic acids (38-44) has also been investigated.²⁰⁹ Monocarboxylate 15C5 and 18C6 carriers (40,41) achieve transport via 2:1 complexes, whereas

Table 11. Novel alkyl- and aryl-substituted crown ethers which have been assessed as complexing agents for alkali and/or alkaline earth metal cations.



Identifier	Description	Ref
(31)	$R^1 = -\text{CH}_3, -\text{C}_2\text{H}_5, -\text{C}_8\text{H}_{17}, -\text{C}_{10}\text{H}_{21}, -\text{C}_{14}\text{H}_{29}$ or $-\text{C}_6\text{H}_5$; $R^2 = R^3 = R^4 = -\text{H}$; $n+m = 2, 3$ or 4	205
(32)	$R^1 = -\text{C}_{12}\text{H}_{25}$; $R^2 = R^3 = R^4 = -\text{H}$; $n+m = 4$	206
(33)	$R^1 = R^4 = -\text{COOH}$; $R^2 = R^3 = X$; $m = n = 2$	207
(34)	$R^1 = R^3 = -\text{COOH}$; $R^2 = R^4 = X$; $m = n = 2$	207
(35)	$R^1 = R^2 = R^3 = R^4 = X$; $m = n = 2$	207
(36)	$R^1 = R^2 = -\text{COOH}$; $R^3 = R^4 = -\text{H}$ or $\text{C}_{10}\text{H}_{21}$; $m+n = 4$	208
(37)	$R^1 = -\text{COOH}$; $R^2 = Y$; $R^3 = R^4 = -\text{H}$; $m+n = 3$ or 4	208
(38)	$R^1 = R^4 = -\text{COOH}$; $R^2 = R^3 = Y$; $m = n = 2$	208, 209
(39)	$R^1 = R^3 = -\text{COOH}$; $R^2 = R^4 = Y$; $m = n = 2$	208, 209
(40)	$R^1 = -\text{COOH}$; $R^2 = -\text{CONHC}_{18}\text{H}_{37}$; $R^3 = R^4 = -\text{H}$; $n+m = 3$	209
(41)	$R^1 = -\text{COOH}$; $R^2 = -\text{CONHC}_{14}\text{H}_{29}$ or Z ; $R^3 = R^4 = -\text{H}$; $n+m = 4$	209
(42)	$R^1 = -\text{COOH}$; $R^2 = -\text{CONHC}_{14}\text{H}_{29}$ or Z ; $R^3 = R^4 = -\text{H}$; $n+m = 4$	209
(43)	$R^1 = R^4 = -\text{COOH}$; $R^2 = R^3 = Z$; $n = m = 2$	209
(44)	$R^1 = R^3 = -\text{COOH}$; $R^2 = R^4 = Z$; $n = m = 2$	209
(45)	$R^1 = R^2 = R^3 = R^4 = -\text{C}_6\text{H}_5$; $n = m = 2$ or 3	210
(46)	$R^1 = R^4 = -(\text{CH}_2)_4\text{C}_6\text{H}_5$; $R^2 = R^3 = -\text{H}$; $n = m = 2$	210

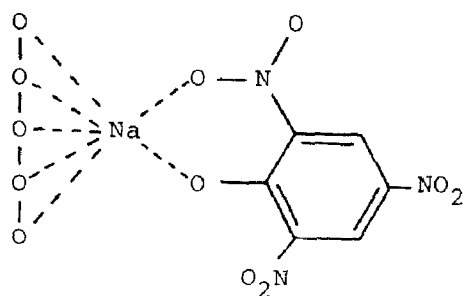
dicarboxylate 18C6 carriers (38,39,42-44) transport ions as 1:1 complexes.²⁰⁹

The ability of phenyl and 4-phenylbutyl substituted 18C6 and 24C8 (45,46) to complex M^+ ($M = \text{Li-Ba}$) and M^{2+} ($M = \text{Sr, Ba}$) ions has been assessed.²¹⁰ The 18C6 derivatives form the most stable complexes with K^+ , Sr^{2+} and Ba^{2+} ; the 24C8 derivatives prefer K^+ , Rb^+ and Ba^{2+} .²¹⁰

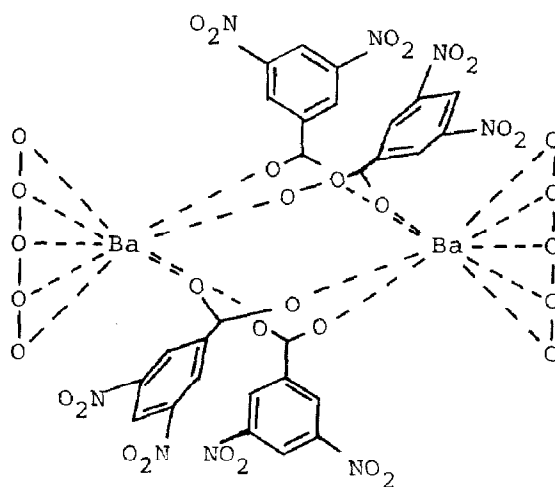
Single crystal XRD studies have been completed for $[(12\text{C}4)_2\text{Li}]^+\text{PPh}_2^-$,²¹¹ $[(12\text{C}4)_2\text{Li}]^+\text{AsPh}_2^-$, thf ,²¹¹ $[(12\text{C}4)\text{Li}]^+\text{N}(\text{SiMe}_3)_2^-$,²¹² $[(\text{B}15\text{C}5)\text{Na}]^+[\text{OC}_6\text{H}_2(\text{NO}_2)_3]^-$,²¹³ $[(\text{B}15\text{C}5)\text{Ba}]^{2+}[\text{O}_2\text{CC}_6\text{H}_3(\text{NO}_2)_2]^-$,²¹⁴ $[(18\text{C}6)\text{Cs}_2]^{2+}[\text{Al}_3\text{Me}_9\text{SO}_4]^{2-}$,²¹⁵ $[(\text{DB}30\text{C}10)\text{K}]^+\text{SCN}^-$,²¹⁶ $[(\text{DB}30\text{C}10)\text{K}]^+\text{SCN}^- \cdot \text{H}_2\text{O}$,²¹⁶ and $[(\text{DB}36\text{C}12)\text{Na}_2]^{2+}(\text{PF}_6^-)_2$.²¹⁷ Contrasting Li atom coordination geometries are observed in the structures of the 12C4 complexes. That in the diorganophosphides and arsenides²¹¹ is novel; it consists of a LiO_8 unit with approximate D_{4d} symmetry generated by two 12C4 polyether rings. The coordination number of 8, previously unknown for lithium, results in unusually long Li-O distances, (average $r(\text{Li} \dots \text{O}) = 235\text{pm}$). That in the bis(trimethylsilyl)amide²¹² is more conventional; it consists of a square pyramidal LiO_4N unit generated by the 12C4 polyether ring (basal positions) and the amide nitrogen atom (apical position). Disparate Li-O distances are observed; two are typical for this bond (209.4, 210.8pm) and two are abnormally long (233.2, 239.3pm). The Li-N bond distance (196.5pm) is similar to those reported for comparable compounds.

Considerably different cation geometries (47,48) are found for the two B15C5 complexes. The Na atom in the picrate (47)²¹³ is seven-coordinate; the NaO_7 unit is composed of all five heteroatoms of the B15C5 ring (240.0-250.1pm), as well as two oxygen atoms, the phenolate (235.0pm) and one from an ortho nitro moiety (251.0pm), of the anion. It is displaced by 90pm from the crown ether cavity in the direction of the picrate.²¹³ The Ba atom in the 3,5-dinitrobenzoate (48)²¹⁴ is nine-coordinate. Two symmetry related Ba atoms are linked by four anions through their carboxylate groups (263.9-269.4pm). The BaO_9 unit is completed by the five heteroatoms of the B15C5 ring (288.8-309.2pm), the Ba atom lying 187.7pm out of the crown ether cavity in the direction of the bridging anions.²¹⁴

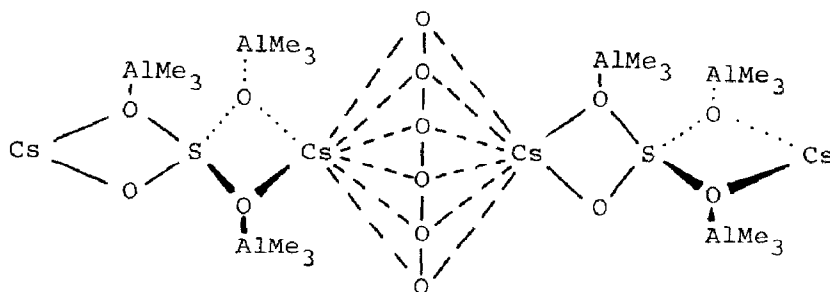
A novel coordination geometry has been observed for the cation



(47)



(48)

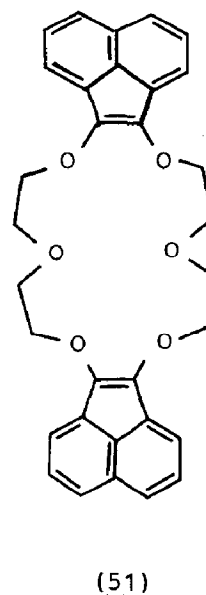
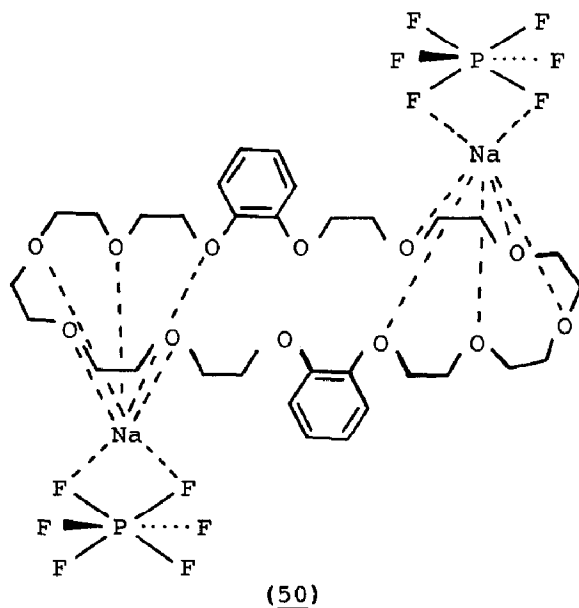


(49)

in the structure of $[(18C6)Cs_2]^{2+}[Al_3Me_9SO_4]^{2-}$ (49);²¹⁵ it contains a Cs...Cs contact (392pm) only slightly longer than the sum of the ionic radii (356pm). The two Cs atoms, which are crystallographically distinct, are located on either side of the 18C6 ring ($r(Cs(1)...O) = 333-359$, $r(Cs(2)...O) = 313-348pm$) and are bridged by the anion ($r(Cs(1)...O) = 308, 324$, $r(Cs(2)...O) = 316, 320pm$). Considerable asymmetry is observed in the disposition of the two Cs atoms relative to the crown ether

cavity, Cs(1) being much closer to the plane of oxygen atoms (179pm) than Cs(2) (237pm) (49).²¹⁵

Only marginal differences occur in the structures of the $[(DB30C10)K]^+$ cations in the anhydrous and monohydrated thiocyanate salts.²¹⁶ Whereas that in the anhydrous material is located on a two-fold axis, that in the monohydrate exhibits no symmetry. The K atom is coordinated by all ten heteroatoms of the DB30C10 molecule in both complexes; the water molecule does not enter the coordination sphere. The two structures show a different pattern of K-O distances. In the anhydrous salt they vary from 285.7 to 293.5pm with the mean distance to aromatic oxygen atoms being greater than that to aliphatic oxygen atoms, while in the monohydrate the range is 286.1-310.6pm with the mean distance to aromatic oxygen atoms being less than that to aliphatic oxygen atoms.²¹⁶



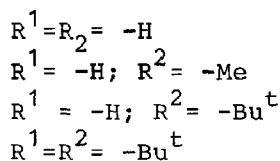
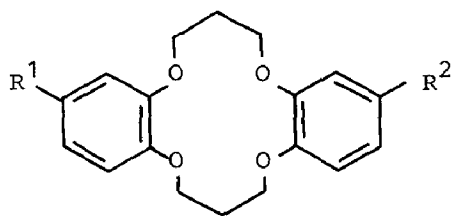
The DB36C12 macrocycle in the hexafluorophosphate salt (50)²¹⁷ contains a centre of symmetry and is twisted such that it possesses two complexing faces at opposite ends of the molecule each of which accommodates a Na atom bound to a PF_6^- anion. The Na atom is seven coordinate with bonding to five oxygen atoms of the DB36C12 molecule (241.9-254.4pm) and two fluorine atoms of the anion (242.4, 252.8pm). It is displaced 45pm from the mean plane of the five heteroatoms towards the phosphorus atom.²¹⁷

The crystal and molecular structures of two more complex crown ether derivatives have also been reported.^{218,219} The coordination geometry of the Na atom in (dibenzo-18-crown-6)bis-(tetrahydrofuran)sodium(meso-tetraphenylporphinato)ferrate, $[(\text{DB18C6})\cdot\text{Na}(\text{thf})_2]^+[\text{FeTPP}]^-$,²¹⁸ consists of a NaO_8 hexagonal bipyramidal unit; the six oxygen atoms of the DB18C6 molecule provide the equatorial plane (257.3-274.5pm) and the thf oxygen atoms occupy the apical positions (227.9, 229.9pm). The coordination geometry of the K atom in 2,3,11,12-(bis-1,2-acenaphtho)-18-crown-6 potassium thiocyanate, $[(51)\text{K}]^+\text{NCS}^-$,²¹⁹ consists of a KO_6N hexagonal pyramidal unit. The K atom is located in the centre of and bonded to the six heteroatoms of the macrocycle (270.6-299.4pm) with a N-bonded thiocyanate anion on one side only (272.7pm).²¹⁹

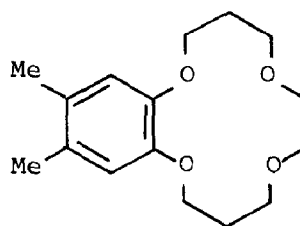
Several papers have been published in which the complexation of alkali metal cations by ring contracted²²⁰ and ring expanded²²¹⁻²²⁴ crown ethers is discussed. Ring contracted 14C5, 17C6 and their sila-analogues showed a drastic decrease in cation binding ability when compared with the corresponding crown ethers;²²⁰ this decrease is attributed not to the diminished cavity size but to the disordered conformation induced by ring contraction.

In an attempt to obtain highly selective ionophores for Li^+ ions, ring expanded 13C4, 14C4, 15C4 and 16C4 derivatives bearing a long aliphatic chain have been synthesised.²²¹ The Li^+ selectivities of these materials were in accord with the size-fit concept, the 14C4 and 15C4 derivatives being the most effective. Incorporation of a methyl group geminal to the aliphatic chain prevents formation of sandwich-type 2:1 complexes with alkali metals other than lithium and hence improves Li^+ selectivity.²²¹

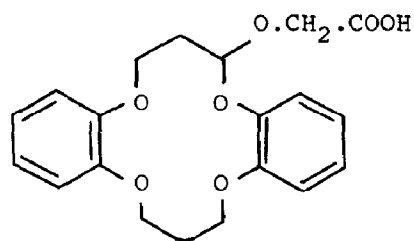
N.m.r. (^7Li) spectroscopic studies²²² of the complexation of Li^+ by ring expanded DB14C4 and its alkyl substituted derivatives (52)



(52)

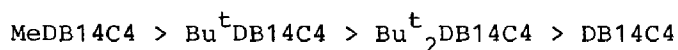


(53)



(54)

provide evidence for the formation of 1:1 complexes; no clear cut evidence for the existence of 2:1 complexes was obtained. Complex formation was found to be solvent dependent, the stability of the complexes varying with the coordinating power of the solvent. The presence of substituent groups on the benzene rings of the crown ethers also influences the stability of the complexes which decreases in the sequence:



Structural analysis of the LiNO_3 complexes of ring expanded B14C4²²³ and its chiral dimethyl derivative (53)²²⁴ has been effected using the results of single crystal XRD studies. The coordination geometry of the Li atom is very similar in the two complexes; although based on a LiO_6 unit it is best perceived as square pyramidal with a bidentate nitrate group occupying the apical position and the four heteroatoms of the crown ether located in the basal plane. Pertinent molecular dimensions for the two complexes are summarised in Table 12.

The crystal and molecular structures of the hydrated lithium salt of the oxyacetic acid derivative of DB14C4 (54) have also been elucidated.²²⁵ The Li atom is coordinated by the four

Table 12. Pertinent molecular dimensions in $[B14C4Li]^+NO_3^-$ ²²³
and in $[Me_2B14C4Li]^+NO_3^-$. ²²⁴

Complex	Average $r(Li...O)/pm$ Crown ether	$r(Li...O)/pm$ Nitrate	$\hat{O}NO/^\circ$	Displacement of Li^+ from plane of heteroatoms/pm
$[B14C4Li]^+NO_3^-$	205.0	207.2, 230.0	57.6	24
$[Me_2B14C4Li]^+NO_3^-$	206.6	207.4, 228.6	51.7	6

heteroatoms of the coronand proper (203.8–207.7pm) and an axial water molecule (191pm) in a near square pyramidal geometry. The water molecule forms a link between the Li atom and the carboxylate moiety which does not directly coordinate the cation. ²²⁵

1.4.3 Complexes of Lariat Ethers

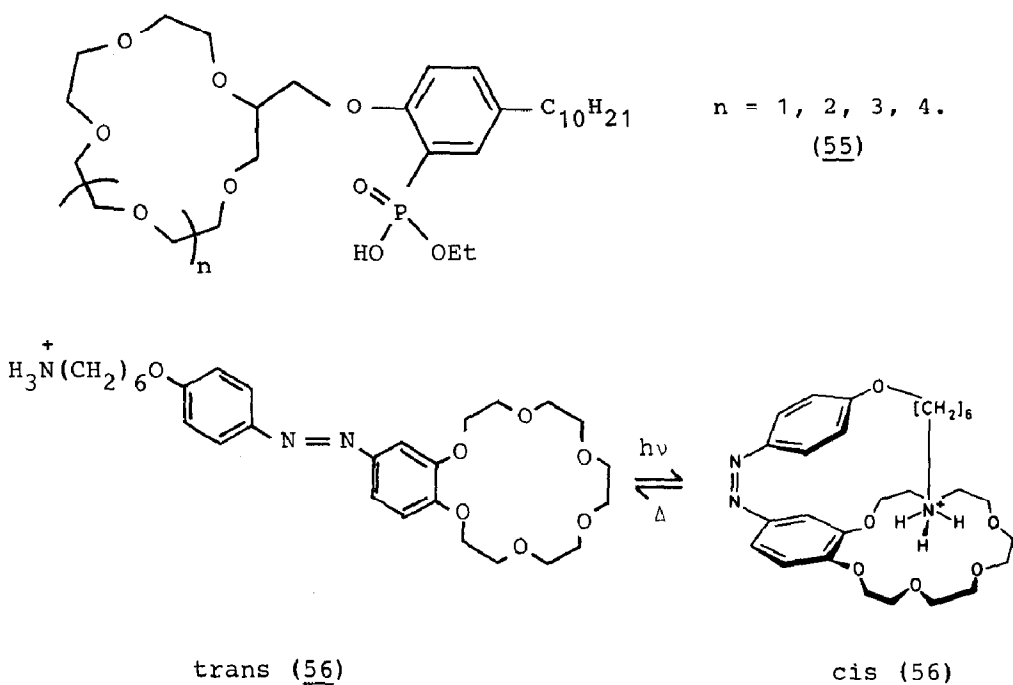
Novel lariat ethers based on crown compounds and their monoaza- and diaza- derivatives have been synthesised and the specificity of their complexing ability for alkali and/or alkaline earth metal cations assessed. The dynamics of the complexation of M^+ ($M = Na, K, Ca$) by various lariat ethers (2-substituted 15C5, N-substituted monoaza 15C5 and N-substituted monoaza 18C6) have been elucidated by ^{13}C nmr spectroscopic techniques. ²²⁶

Comparison of the complexing abilities of lariat ethers bearing alkyl and polyether side chains (2-substituted-12C4, -15C5, -18C6, N-substituted monoaza-12C4, -15C5 and -18C6) for M^+ ($M = Li-Cs$) has been effected; ²²⁷ the incorporation of oxygen atoms in the side chains did not significantly improve the complexing abilities of the lariat ethers towards Na^+ and K^+ .

The series of 2-substituted crown ethers (55) have been prepared. ²²⁸ They have been tested in competitive alkali metal solvent extraction experiments ($M = Li-Cs$) and have been shown to be capable of anion independent metal ion transport from acidic and neutral aqueous solutions into organic media. Whereas the 15C5 and 18C6 derivatives were fairly selective for Na^+ and K^+ , respectively, the 21C7 and 24C8 derivatives were less discriminating, the extracts containing at least 10% of each

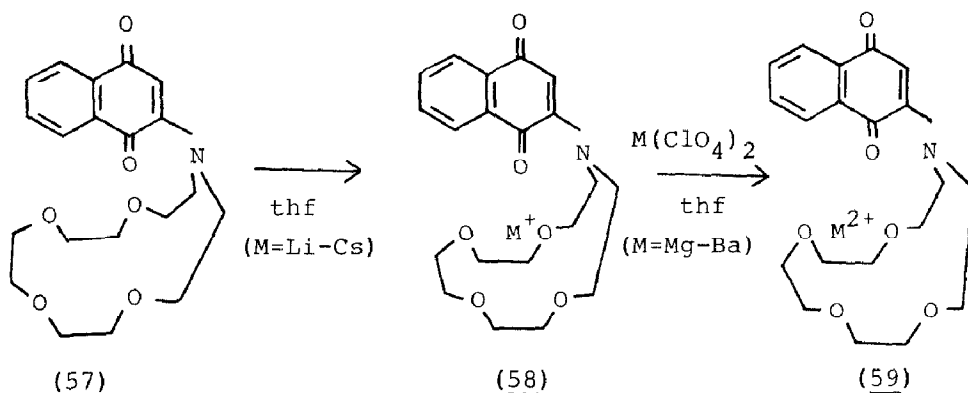
alkali metal.²²⁸

A novel photoresponsive crown ether with an ammonium group tail (56) has been synthesised.²²⁹ Its photoresponsive ionophoric properties have been evaluated through solvent extraction of alkali metal toluene-p-sulphonates ($M = K-Cs$). Trans (56) clearly exhibits a higher affinity for K^+ than for Rb^+ or Cs^+ .

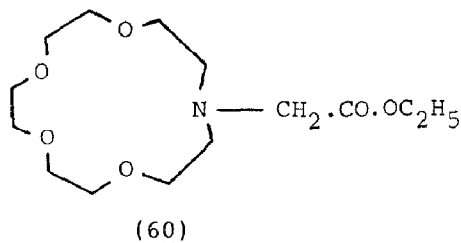


Cis (56), however, is capable of ejecting K^+ , but not Rb^+ or Cs^+ from the crown ether ring. Presumably, the K^+ ion nests in the B18C6 cavity while the larger Rb^+ and Cs^+ ions perch on its edge. Thus interaction with Rb^+ and Cs^+ would be less affected by an ammonium group bound (probably) to the opposite side of the crown ether ring.²²⁹

Reduction of 1,4-naphthoquinone N-substituted monoaza 15C5 (57) by an alkali metal in thf at 298K generates the azacoronand-naphthoquinone radical anion which forms a cage into which the cation can be inserted (58).²³⁰ Reaction of this product with alkaline earth metal perchlorates yields the corresponding alkaline earth metal complex (59). Characterisation of all products was achieved using esr/endor spectroscopy.²³⁰



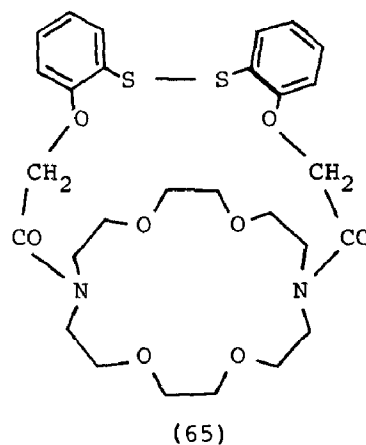
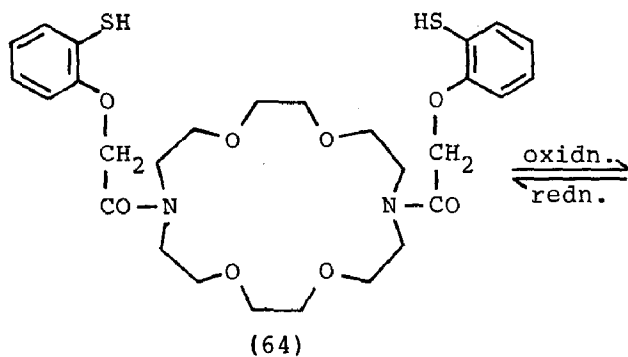
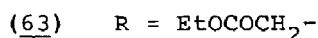
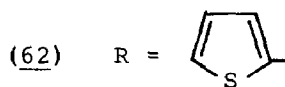
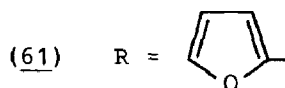
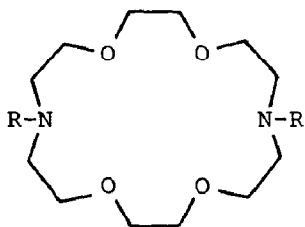
The molecular structure of the complex formed between NaBr and the N-substituted monoaza-15C5 (60) has been determined.²³¹ It is the first structurally characterised example of a lariat ether in which an ester carbonyl group interacts directly with a ring bound cation. Thus, the Na atom is coordinated by the five heteroatoms of the monoaza 15C5 coronand ($r(\text{Na} \dots \text{O}) = 248.3\text{--}251.5$



pm; $r(\text{Na} \dots \text{N}) = 257.8\text{pm}$), the carbonyl oxygen atom of the lariat side chain (245.1pm) and the bromide anion (311.6pm) in a pentagonal bipyramidal geometry.²³¹

N,N'-disubstituted diaza 18C6 coronands, having two functionalised side chains for cation binding, provide new and characteristic transport selectivities. Tsukube²³² has shown that the furan derivative (61) exhibited clearly enhanced complexing and transporting abilities for the K^+ ion when compared with those of simple diazacrown ethers. Replacement of furan with thiophene, however, resulted in a carrier (62) which exhibited decreased transport efficiencies for K^+ and Ba^{2+} ions.²³² Gokel et al,²³³ in a separate study, have shown that

utilisation of polar yet uncharged donor groups such as carbethoxymethyl gives a "bibracchial" lariat ether (63) capable of selectivity of Ca^{2+} over Na^+ or K^+ .

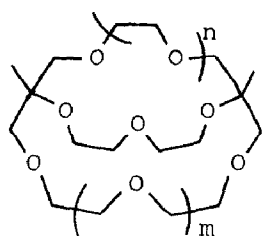


Synthesis of a disubstituted N,N'-diazacycloocta-1,4-diene bearing redox functional thiol groups has been achieved;²³⁴ redox-responsive interconversion between the "bibracchial" lariat ether (64) and the cryptand (65) readily occurs. For Na^+ ions, (64) and (65) showed a similar affinity. For M^+ ($\text{M} = \text{K}-\text{Cs}$), however, (65) was a more effective complexing agent presumably because of coordination of the complexed metal ions by the bridging oxygen atoms.²³⁴

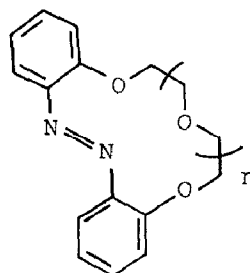
1.4.4 Complexes of Macrocyclic Polyethers of Novel Design

Japanese chemists are interested in the design, synthesis and coordination properties of novel macrocyclic polyethers to such an extent that papers submitted by six independent groups²³⁵⁻²⁴⁰ have been abstracted for this subsection. The macrocyclic polyether

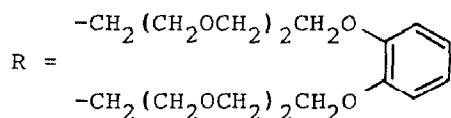
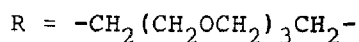
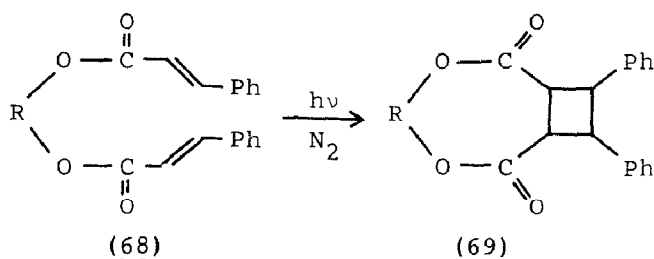
(66) with novel ring structures complex with Na^+ and K^+ in accordance with the size-fit concept.²³⁵ Crown ethers containing an azo-linkage (67) are somewhat ineffective as ligands for M^+ ($\text{M} = \text{Li-Cs}$) and M^{2+} ($\text{M} = \text{Mg-Ba}$) ions;²³⁶ it is concluded that incorporation of the azo moiety into the macrocycle does not lead to stabilisation of complexes. Acyclic polyethers containing two cinnamoyl moieties (68) and their cyclised derivatives (69) exhibit but little difference in their selectivity and complexing ability for M^+ ($\text{M} = \text{Na, K}$);²³⁷ it is suggested that the cyclobutane structure distorts the macrocyclic polyether to such an extent that its presence negates the anticipated increase in complexing ability on cyclisation. The bis(polyetheramide) derivative (70) is more selective than the corresponding monocyclic analogue (71) for the Ca^{2+} ion.²³⁸ Furthermore, the potentiometric selectivity for Ca^{2+} relative to

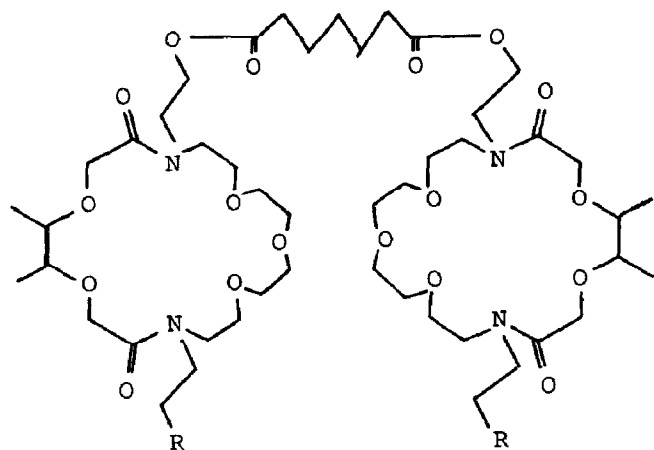


$n=2, m=1$
 $n=1, m=1$
 $n=1, m=0$
 (66)

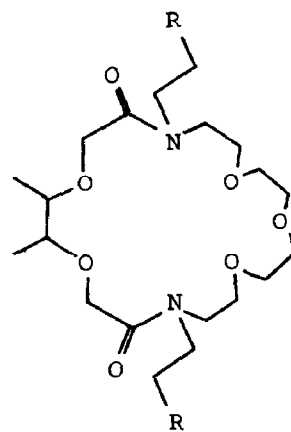


$n=1, 2, 3 \text{ or } 4$
 (67)

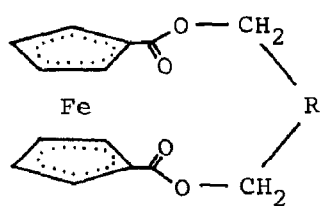
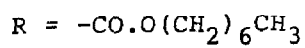




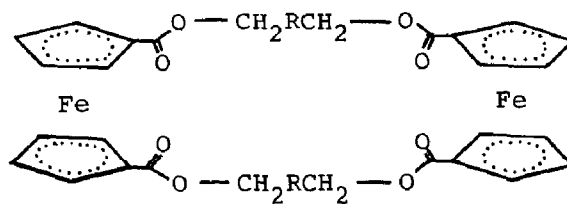
(70)



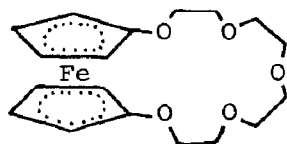
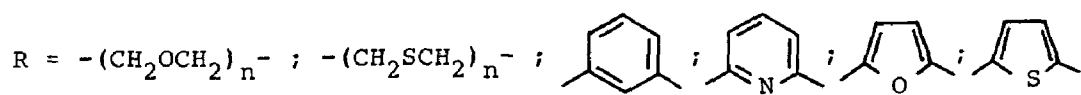
(71)



(72)



(73)



(74)

Mg^{2+} is improved by more than an order of magnitude.

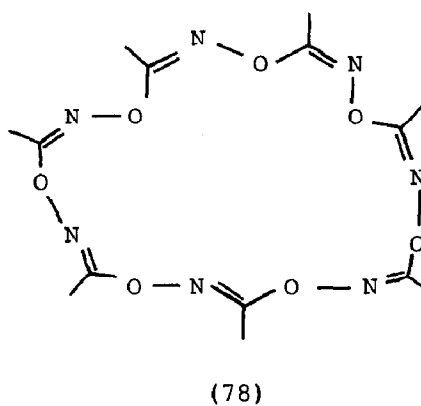
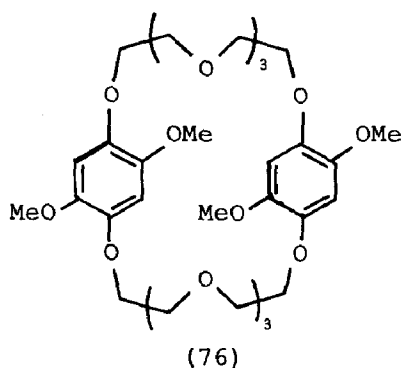
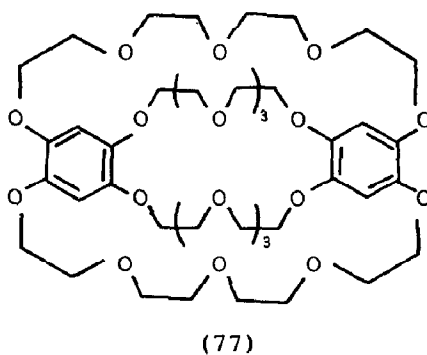
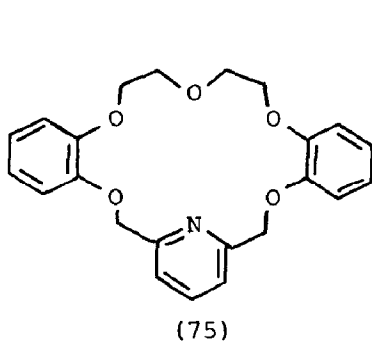
A number of novel crown ethers containing a ferrocene unit as an integral part of the ring have also been reported.^{239,240} The complexing ability of some of these ferrocenophanes (72,73) towards, inter alia, M^+ ($\text{M} = \text{Li-Cs}$) and M^{2+} ($\text{M} = \text{Mg-Ba}$) has been examined;²³⁹ in general they exhibit low complexing power and little selectivity for these ions. Alkali metal thiocyanate complexes with polyoxa[n]-ferrocenophanes (e.g. 74) have been studied²⁴⁰ using multinuclear (^1H and ^{13}C) nmr spectroscopic methods; chemical shift data are rationalised in terms of an electronic field effect and a conformational change on metal complexation. The crystal and molecular structures of $[(74)\text{Na}]^+\text{NCS}^-$ have also been determined in a complementary single crystal XRD study.²⁴⁰ The Na atom is coordinated by the five heteroatoms of the cyclic moiety (239.6-263.1pm) and the nitrogen atom of an anion (254.1pm) in a pentagonalpyramidal geometry. The Fe-Na distance (412.9pm) is too long relative to the sum of the van der Waals radii for the iron atom to take part in complex formation although the possibility of a very weak Fe...Na interaction cannot be excluded.²⁴⁰

Four other papers, all of which describe the results of structural studies,²⁴¹⁻²⁴⁴ have been abstracted for this section; as for the 1983 review the majority are submitted by either Weber²⁴¹ or Owen.^{242,243} Weber has determined the crystal structure of $[(75)\text{Na}]^+\text{NCS}^-$,²⁴¹ Owen those of $[(76)\text{Na}_2]^{2+}(\text{SCN})_2^-, 2\text{H}_2\text{O}$ ²⁴² and $[(77)\text{K}_2]^{2+}(\text{OC}_6\text{H}_2(\text{NO}_2)_3)_2^-$ ²⁴³ and Casini et al that of $[(78)\text{K}]^+\text{SCN}^-$.²⁴⁴

The crystal structure of $[(75)\text{Na}]^+\text{NCS}^-$ ²⁴¹ contains two crystallographically distinct complexes. The Na atom is located close to the centre of the macrocycle in both complexes; it is coordinated by all six heteroatoms of the ring ($r(\text{Na}(1)\dots\text{O}) = 263.1-277.2$; $r(\text{Na}(1)\dots\text{N}) = 260.1$; $r(\text{Na}(2)\dots\text{O}) = 259.6-269.6$; $r(\text{Na}(2)\dots\text{N}) = 250.1\text{pm}$) and the nitrogen atom of the NCS anion ($r(\text{Na}(1)\dots\text{N}) = 233.5$; $r(\text{Na}(2)\dots\text{N}) = 238.2\text{pm}$), the NaO_5N_2 coordination geometries being essentially hexagonal pyramidal.²⁴¹

In $[(76)\text{Na}_2]^{2+}(\text{SCN})_2^-, 2\text{H}_2\text{O}$,²⁴² two Na atoms, separated by 816.9 pm are coordinated by each ligand molecule. Na(1) is surrounded by the five heteroatoms of one polyether chain (there are four normal Na-O distances (241.5-250.4pm) and one longer interaction

(298.8pm)), an adjacent methoxy oxygen atom (249.5pm) and the nitrogen atom of an NCS anion; the NaO_6N coordination geometry is



approximately pentagonal bipyramidal. $\text{Na}(2)$ forms part of an eight coordinate NaO_8 unit, of no particular geometry, generated by the five heteroatoms of the other polyether chain (245.0-266.1 pm), two methoxy oxygen atoms (248.4, 259.2) and a water molecule (237.6pm). Neither the second anion nor the second water molecule is coordinated to a Na atom.²⁴² Two metal atoms are also coordinated by a single ligand molecule in the structure of $[(77)\text{K}_2]^{2+}(\text{OC}_6\text{H}_2(\text{NO}_2)_3)_2^-$; ²⁴³ two K atoms, related by a crystallographic centre of symmetry are each encapsulated by ten oxygen atoms of the ligand (282.2-319.5pm) to the exclusion of the picrate anions.²⁴³

The K atom in the KNCS complex of acetonitrile oxide cyclic heptamer (78)²⁴⁴ is located in a heptagonal bipyramidal KO_7NS unit generated by the seven oxygen atoms of the macrocycle (average $r(\text{K}\dots\text{O}) = 282\text{pm}$), the nitrogen atom of the anion (287pm) and, to a weaker extent, the sulphur atom of a symmetry related anion (323pm); it is displaced by 10pm from the plane of the seven oxygen atoms in the direction of the N-bonded NCS anion.²⁴⁴

1.4.5 Cryptates and Related Complexes

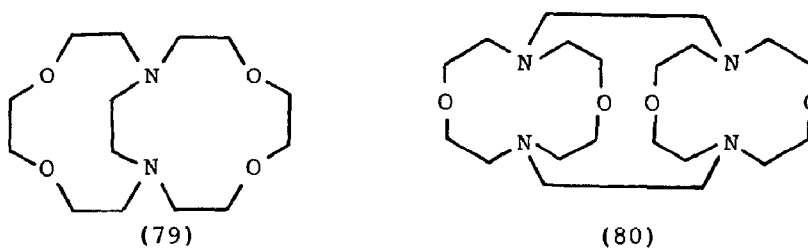
Thermodynamic^{245,246} and kinetic^{246,247} data for the complexation of alkali and/or alkaline earth metal cations by diverse cryptates have been reported. Enthalpies of complexation for M^+ ($\text{M} = \text{Na}-\text{Cs}$) with C222 in dmf and dmsO and for Li^+ with C222 in methanol have been determined²⁴⁵ using a calorimetric technique; corresponding entropy data were derived from known free energy data.²⁴⁵ The stability constants of complexes of M^{2+} ($\text{M} = \text{Ca}-\text{Ba}$) with C211, C221, C222, $\text{C2}_{\text{B}}22$ and $\text{C2}_{\text{B}}2_{\text{B}}2$ have also been measured²⁴⁶ in dmf, dmsO, methanol and water. The formation and dissociation rate constants of M^{2+} ($\text{M} = \text{Ca}-\text{Ba}$) complexes of C222, $\text{C2}_{\text{B}}22$ and $\text{C2}_{\text{B}}2_{\text{B}}2$ have been determined independently by two groups of authors;^{246,247} in one study²⁴⁶ the results are compared with analogous data for complexes containing C211 and C221. The introduction of the benzene rings in the sequence $\text{C222} - \text{C2}_{\text{B}}22 - \text{C2}_{\text{B}}2_{\text{B}}2$ causes (i) a progressive decrease in the formation rate constants for all three cations, (ii) no change in the dissociation rate constants for Ca^{2+} , and (iii) a marked increase in the dissociation rate constants for Sr^{2+} and Ba^{2+} .²⁴⁷

Reaction of KGeSb with C222 in ethylenediamine(en) produces a dark red solution from which crystals of both $[\text{C222K}]_2^+\text{Sb}_4^{2-}$ and $[\text{C222K}]_3^+\text{Sb}_7^{3-}\cdot 2\text{en}$ have been isolated.²⁴⁸ Whereas the structure of the former complex is centrosymmetric, that of the latter complex contains three crystallographically independent $[\text{C222K}]^+$ cations. All of the cations have normal configurations with the K atom centrally located along the $\text{N}\dots\text{N}$ axis. Details of the K atom coordination spheres are only available as supplementary material.²⁴⁸

Coloured 1:1 complexes of diaza-18C6 with potassium 4-nitrophenolate and with potassium 2,4-dinitrophenolate and of diaza-15C5 with sodium and potassium 4-nitrophenolate have been isolated

and characterised using chemical analytical and spectroscopic (i.r.; u.v.-visible; n.m.r.) techniques;²⁴⁹ no complexes of diaza-18C6 with sodium salts could be isolated.

Groth et al have isolated and structurally characterised alkali metal thiocyanate complexes of (79) ($M = \text{Li, Na, K}$)²⁵⁰ and of (80) ($M = \text{K}$);²⁵¹ with the exception of the lithium complex which is a hemihydrate, the complexes are anhydrous. Significant features of the structures of the MNCS ($M = \text{Li-K}$) complexes of (79)²⁵⁰ are shown in Figure 6; details are only available as supplementary material. The structures are similar. As the size of the alkali metal atom increases it moves from a location within the trigonal bipyramidal N_2O_4 cage of the ligand (for Li^+), through a point close to the centre of the O_4 square plane (for Na^+) to a



position above the O_4 square plane (for K^+). The gap in the coordination spheres of Na^+ and K^+ is filled by the nitrogen atom of the NCS^- anion. Only the Na atom ($\text{CN} = 7$) attains its optimum coordination number, the K atom ($\text{CN} = 7$) being coordinatively unsaturated and the Li atom ($\text{CN} = 6$) having too many neighbours. As a result the ligand clearly has the least conformational strain in the sodium complex.²⁵⁰ The structure of the KNCS complex of (80)²⁵¹ is such that the K atom is located inside a cavity generated by all eight heteroatoms ($r(\text{K} \dots \text{O}) = 258\text{--}284$; $r(\text{K} \dots \text{N}) = 274\text{--}281\text{pm}$) in a pseudo cubic arrangement.

1.4.6 Complexes of Macrocyclic Polyimine and Related Ligands

Russian authors have considered the complexation of alkali metal 2,4-dinitrophenolates ($M = \text{Li-K, Cs}$)²⁵² and of alkaline earth metal iodides ($M = \text{Mg, Ca}$)²⁵³ by the tripodand triaza-[9]-annulene (81). Solution (thf-CHCl_3 ; 4/1) studies²⁵² of the alkali metal complexes using conductometric methods indicate that their stabilities decrease with increasing cation size. Formation constant studies²⁵³ of the alkaline earth metal complexes in organic

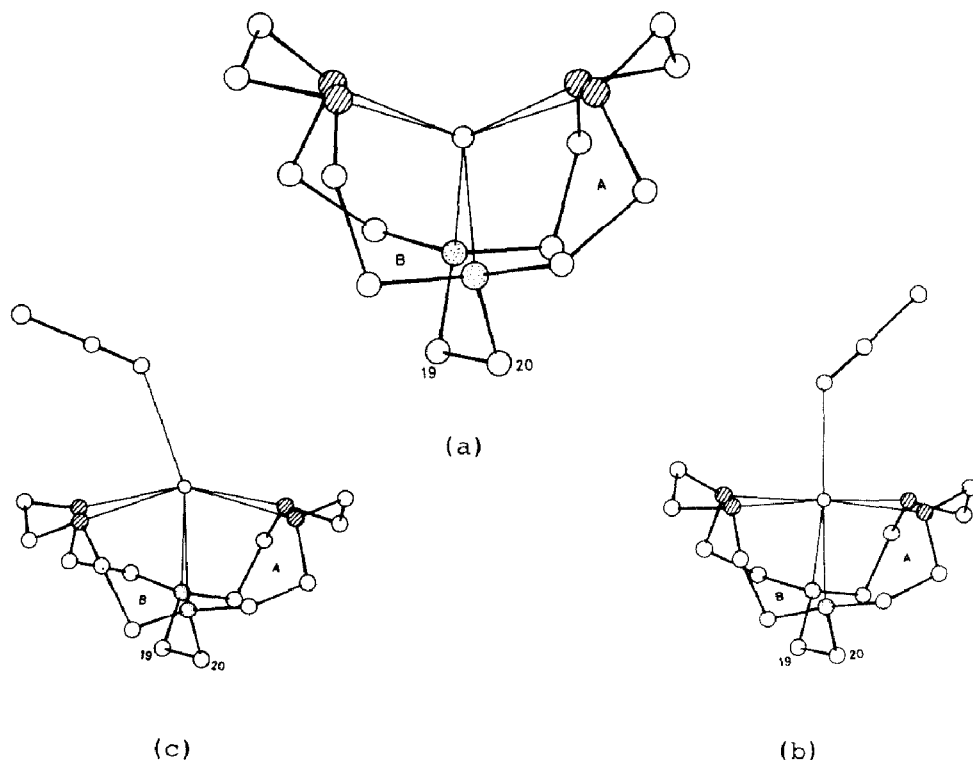
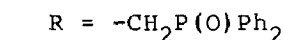
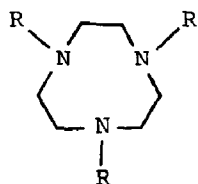


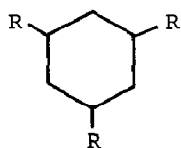
Figure 6. The molecular geometries around the alkali metal atom in (a) $[(79)\text{Li}]^+\text{SCN}^-, \frac{1}{2}\text{H}_2\text{O}$, (b) $[(79)\text{Na}]^+\text{SCN}^-$, and (c) $[(79)\text{K}]^+\text{SCN}^-$ (reproduced by permission from J. Chem. Soc., Chem. Commun., (1984)1502).

solvents suggest that complex formation involves interaction with not only the phosphoryl groups but also the nitrogen atoms of the macrocycle. Two complexes, $[(81)_2\text{Mg}_3]^{6+}6\text{I}^-, 3\text{H}_2\text{O}$ and $[(81)\text{Ca}]^{2+}2\text{I}^-, 3\text{H}_2\text{O}$ have been isolated from these solutions.²⁵³ In both investigations, the results were compared with analogous data for the ligands, $\text{Ph}_2\text{P}(\text{O})\text{CH}_2\text{P}(\text{O})\text{Ph}_2$, $\text{Ph}_2\text{P}(\text{O})\text{CH}_2\text{NH}(\text{CH}_2)_2.\text{NH}-\text{CH}_2\text{P}(\text{O})\text{Ph}_2$ and (82).^{252,253}

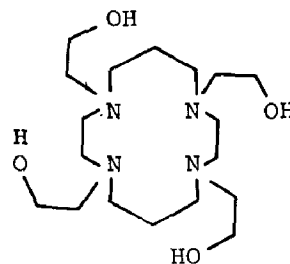
Complex formation between Na^+ and the tetrapodand tetraaza-[14]-annulene (83) has been monitored in aqueous solution by ^{23}Na nmr using Dy^{3+} as a shift reagent.²⁵⁴ The spectra are consistent with the formation of a complex in which three of the arms of the ligand coordinate a Na atom located in the macrocyclic cavity and the fourth arm interacts with Dy^{3+} .²⁵⁴ An analogous Na atom coordination geometry has been observed previously in the solid phase.²⁵⁵



(81)

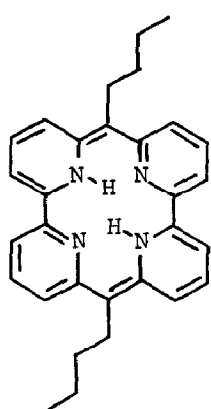


(82)

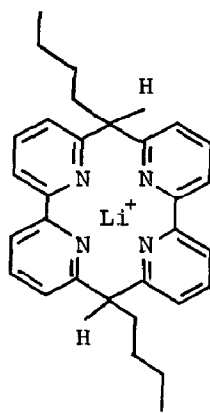
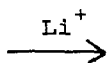


(83)

A tetraaza-[1,4]-annulene (84) that selectively binds Li^+ with a concomitant colour change has been synthesised.²⁵⁶ Addition of solid $LiCl$ to the red solution of (84) in CH_2Cl_2 results in its decolourisation. Incorporation of Li^+ into the cavity of the macrocycle, induces proton transfer from nitrogen to bridging carbon and hence reduction of the ligand's conjugated π -system (85). Neither sodium, potassium nor alkaline earth metal salts are capable of effecting this spectral change.²⁵⁶



(84)



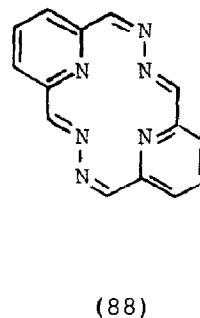
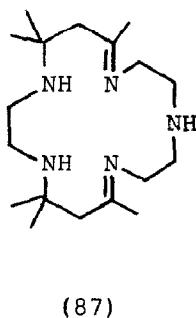
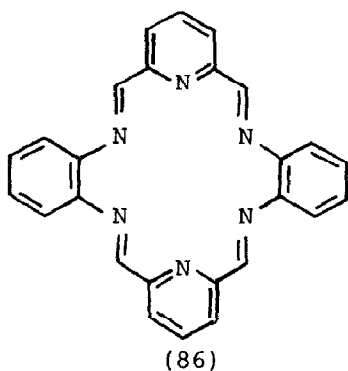
(85)

1H -nmr studies of the $KClO_4$ complex of the hexaaza-[18]-annulene (86) indicate that the stability of $[(86)K]^+ClO_4^-$ is an order of magnitude greater than that of the corresponding 18C6 complex in the same solvent (dmsO).²⁵⁷

Novel complexes, $[(87)Mg]^{2+}(ClO_4)_2^-, 2H_2O$ and $[(88)Mg]^{2+}(ClO_4)_2^-, H_2O$ have been isolated and identified by field desorption mass spectroscopic methods.²⁵⁸ It is inferred that the Mg atom is located in cavities formed by just four of the

nitrogen atoms of the pentaaza-[17]- and hexaaza-[14]-annulenes; incorporation of the water molecules into the Mg coordination sphere is also thought to be possible.

The crystal and molecular structures of the magnesium tetraphenylporphyrin complexes, $\text{MgTPP}(1\text{-methylimidazole})_2$, $\text{MgTPP}(4\text{-picoline})_2$ and $\text{MgTPP}(\text{piperidine})_2$ have been reported.²⁵⁹ All three complexes exhibit distorted octahedral Mg coordination spheres with the four nitrogen atoms of the tetraaza-[16]-annulene in the equatorial positions and the nitrogeneous bases in



the axial positions. Compared with the Mg-N equatorial bond distances, which fall in a very limited range (206.9-208.2pm), the Mg-N axial bond distances are long, varying from 229.7pm (for 1-methylimidazole) through 238.6pm (for 4-picoline) to 241.9pm (for piperidine).²⁵⁷

1.4.7 Salts of Carboxylic and Thiocarboxylic Acids.

A significant number of papers, have been abstracted, mainly from Acta Crystallographica, for this subsection. They are concerned exclusively with structural chemistry, four lithium,²⁶⁰⁻²⁶³ seven sodium,²⁶⁴⁻²⁶⁹ four potassium^{266,270-272} and a single caesium salt²⁷³ being considered. The salts studied are listed in Table 13 which also incorporates pertinent features of the cations' coordination spheres. Whereas the coordination number of Li^+ is exclusively 4, for Na^+ it is either 5 or 6, for K^+ it ranges from 6 to 8 and for the single Cs^+ example it is 8. Although in anhydrous salts the cations are normally coordinated by either the carboxylate oxygen atoms or the thiocarboxylate sulphur atoms, as appropriate, a preference for coordination by water molecules is shown in the hydrated

Table 13. Pertinent features of the cation coordination spheres in a number of salts of carboxylic and thiocarboxylic acids.

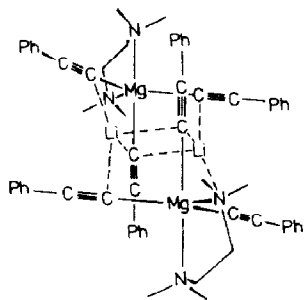
Structural Formula	Cation Unit	Coordination Geometry	Interatomic Distances/pm				Ref.
			Anion		Water		
			M...O	M...X	M...O	M...O	
$[\text{HO}_2\text{C}(\text{CH}_2)_4\text{CO}_2]\text{Li}$	LiO_4	dist. T_d	189.6-197.7	-	-	-	260
$[(\text{CH}_3)_2\text{NCS}_2]\text{Li}_4\text{H}_2\text{O}$	LiO_4	dist. T_d	-	-	190.7-195.4	-	261
$[(\text{C}_2\text{H}_5)_2\text{NCS}_2]\text{Li}_4\text{H}_2\text{O}$	LiO_4	dist. T_d	-	-	189.5-204.9	-	262
$[(\text{C}_3\text{H}_7)_2\text{NCS}_2]\text{Li}_4\text{H}_2\text{O}$	LiO_4	dist. T_d	-	-	187.0-203.1	-	263
$[\text{HO}_2\text{C.CO}_2]\text{Na.H}_2\text{O}$	NaO_6	irregular	235.2-244.3	-	230.7, 238.3	-	264
$[\text{HO}_2\text{C.CH=CH.CO}_2]\text{Na.3H}_2\text{O}$	NaO_6	dist. O_h	237.4-244.6	-	237.6	-	265
$[\text{HO}_2\text{C}(\text{CH}_2)_2\text{CO.CO}_2]\text{Na}$	NaO_6	dist. O_h	235.5-260.5	-	-	-	266
$[\text{HOCH}_2(\text{CHOH})_4\text{CO}_2]\text{Na}$	NaO_6	dist. O_h	234.0-254.0	-	-	-	267
$[\text{HN}(\text{CH}_2\text{CO}_2)_3]\text{Na}_2$	NaO_6	O_h	230.4-243.2	-	-	-	268
	NaO_6	O_h	241.6-251.2	-	-	-	
$[\text{N}(\text{CH}_2\text{CO}_2)_3]\text{NaZn.H}_2\text{O}$	NaO_5	irregular	224.2-241.0	-	231.0	-	268
$[\text{S}_2\text{C.N}(\text{NCS}_2)_2]\text{Na}_2.6\text{H}_2\text{O}$	NaO_4S	dist. O_h	-	299.0 (X=S)	231.6-245.0	-	269
$[\text{PhSCH}_2\text{CO}_2]\text{K.PhSCH}_2\text{CO}_2\text{H}$	KO_7	irregular	272.9-303.4	-	-	-	270
$[\text{HO}_2\text{C}(\text{CH}_2)_2\text{CO.CO}_2]\text{K}$	KO_8	irregular	274.7-301.3	-	-	-	266
$[\text{SC}(\text{CH}_3)_2\text{CH}(\text{NH}_2)\text{CO}_2]\text{K}_2.3\text{H}_2\text{O}$	KO_5N	dist. O_h	268.4-293.3	296.5 (X=N)	268.3, 282.7	-	271
	KO_6	dist. D_{3h}	274.6-288.7	-	287.6, 291.7	-	
$[\text{S}_2\text{C.NH.NH.CS}_2]\text{K}_2.4\text{CH}_3\text{OH}$	KO_4S_4	D_{4d}	-	341.2, 342.6 (X=S)	276.6, 292.0 (methanol)	-	272
$[\text{CH}(\text{CO}_2)\{\text{CH}(\text{CO}_2\text{H})\}_3\text{O}]\text{Cs}$	CsO_8	irregular	300.9-334.2	-	-	-	273

materials.

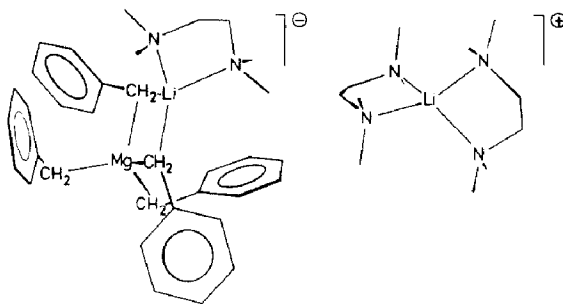
1.4.8 Heterobimetallic Complexes containing Alkali Metals

A significant number of heterobimetallic complexes containing lithium²⁷⁴⁻²⁷⁸ and sodium^{279,280} have been isolated. In every instance they have been structurally characterised using single crystal XRD methods.

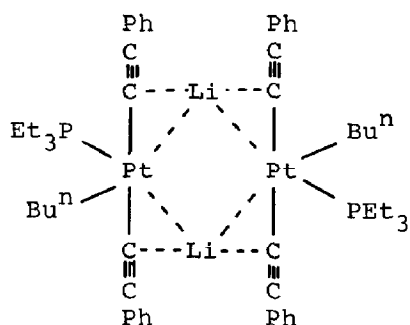
The Li-Mg complexes, $[\text{Li}_2\text{Mg}_2(\text{tmeda})_2(\text{PhC}\equiv\text{C})_6]$ (89) and $[\text{Li}(\text{tmeda})_2]^+[\text{LiMg}(\text{tmeda})(\text{C}_6\text{H}_5\text{CH}_2)_4]^-$ (90) have been synthesised²⁷⁴ by reaction of $\text{PhC}\equiv\text{CLi}$ with $(\text{PhC}\equiv\text{C})_2\text{Mg}$ in the presence of tmeda and by reaction (273K) of EtLi with Et_2Mg and toluene in hexane solution containing tmeda. The asymmetric unit of (89) is centrosymmetric.²⁷⁴ The Li atom is surrounded by four carbon atoms of separate acetylide molecules; two bridge to Li ($r(\text{Li}\dots\text{C}) = 230.1, 231.5\text{pm}$) and two bridge to Mg ($r(\text{Li}\dots\text{C}) = 225.7, 234.2\text{pm}$) in a distorted tetrahedral arrangement. The Mg atom is coordinated by three carbon atoms of separate acetylide molecules, ($r(\text{Mg}\dots\text{C}) = 218.3, 218.8, 230.7\text{pm}$) all of which bridge to Li, and the two nitrogen atoms of a tmeda molecule ($220.2, 235.0\text{pm}$) in a distorted trigonal pyramidal geometry. The structure of (90) contains clearly separated $[\text{Li}(\text{tmeda})_2]^+$ cations and $[\text{LiMg}(\text{tmeda})(\text{C}_6\text{H}_5\text{CH}_2)_4]^-$ anions.²⁷⁴ The Li atom in the cation is surrounded by the four nitrogen atoms of two tmeda molecules ($207.6-221.3\text{pm}$) in a distorted tetrahedral configuration. The anion is based on a LiCMgC ring containing bridging benzyl molecules ($r(\text{Li}\dots\text{C}) = 222.9, 227.2$; $r(\text{Mg}\dots\text{C}) = 231.3, 232.2\text{pm}$) with the approximately tetrahedral coordination geometries of the metal atoms being completed by (for Li) the two



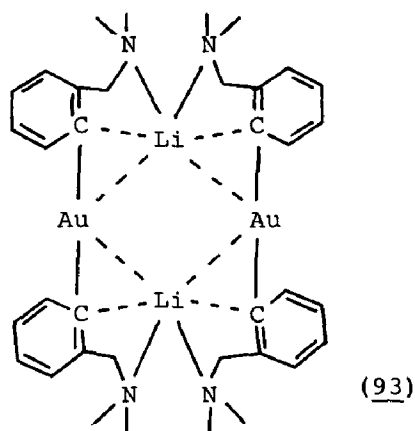
(89)



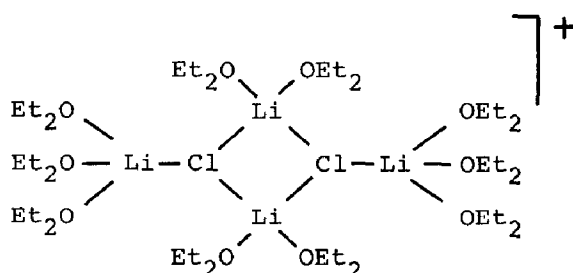
(90)



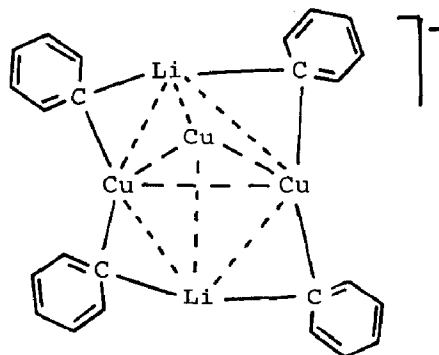
(91)



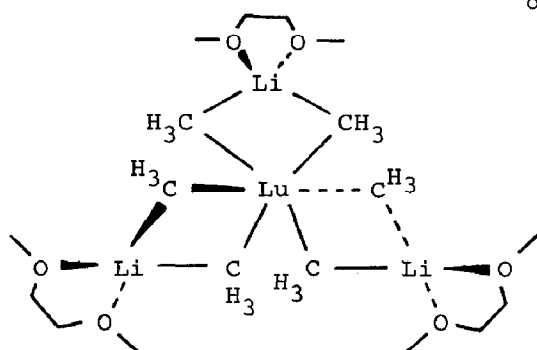
(93)



(92)



Two phenyl groups have been omitted for clarity



(94)

nitrogen atoms of a tmeda molecule (210.9,216.7pm) and (for Mg) the carbon atoms of two terminal benzyl molecules (222.5,226.3 pm).²⁷⁴

Treatment of $[(\text{PhC}\equiv\text{C})_2\text{Pt}(\text{PEt}_3)_2]$ with Bu^nLi results in loss of one equivalent of PEt_3 and formation of the Li-Pt complex $[\text{Li}_2\text{Pt}_2(\text{PEt}_3)_2(\text{PhC}\equiv\text{C})_4\text{Bu}_2^n]$ (91).²⁷⁵ The bonding in this material, which does not exhibit a centre of symmetry, is complex. Close contacts occur between the Li atoms and both the Pt atoms

(average $r(\text{Li} \dots \text{Pt}) = 280.7\text{pm}$) and the acetylenic carbon atoms (average $r(\text{Li} \dots \text{C}) = 215.5\text{pm}$). The relative significance of the Li-Pt and Li-C interactions is as yet unresolved, despite a detailed multinuclear nmr (^1H , ^7Li , ^{13}C , ^{31}P , ^{195}Pt) study of this, and several related, complexes.²⁷⁵

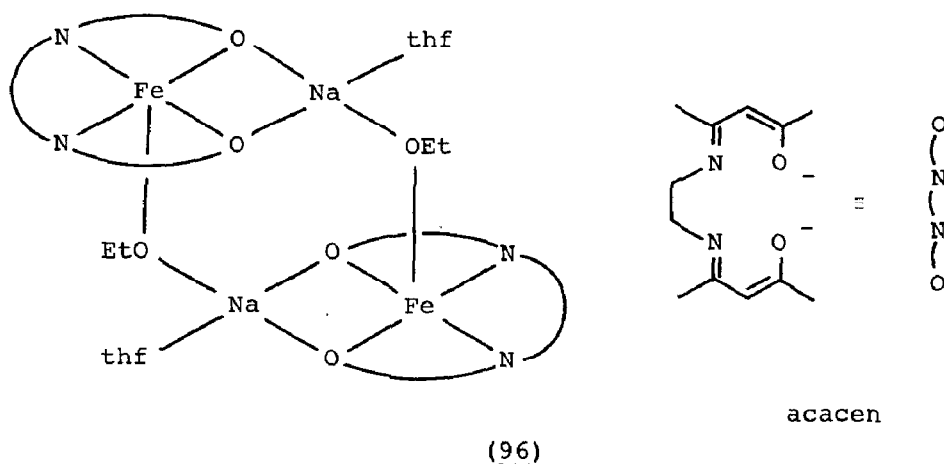
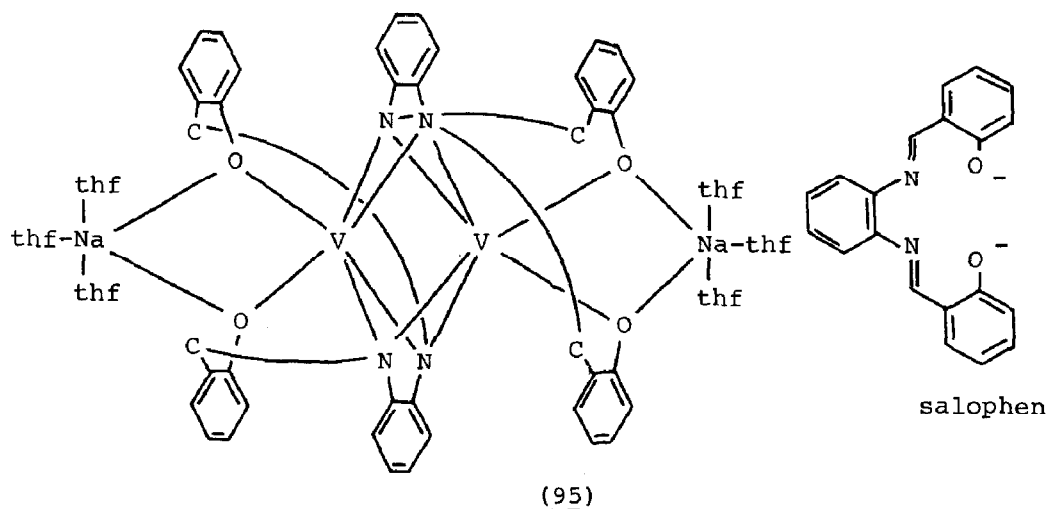
Addition of PhLi to CuCN in ether at 253K yields yellow crystals of the Li-Cu complex, $[\text{Li}_4\text{Cl}_2(\text{Et}_2\text{O})_{10}]^{4+}[\text{Li}_2\text{Cu}_3\text{Ph}_6]^{2-}$ (92).²⁷⁶ The cation consists of a planar Li_2Cl_2 core (250.5, 253.7pm) each Cl atom also being coordinated by a terminal Li atom (269.7pm). All the Li atoms are four coordinate due to the presence of either two or three ether molecules (average $r(\text{Li} \dots \text{O}) = 196\text{pm}$). The anion is based on a trigonal bipyramid containing two Li (axial) and three Cu (equatorial) atoms, each Li-Cu vector being bridged by a phenyl group (typical $r(\text{Li} \dots \text{C}) = 224.0$; typical $r(\text{Cu} \dots \text{C}) = 192.9\text{pm}$). The Li atoms are essentially three coordinate, the sites along the 3-fold axes of the Li_2Cu_3 cluster being blocked by protons of the phenyl group.²⁷⁶

The structure of the Li-Au complex, $[\text{Li}_2\text{Au}_2(\text{Me}_2\text{NC}_6\text{H}_4\text{CH}_2)_4]$ (93),²⁷⁷ for which no preparative details are given, is comparable to that of the Li-Pt complex (91). Close contacts occur between the Li atoms and both the Au atoms (typical $r(\text{Li} \dots \text{Au}) = 286, 290\text{pm}$) and the ipso carbon atoms of the aryl anion (typical $r(\text{Li} \dots \text{C}) = 245, 258\text{pm}$). Although the relative significance of these two interactions is still uncertain, multinuclear nmr (^1H , ^{13}C , ^6Li , ^7Li) studies of $[\text{Li}_2\text{M}_2(\text{Me}_2\text{NC}_6\text{H}_4\text{CH}_2)_4]$ ($\text{M} = \text{Cu}, \text{Ag}, \text{Au}$) in solution indicate that the carbon sp^2 lone pair of the aryl anion interacts with both Li and M atoms.²⁷⁷ The Li coordination sphere is completed by nitrogen atoms (average $r(\text{Li} \dots \text{N}) = 224\text{pm}$) of two pendant amine groups.

Reaction of MeLi with LuCl_3 in ether containing 1,2-dme gives $[\text{Li}_3\text{Lu}(\text{dme})_3(\text{CH}_3)_6]$ (94).²⁷⁸ Structural analysis shows it to contain an octahedral $\text{Lu}(\text{CH}_3)_6$ arrangement bridged to each of the three Li atoms via two methyl groups (202-219pm), the distorted tetrahedral geometry of each Li atom being completed by a bidentate chelating 1,2-dme molecule (194-214pm).²⁷⁸

Na-V and Na-Fe heterobimetallic complexes have been synthesised and characterised by Floriani et al.^{279,280} using tetradentate Schiff bases (salophen or acacen) to stabilise the metal cluster. The Na-V complex $[\text{Na}_2\text{V}_2(\text{salophen})_2(\text{thf})_6]$ (95)²⁷⁹ was prepared by reduction of $[\text{V}(\text{salophen})(\text{thf})\text{Cl}]$ with sodium metal. The

approximately trigonal bipyramidal Na coordination sphere is composed of the two oxygen atoms of a salophen molecule (equatorial; 228.0, 233.4 pm) which bridge to a vanadium atom (199.4, 200.3 pm) and three thf oxygen atoms (one equatorial, two axial; bond distances not quoted). The two vanadium atoms are bridged by the four nitrogen atoms of the two salophen molecules (205.0–208.7 pm) and are joined by a V(III)–V(III) double bond (240.6 pm).²⁷⁹ Reaction of FeCl_2 with acacen in the presence of MeONa affords $[\text{Fe}(\text{acacen})_2]$ which reacts with EtONa to form the



Na-Fe complex, $[\text{Na}_2\text{Fe}_2(\text{acacen})_2(\text{thf})_2(\text{EtO})_2]$ (96).²⁸⁰ It contains two centrosymmetrically related, five coordinate Fe^{II} atoms doubly bridged by EtONa ion pairs. The distorted tetra-

hedral Na coordination sphere consists of four oxygen atoms provided by the acacen molecule (234.7, 235.5 pm) the ethoxy anion (224.1 pm) and the thf molecule (236.9 pm). The approximately square pyramidal Fe coordination geometry is composed of the heteroatoms of the Schiff base (equatorial; $r(\text{Fe} \dots \text{O}) = 206.2, 207.1$; $r(\text{Fe} \dots \text{N}) = 206.5, 209.9$ pm) and the oxygen atom of the ethoxy anion (axial; 193.1 pm).²⁸⁰

1.4.9 Lithium Derivatives

Following the precedent set for the 1983 review,²⁸¹ many papers have been abstracted in which the inorganic chemistry of lithium is discussed. Four principle of areas interest can be perceived: (i) theoretical analysis of small molecules containing lithium, including low molecular weight organolithiums, (ii) synthesis of novel heterobimetallic complexes of lithium, (iii) characterisation of lithium containing oligomers, and (iv) structural analysis of diverse monomeric lithium derivatives. The former two topics are considered in subsections 1.3.2 and 1.4.8, respectively, the latter two in the present subsection.

It is important to remind the reader that, with the sole exception of novel structural data, the organometallic chemistry of lithium is not covered here since it is the subject of a separate annual review.

Oligomerisation is currently of great interest to lithium chemists. Reports describing the synthesis and characterisation, principally by single crystal XRD structural methods, of octameric,²⁸² pentameric,²⁸³ tetrameric,²⁸⁴⁻²⁸⁷ trimeric²⁸⁸ and dimeric²⁸⁸⁻³⁰² lithium derivatives have been published. The complex $[\text{Li}_8(\text{Me}_3\text{COS}(\text{N})\text{F})_4\text{F}_2][\text{Li}_4(\text{OCMe}_3)_5]_2, 4\text{C}_5\text{H}_{12}$,²⁸² which was isolated from a reaction mixture of $\text{N}\equiv\text{SF}$ and Me_3COLi in n-pentane, contains an unprecedented octanuclear Li_8 cluster. Its structure (Figure 7a) arises from the linkage of two $\text{Li}_8(\text{OCMe}_3)_5\text{F}$ clusters by four $\text{Me}_3\text{COS}(\text{N})\text{F}^-$ anions, which act as bridges. The eight Li atoms form a tetragonal antiprism, bond distances between the inner Li' atoms (Figure 7a), which are bridged by fluorine or nitrogen are 264-270 pm, those between the outer Li'' atoms (Figure 7a), which are oxygen bridged are 233-243 pm, and the Li'-Li'' distances lie between 275 and 280 pm. The triangular faces of the antiprism are bridged by four Me_3CO groups ($r(\text{Li}' \dots \text{O}) = 190.1$; $r(\text{Li}'' \dots \text{O}) = 188.3$ pm) and the outer quadrangular face is capped by an

additional Me_3CO moiety ($r(\text{Li}''\dots\text{O}) = 199.1\text{pm}$). The fluorine atom which bridges the inner quadrangular face lies within the antiprism (Figure 7a) and hence interacts with all the Li atoms ($r(\text{Li}'\dots\text{F}) = 198.5$, $r(\text{Li}''\dots\text{F}) = 246.4\text{pm}$).²⁸²

A novel pentanuclear Li_5 cluster is present in the anion of the complex $[\text{Li}(\text{hmpa})_4]^+[\text{Li}_5(\text{hmpa})\{\text{N}=\text{CPh}_2\}_6]^{283}$ which has been crystallised from an ether/toluene solvent mixture containing $[\text{LiN}=\text{CPh}_2]$ and hexamethylphosphoramide (hmpa). The five Li atoms in the anion (Figure 7b) are arranged in a distorted trigonal bipyramidal arrangement such that four Li atoms (Li(2)-Li(5)) form a tetrahedron (average $r(\text{Li}\dots\text{Li}) = 302\text{pm}$) while the fifth Li atom (Li(1)), which is bonded to the single hmpa molecule ($r(\text{Li}\dots\text{O}) = 183\text{pm}$), caps the face at the base of the tetrahedron but with significantly shorter contacts (average $r(\text{Li}\dots\text{Li}) = 260\text{pm}$). Three imido nitrogen atoms bridge the Li_3 faces involving this unique Li atom (average $r(\text{Li}\dots\text{N}) = 205\text{pm}$) while the remaining three bridge the Li_2 edges involving Li(5) (average $r(\text{Li}\dots\text{N}) = 202\text{pm}$). The structure of the cation is conventional with the Li atom tetrahedrally coordinated by four oxygen atoms (average $r(\text{Li}\dots\text{O}) = 184\text{pm}$) of the hmpa molecules.²⁸³

Tetrahedral Li_4 clusters have been observed in the structures of $[\text{CH}_3\text{OCH}_2\text{CH}_2(\text{CH}_3)\text{CHLi}]_4$ (97),²⁸⁴ $[(\text{Ph}_2\text{C}=\text{N})\text{Li}.\text{C}_5\text{H}_5\text{N}]_4$ (98),²⁸⁵ $[\text{LiCl}.\text{hmpa}]_4$ (99),²⁸⁵ and $[\text{Bu}^t_2\text{Si}(\text{NH}_2)\text{OLi}]_4$ (100).²⁸⁶ In (97),²⁸⁴ each face of the Li_4 tetrahedron (average $r(\text{Li}\dots\text{Li}) = 249.0\text{pm}$) is capped by a μ_3 -bridging anion attached at the chiral C(2) atom, to form a pseudo-cubane Li_4C_4 configuration (average $r(\text{Li}\dots\text{C}) = 231.4\text{pm}$). In addition each Li atom is coordinated intramolecularly by the pendant oxygen atom of an ether side chain (192.3pm).²⁸⁴ Similar structures are adopted by (98), obtained by reaction of $[\text{LiN}=\text{CPh}_2]$ with pyridine in hot toluene,²⁸⁵ and by (99), isolated from the reaction of a 1:1 mixture of $[\text{LiN}=\text{CBu}^t_2]$ and hmpa in hexane with 1/3 molar equivalent of AlCl_3 in ether.²⁸⁵ The faces of the tetrahedral Li_4 cluster in the former complex ($r(\text{Li}\dots\text{Li}) = 257.1\text{--}274.6\text{pm}$) are capped by μ_3 -bridging $\text{Ph}_2\text{C}=\text{N}$ anions attached at the nitrogen atom ($r(\text{Li}\dots\text{N}) = 201.9\text{--}217.1\text{pm}$) whereas those in the latter complex ($r(\text{Li}\dots\text{Li}) = 306.4\text{--}312.1\text{pm}$) are capped by μ_3 -bridging Cl atoms ($r(\text{Li}\dots\text{Cl}) = 235.7\text{--}244.1\text{pm}$) to form pseudocubane Li_4N_4 and Li_4Cl_4 frameworks. In the former complex the coordination sites along the 3-fold axes of the Li_4 tetrahedron are occupied by the nitrogen atom of a donor pyridine

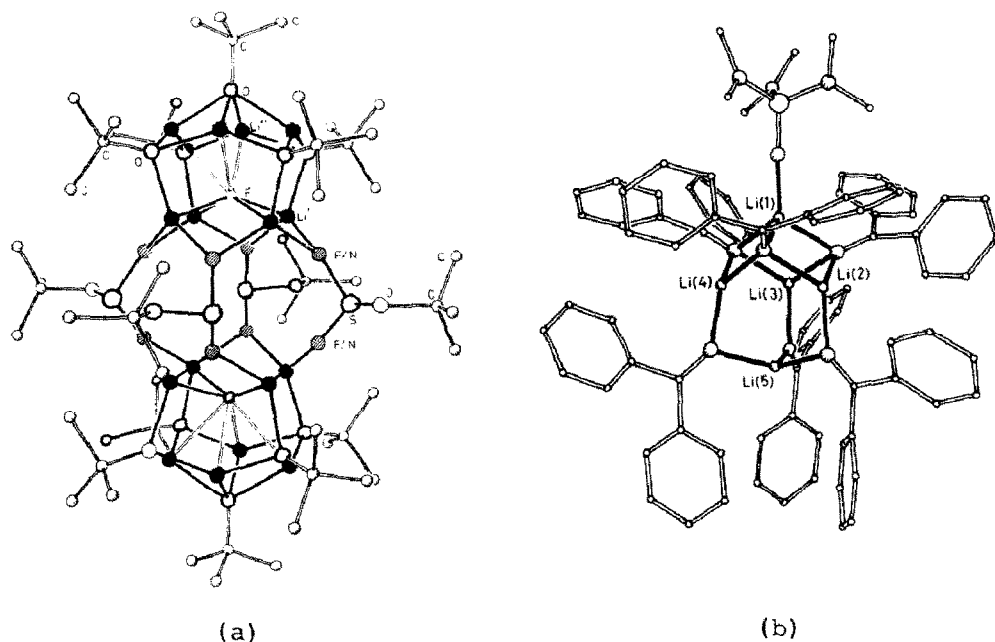


Figure 7. Molecular structures of (a) the two Li_8 clusters in $[\text{Li}_8(\text{Me}_3\text{COS}(\text{N})\text{F})_4\text{F}_2][\text{Li}_4(\text{OCMe}_3)_5]_2 \cdot 4\text{C}_5\text{H}_{12}$ and of (b) the Li_5 cluster in $[\text{Li}_5(\text{hmpa})\{\text{N}=\text{CPh}_2\}_6]^-$ (reproduced by permission from (a) *Angew. Chem., Int. Ed. Engl.*, 23(1984)795, and (b) *J. Chem. Soc., Chem. Commun.*, (1984)220).

molecule (207.5–211.4pm); those in the latter complex are filled by the oxygen atom of a donor hmpa molecule.²⁸⁵ In (100),²⁸⁶ prepared by reaction of $\text{Bu}^t\text{Si}(\text{Cl})\text{OH}$ with NH_3 followed by Bu^nLi , the pseudocubane Li_4O_4 configuration is generated by attachment of μ_3 -bridging anions via the oxygen atom ($r(\text{Li} \dots \text{O}) = 191\text{--}211\text{pm}$) to each face of the Li_4 tetrahedron ($r(\text{Li} \dots \text{Li}) = 255\text{--}262\text{pm}$). The Li coordination sphere is completed by the amine nitrogen atom of the anion ($r(\text{Li} \dots \text{N}) = 220\text{--}230\text{pm}$).²⁸⁶

The room temperature solution structures of phenyllithium have been established by nmr techniques.²⁸⁷ In ether-rich, cyclohexane-ether mixtures, it is tetrameric with essentially the same geometry as in the solid state. In cyclohexane-rich solutions, however, tetramers and dimers exist in equilibrium. In thf solutions, it is invariably dimeric.²⁸⁷

Addition of Bu^nLi in hexane to chilled solutions of $(\text{PhCH}_2)_2\text{NH}$ in hexane, diethylether-hexane or hmpa-hexane yields trimeric

$[(\text{PhCH}_2)_2\text{NLi}]_3$ (101), dimeric $[(\text{PhCH}_2)_2\text{NLi.OEt}_2]_2$ (102) and dimeric $[(\text{PhCH}_2)_2\text{NLi.(hmpa)}]_2$ (103), respectively.²⁸⁸ The molecules contain planar Li_3N_3 ((101) — 190.7–203.8pm) or Li_2N_2 ((102) — 198.2–199.1; (103) — 200.1–201.3pm) rings with formal Li coordination numbers of 2 or 3, the third coordination site in the dimers being occupied by either ether ((102) — 200.9pm) or hmpa ((103) — 185.0pm) molecules.²⁸⁸ In the trimer, however, all the benzyl units bend towards neighbouring Li atoms of the Li_3N_3 ring to give each Li atom contacts to four CH_2 units (average $r(\text{Li}\dots\text{C}) = 281$, average $r(\text{Li}\dots\text{H}) = 280$, to two α -C ring carbon atoms (average $r(\text{Li}\dots\text{C}) = 280\text{pm}$) and to two ortho-CH units (average $r(\text{Li}\dots\text{C}) = 280$; average $r(\text{Li}\dots\text{H}) = 266\text{pm}$).^{288,289} It is suggested²⁸⁹ that these Li-benzyl interactions are responsible for the changed state of association in the absence of coordinating ligands, in that the decrease in formal Li coordination number from 3 (in 102, 103) to 2 (in 101) may cause the much closer approach of the benzyl units to the Li atoms (in 101) which in turn necessitates expansion to a larger ring system. Spectroscopic studies²⁸⁹ of the coloured solutions from which these complexes crystallise, are thought to provide evidence for a low association (monomeric) $(\text{PhCH}_2)_2\text{NLi}$ species which absorbs in the visible region of the spectrum owing to a benzyl \rightarrow Li charge transfer excitation.

Although no other trimeric lithium derivatives have been studied in 1984, many novel dimers have been prepared and structurally characterised. Of these, one contains a planar Li_2X_2 framework with 3-coordinate Li atoms similar to those in (102, 103). Treatment of 2,4,6-tri-*t*-butylaniline (NH_2Ar) with Bu^nLi in ether yields $[\text{ArNHLi.Et}_2\text{O}]_2$ (104) in which the Li_2N_2 framework (204.1pm) has ether substituents to complete the Li coordination sphere (190.6pm).²⁹⁰

More conventional 4-coordinate Li atoms are found in the Li_2O_2 frameworks of $[\text{Ph}_2(\text{O})\text{P-P-P}(\text{O})\text{Ph}_2\text{Li.MeCN}]_2$ (105),²⁹¹ obtained by degradation of P_4 by LiOPPh_2 , $[\text{LiCl.dmf.}\frac{1}{2}\text{H}_2\text{O}]_2$ (106),²⁹² prepared by interaction of solid LiCl with neat dmf, $[\text{Li}(\text{H}_2\text{O})_2, (\text{hmpa})]_2^{2+}2\text{Cl}^-$ (107),²⁹³ isolated from the reaction of hydrated LiCl and hmpa in toluene, and $[\text{Ph}(2\text{-pyridyl})\text{NLi.(hmpa)}]_2$ (108),²⁹⁴ synthesised in the 1:1:1 reaction of 2-anilinopyridine with Bu^nLi and hmpa. Whereas the former complex contains a conventional oxygen bridging anion, the latter three complexes

exhibit formally neutral oxygen bridging molecules, a previously unknown phenomenon. The centrosymmetric Li_2O_2 ring in (105)²⁹¹ is bridged by one of the two oxygen atoms of the $(\text{Ph}_2(\text{O})\text{P}-\text{P}-\text{P}(\text{O})\text{Ph}_2)^-$ anion (198.9pm); the other oxygen atom completes the distorted tetrahedral Li coordination sphere (185.0pm) together with the nitrogen atom of an acetonitrile molecule. The two Li atoms of the Li_2O_2 ring of (106),²⁹² which contains bridging dmf molecules, are crystallographically distinct; whereas Li(1) is surrounded by the bridging oxygen atoms (195.2, 198.4pm), a chlorine atom (236.1pm) and a water molecule (190.4 pm), Li(2) is associated with the bridging oxygen atoms (194.9, 197.5pm) and two chlorine atoms (234.1, 234.7pm). The Li_2O_2 frameworks of (107)²⁹³ and (108)²⁹⁴ are centrosymmetric with bridging hmpa molecules. The Li atom in (107) is coordinated by two bridging oxygen atoms (198.4, 201.3pm) and two water molecules (193.6, 194.0pm).²⁹³ That in (108) is surrounded by the two bridging oxygen atoms (average $r(\text{Li}\dots\text{O}) = 192.4\text{pm}$) and the two nitrogen atoms of a bidentate anion (198.3, 217.2pm),²⁹⁴ The structure of the latter complex (Figure 8a) is of particular interest because it is one of two entirely different structural isomers. The structure of the alternative isomer (Figure 8b) is based on a centrosymmetric Li_2N_2 framework, the amido nitrogen atoms of the anions providing the bridging atoms (average $r(\text{Li}\dots\text{N}) = 214.2\text{pm}$). The terminal positions of the distorted tetrahedral coordination geometry of the Li atom are occupied by a pyridyl nitrogen atom of the anion (205.5pm) and an oxygen atom of the hmpa molecule (187.0pm).²⁹⁴ In the presence of excess 2-anilinopyridine, neither of the dimeric isomers is found. The product, $[\text{Ph}(2\text{-Pyr})\text{NLi}, \text{Ph}(2\text{-pyr})\text{NH}, \text{hmpa}]$,³⁰⁴ is a monomeric species in which the 4-coordinate Li atom is surrounded by the two nitrogen atoms of the anion (209.1, 211.1pm), the pyridyl nitrogen atom of a neutral 2-anilinopyridine molecule (207.8pm) and the oxygen atom of a hmpa molecule (181.5pm). The protonated ligand forms a hydrogen bond to the amido nitrogen atom of the anion resulting in a short Li-H contact (251.6pm).³⁰⁴

Another two dimers based on Li_2N_2 frameworks for which structural data are now available are the lithiated bis-lactim ether of the diketopiperazine from alanine (109),²⁹⁵ and the lithium complex derived by metallation of 2-(Me_3Si) $\text{CH}_2\text{C}_5\text{H}_4\text{N}$ (110).²⁹⁶ The Li atoms in (109), although lying on an

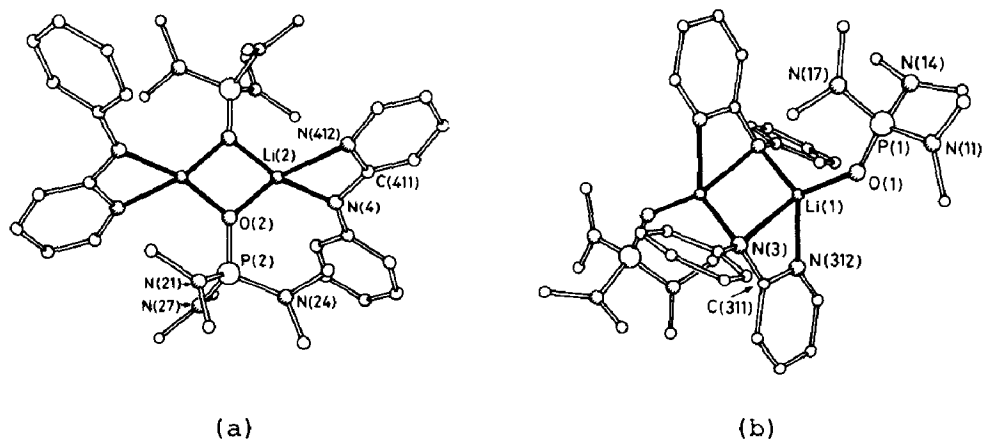
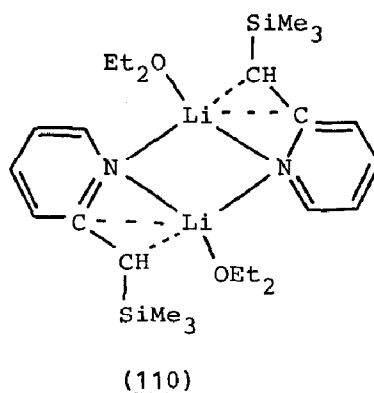
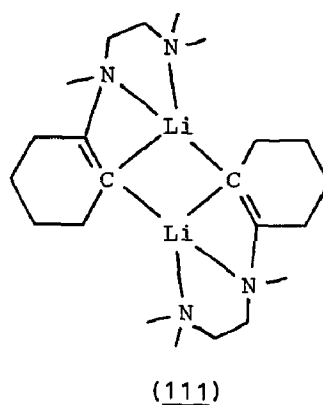
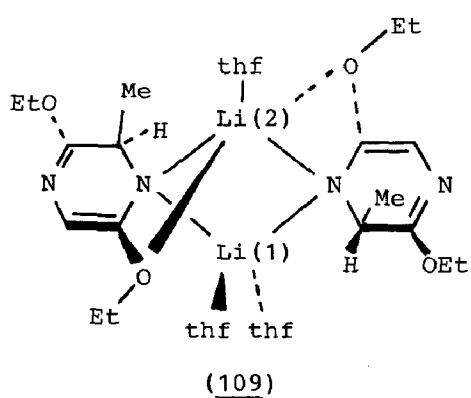


Figure 8. Molecular structures of (a) the μ_2 -O-isomer and (b) the μ_2 -N-isomer of $[\text{Ph}(2\text{-pyr})\text{NLi},\text{hmpa}]_2$ (reproduced by permission from J. Chem. Soc., Chem. Commun., (1984) 700).

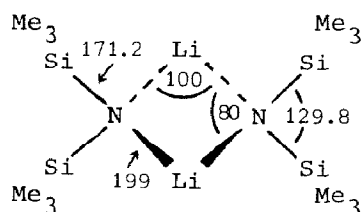


approximate 2-fold axis are crystallographically distinct. Whereas Li(1) is coordinated by the two bridging nitrogen atoms of the anions (205,206pm) and two thf oxygen atoms (198,198pm) in an approximately tetrahedral geometry, Li(2) is surrounded by the two bridging nitrogen atoms (204,206pm), a single thf oxygen atom (192pm), and the two oxygen atoms of the ethoxy moieties attached to the heterocycles in the 2-position (224,225pm) to form a distorted square pyramidal geometry.²⁹⁵

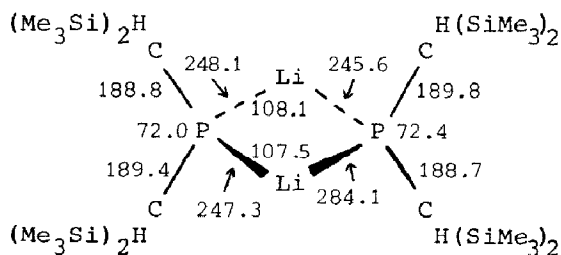
In the centrosymmetric structure of (110),²⁹⁶ the anion adopts a novel η^3 -azaallyl ligand geometry ($r(\text{Li}\dots\text{N}) = 219$, $r(\text{Li}\dots\text{C}) = 234, 236\text{pm}$), the nitrogen atom bridging to the related Li atom (204pm). The coordination geometry of the Li atom is completed by an ether oxygen atom (191pm).²⁹⁶

The only Li_2C_2 4-membered ring structurally characterised this year is that which forms the basis of the dimeric vinyl lithium derivative N-(2-lithiocyclohexenyl)-N,N',N'-trimethyl-1,3-propane diamine (111).²⁹⁷ The bridging carbon atoms are provided by the cyclohexenyl ring (216,220pm) and the four-coordinate geometry of the Li atom is completed by the two nitrogen atoms of the pendant diamine side chain (205,210pm).²⁹⁷

Lappert et al²⁹⁸⁻³⁰⁰ have synthesised the two lithiated trimethylsilyl derivatives $[(\text{Me}_3\text{Si})_2\text{NLi}]_2$ (112) and $[(\text{Me}_3\text{Si})_2\text{CH}]_2\text{PLi}]_2$ (113). Whereas the former (112) has been structurally characterised in the gas phase using electron diffraction methods,^{298,299} the latter (113) has been studied in the solid phase using conventional XRD techniques.³⁰⁰ Structurally similar, they are dimeric with Li_2X_2 frameworks, none of the Li atoms bearing any other substituents. Although the Li_2N_2 ring exhibits D_2 symmetry,^{298,299} the Li_2P_2 ring has no



(112)

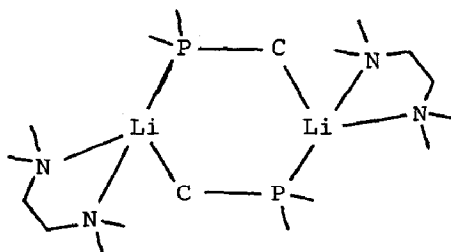


(113)

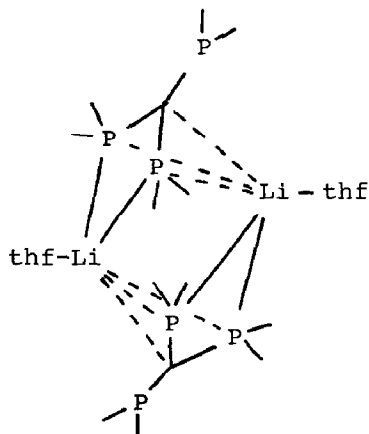
distances/pm; angles/°

apparent symmetry.³⁰⁰

The crystal and molecular structures of the related lithiated phosphine complexes $[\text{Me}_2\text{PCH}_2\text{Li}, \text{tmeda}]_2$ (114)³⁰¹ and $[(\text{Me}_2\text{P})_3\text{CLi}, \text{thf}]_2$ (115)^{302,303} have been reported by two independent groups. White et al³⁰¹ have shown that (114) is a dimer with a simple LiCPLiC ring structure. Thus the Li atoms are coordinated by a carbon atom ($r(\text{Li}(1)\dots\text{C}) = 214.1$, $r(\text{Li}(2)\dots\text{C}) = 215.0\text{pm}$) and a phosphorus atom ($r(\text{Li}(1)\dots\text{P}) = 261.5$, $r(\text{Li}(2)\dots\text{P}) = 259.3\text{pm}$) from separate bridging anions and by the two nitrogen atoms of a bidentate tmeda molecule ($r(\text{Li}(1)\dots\text{N}) = 216.9, 221.6$, $r(\text{Li}(2)\dots\text{N}) = 217.7, 221.8\text{pm}$) in a distorted tetrahedral geometry.³⁰¹ Karsh, Muller et al^{302,303} have ascertained that $[(\text{Me}_2\text{P})_3\text{CLi}, \text{thf}]_2$ is also a dimer, but in this case, despite the centrosymmetric structure, the bridging



(114)



(115)

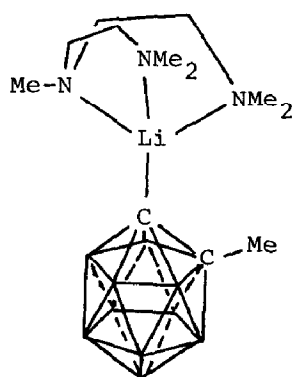
conformation is much more complex (115). Each Li atom is bonded to the oxygen atom of a thf molecule (192.3pm) and to the phosphorus atoms of two phosphino groups of one $[(\text{Me}_2\text{P})_3\text{Cl}]^-$ anion ($258.8, 268.4\text{pm}$). The pseudo-tetrahedral Li coordination sphere is completed by an η^3 -contact ion pair interaction with the carbanionoid centre of the second anion.^{302,303}

Several monomeric lithium complexes have been structurally characterised. They fall into two categories: those with conventional σ -bonded ligands only and those also containing η^n -bonded ligands. With two exceptions, namely the 3- and 6-coordinate Li atoms in $[2,4,6\text{-Bu}^t_3\text{C}_6\text{H}_2\text{NHLi}, \text{tmeda}]$ (116)²⁹⁸ and

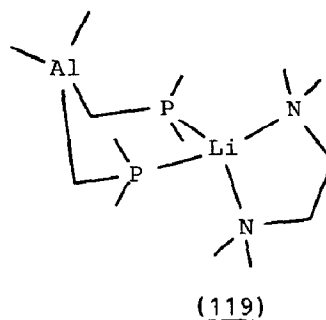
$[(\text{PhMe}_2\text{Si})_3\text{CBH}_3\text{Li}, (\text{thf})_3]$ (117),³⁰⁵ respectively, 4-coordinate Li atoms are found in the former compounds;^{304,306-309} in the latter complexes, however, higher coordination numbers are generally favoured.^{296,310-315} The Li atom in (116) is simply attached to the anilino nitrogen atom of the anion (189.5pm) and the two nitrogen atoms of a bidentate tmeda ligand (213.7, 216.5pm).²⁹⁸ That in (117) is located on the three-fold axis of symmetry, $(\text{Me}_3\text{Si})_3\text{C-B-Li}(\text{thf})_3$, implying tridentate coordination of the Li atom by the hydrogen atoms of the alkyltrihydroborate moiety; in conjunction with the three oxygen atoms of the thf solvate molecules (average $r(\text{Li}\dots\text{O}) = 200\text{pm}$) this gives a distorted octahedral coordination sphere. If the hydrogen atoms are ignored (they were not located owing to the relatively poor quality of the diffraction data) the Li atom is situated in a pseudo-tetrahedral coordination geometry comprising the thf oxygen atoms and the boron atom of the anion (219pm).³⁰⁵

Four-coordinate Li atoms have been observed in the cations of $[\text{Li}(\text{thf})_4]^+ [(\text{Me}_3\text{Si})_3\text{C}_2\text{Ag}]^-$ ³⁰⁶ and $[\text{Li}(\text{tmeda})_2]^+ [(\text{C}_5\text{H}_5)\text{Lu}(\text{CH}_3)_3]^-$ ³⁰⁷ and in the molecular species, $[\text{C}_2\text{B}_{10}\text{H}_{10}\text{MeLi}, \text{pmdeta}]$ (118),³⁰⁸ $[\text{Ph}(2\text{-pyr})\text{NLi}, \text{Ph}(2\text{-pyr})\text{NH}, \text{hmpa}]$ (119),³⁰⁴ and $[\text{Me}_2\text{Al}(\text{CH}_2\text{PMe}_2)_2\text{Li}, \text{tmeda}]$ (120).³⁰⁹ The structures of the cations are conventional and need not be discussed further.^{306,307} Those of the molecular species, however, are novel. Both the dicarbadodecaborane³⁰⁸ and phosphinomethyl substituted aluminate³⁰⁹ derivatives exhibit mirror symmetry. In the former complex (118),³⁰⁸ the Li atom is bonded to a six coordinate carbon atom (217.6pm) of the carborane unit and to the three nitrogen atoms of a tridentate pmdeta molecule (213.4, 216.9 pm). In the latter complex (119),³⁰⁹ the Li atom has a distorted tetrahedral coordination geometry provided by the two phosphorus atoms of the chelating anion (260.5pm) and the two nitrogen atoms of the bidentate tmeda molecule. The structure of the monomeric 2-anilinopyridine derivative $[\text{Ph}(2\text{-pyr})\text{NLi}, \text{Ph}(2\text{-pyr})\text{NH}, \text{hmpa}]$ ³⁰⁴ is compared to that of the corresponding dimeric complex $[\text{Ph}(2\text{-pyr})\text{NLi}, \text{hmpa}]_2$ ²⁹⁴ earlier in this section.

The classical example of a lithiated compound containing a η^n -bonded ligand is cyclopentadienyllithium. Ab initio SCF MO calculations³¹⁰ have shown that the hydrogen atoms on this molecule are bent away from the lithium atom to a significant degree (1.9° using the 4-31G** basis set level) thereby increasing

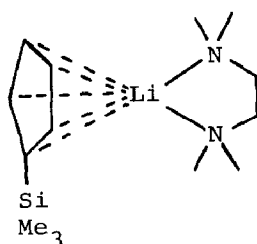


(118)



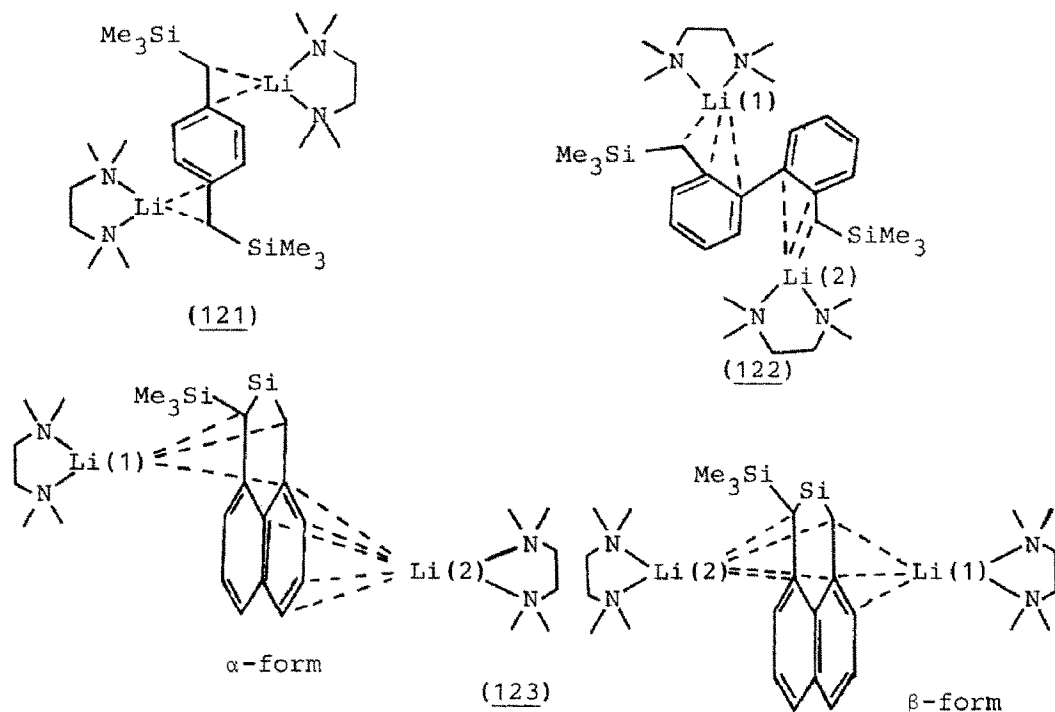
(119)

the negative charge on the side of the ring adjacent the Li atom. These results imply that (η^5 -C₅H₅)Li is an ion pair and that the binding therein is essentially a Coulombic effect of the Li⁺ cation.³¹⁰ Structural analysis of the cyclopentadienyllithium derivative, [η^5 -C₅H₄SiMe₃Li, tmeda] (120),³¹¹ synthesised by addition of an equimolar mixture of BuⁿLi and tmeda in n-hexane to trimethylsilylcyclopentadiene and recrystallised from n-pentane, has shown that the Li atom has a pseudo-trigonal planar coordination sphere with bonds to the centroid of the planar η^5 -C₅H₄SiMe₃ ring ($r(\text{Li} \cdots \text{C}) = 225.7\text{--}228.6\text{pm}$) and to the two nitrogen atoms of the bidentate tmeda molecule (211.9, 214.2 pm).



(120)

Figure 9. Schematic representation of the structures of the lithiated trimethylsilyl derivatives of 1,4-xylene (121),³¹² 2,2'-dimethylbiphenyl (122)³¹³ and 1,8-dimethylnaphthalene (123).³¹⁴



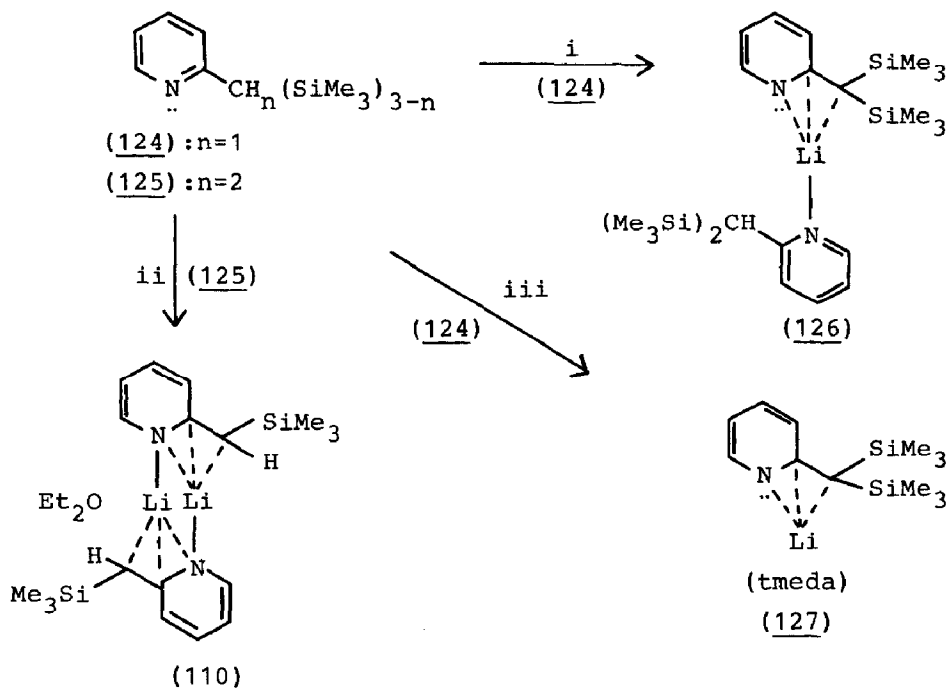
Pertinent interatomic distances/pm in (121)-(123):

	(<u>121</u>) [†]	(<u>122</u>) Li (1)	(<u>122</u>) Li (2)	α-(<u>123</u>) Li (1)	α-(<u>123</u>) Li (2)	β-(<u>123</u>) Li (1)	β-(<u>123</u>) Li (2)
r(Li...tmeda)	204 206	204 210	204 210	213 218	208 212	* *	* *
r(Li... ⁿ C _n)	210 238	219 233 248	222 242 263	235 246 251	234 240 243 249 249	212 217 219	224 239 249 264

[†] centrosymmetric

* Not quoted

Figure 10. Schematic representations of, and synthetic routes to, lithium η^3 -azaallyl derivatives (110, 126, 127).²⁹⁶



Reagents and conditions: (i) Bu^nLi (ca. 1.6M in hexane); (ii) as for (i) + OEt_2 ; (iii) as for (i) + tmeda.

Pertinent interatomic distances/pm in (110), (126) and (127).

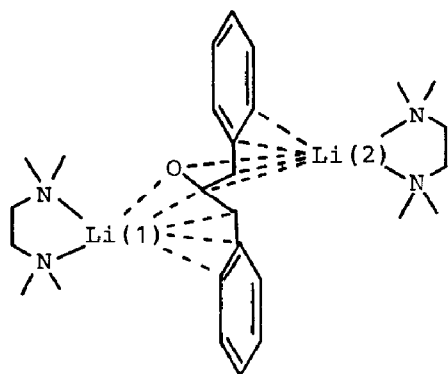
	$r(\text{Li} \dots \text{N})$	$\frac{r(\text{Li} \dots \eta^3\text{C}_2\text{N})}{\text{N} \quad \text{C} \quad \text{C}}$	$r(\text{Li} \dots \text{tmeda})$	$r(\text{Li} \dots \text{OEt}_2)$
(<u>110</u>)	204	219, 234, 236	-	191
(<u>126</u>)	201	200, 222, 232	-	-
(<u>127</u>)	-	196, 243, 246	206, 207	-

Raston, White et al.³¹²⁻³¹⁴ have made a substantial contribution to the study of the chemistry of lithiated complexes of trimethylsilyl derivatives of aromatic materials. As part of their investigation they have determined the crystal and molecular structures of the 1,4-xylene, 2,2'-dimethylbiphenyl and

1,8-dimethylnaphthalene derivatives, $[1,4-(\text{Me}_3\text{SiCH})_2\text{C}_6\text{H}_4\text{Li}_2, (\text{tmeda})_2]$ (121),³¹² $[2,2'-(\text{Me}_3\text{SiCH})_2\text{C}_{12}\text{H}_8\text{Li}_2, (\text{tmeda})_2]$ (122)³¹³ and $[\text{C}(\text{SiMe}_3)\text{SiMe}_2\text{CHC}_{10}\text{H}_6\text{Li}_2, (\text{tmeda})_2]$ (123),³¹⁴ respectively. Their structures are shown schematically in Figure 9; the 1,8-dimethylnaphthalene derivative exists in two polymorphic modifications.³¹⁴ The asymmetric units of all four structures contain two $[\text{Li}(\text{tmeda})]^+$ cations and a single dicarbanion; they differ in the configuration of the contact ion pair interaction. Whereas the two cations in (121)³¹² bond to the π -system of the anion by an η^2 -interaction, those in (122)³¹³ interact through an η^3 -configuration. The α -polymorph of (123) exhibits η^3 - and η^6 -configurations; the β -polymorph contains η^3 - and η^4 -arrangements.³¹⁴ Pertinent interatomic distances are summarised in Figure 9.

Raston, White et al.²⁹⁶ have also effected a detailed study of lithium η^3 -azaallyl-type complexes derived from the metallation of $2-(\text{Me}_3\text{Si})_3\text{-}\eta^5\text{-CH}_5\text{C}_5\text{H}_4\text{N}$. Details of the synthetic routes and products are summarised in Figure 10. Metallation of (124) with Bu^nLi in hexane yields the monomeric pyridine adduct (126); in the presence of tmeda, however, the chelating agent replaces the pyridine molecule to form the monomeric tmeda adduct (127). Metallation of (125) with Bu^nLi in hexane-ether mixtures affords the dimeric solvated product (110). [This product has been discussed previously in the section covering dimeric complexes with Li_2N_2 frameworks]. Single crystal XRD structural analysis of the three products has shown them all to contain novel η^3 -azaallyl ligand geometries.²⁹⁶ Pertinent details are incorporated in Figure 10.

A similar contact-ion pair interaction occurs in lithiated dibenzylketone, $[(\text{C}_6\text{H}_5\text{CH})_2\text{COLi}_2, (\text{tmeda})_2]$ (128).³¹⁵ Each of the two crystallographically distinct Li atoms is involved in an $\eta^5\text{-C}_4\text{O}$ interaction with the dicarbanion. The pseudo trigonal coordination of the Li atoms is completed by the nitrogen atoms of a bidentate tmeda molecule. Experimental structural data for the contact ion pair interaction were compared with those calculated in a MNDO theoretical study. Although they agreed in principle, they differed in detail; calculated Li-C contacts were too short and the calculated Li-O contact too long.

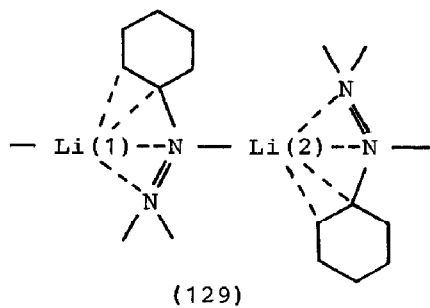


	Li(1)	Li(2)	MNDO
$r(\text{Li} \dots \text{C})$	215.0	241.5	216.7
	246.9	242.5	225.5
	265.3	250.5	232.6
	273.1	255.0	244.1
$r(\text{Li} \dots \text{O})$	184.9	187.0	201.3

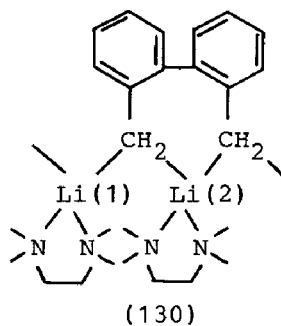
distances/pm

(128)

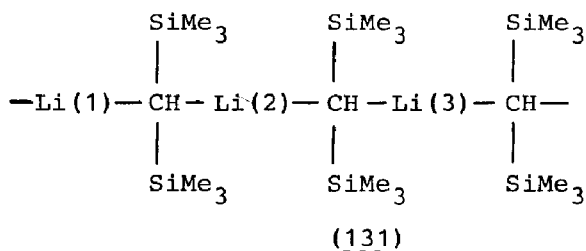
Single crystal XRD studies have shown that the three lithiated species, $[\text{C}_6\text{H}_{10}\text{N}=\text{NMe}_2\text{Li}]_n$ (129),³¹⁶ $[(2\text{-CH}_2\text{C}_6\text{H}_4)_2\text{Li}_2(\text{tmeda})_2]_n$ (130),³¹³ and $[(\text{SiMe}_3)_2\text{CHLi}]_n$ (131),³¹⁷ adopt polymeric extended arrays in the solid state. The two crystallographically distinct Li atoms in (129)³¹⁶ are coordinated to one anion in an $\eta^4\text{-C}_2\text{N}_2$ configuration ($r(\text{Li}(1) \dots \text{C}) = 219.6, 229.8$; $r(\text{Li}(1) \dots \text{N}) = 206.2, 215.6$, $r(\text{Li}(2) \dots \text{C}) = 225.5, 229.8$, $r(\text{Li}(2) \dots \text{N}) = 199.5, 217.6$ pm and to a second anion by a simple Li-N contact ($r(\text{Li}(1) \dots \text{N}) = 193.4$, $r(\text{Li}(2) \dots \text{N}) = 193.4$ pm). In the other two compounds (130, 131), the Li atom coordination sphere does not involve any η^n -type ($n > 1$) interactions. One of the Li atoms in (130)³¹³ bridges the two methylene groups of a biphenyl dianion



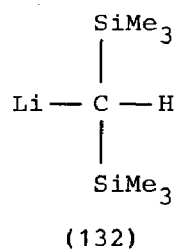
(129)



(130)



(131)



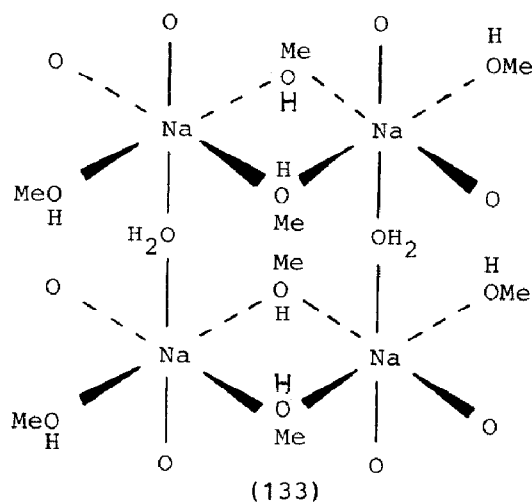
(132)

($r(\text{Li}(1)\dots\text{C}) = 216,228\text{pm}$); the other bridges two methylene groups of adjacent biphenyl dianions ($r(\text{Li}(2)\dots\text{C}) = 228,246\text{pm}$). The four-fold, approximately tetrahedral, coordination geometries of the two Li atoms are completed by nitrogen atoms of bidentate tmeda molecules ($r(\text{Li}(1)\dots\text{N}) = 210,221$, $r(\text{Li}(2)\dots\text{N}) = 214,218\text{pm}$). The three Li atoms in the asymmetric unit of (131)³¹⁷ simply bridge alkyl groups ($r(\text{Li}(1)\dots\text{C}) = 214,221$, $r(\text{Li}(2)\dots\text{C}) = 218,222$, $r(\text{Li}(3)\dots\text{C}) = 213,227\text{pm}$) forming nearly linear 2-fold coordination geometries ($\text{C-Li}(1)\text{-C} = 152^\circ$, $\text{C-Li}(2)\text{-C} = 147^\circ$, $\text{C-Li}(3)\text{-C} = 151^\circ$). This latter compound has also been the subject of a gas-phase electron diffraction study at 413K;³¹⁷ it adopts a monomeric configuration (132) with $r(\text{Li}\dots\text{C}) = 203\text{pm}$.

1.4.10 Sodium Derivatives

As for previous reviews, the majority of the papers abstracted for this subsection contain novel structural data for diverse sodium salts. The compounds studied fall into two broad classifications; those containing inorganic anions³¹⁸⁻³²⁰ and those containing organic anions.³²¹⁻³²⁵

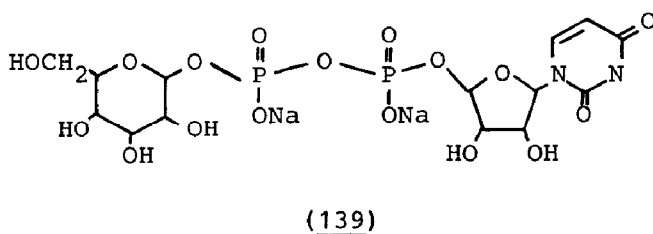
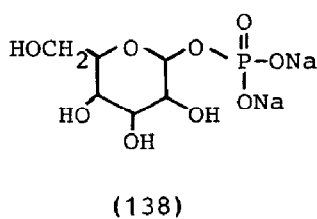
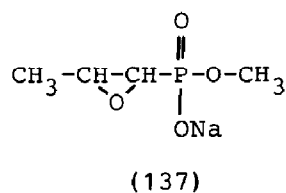
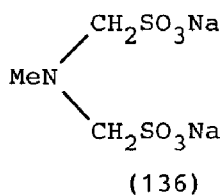
Novel tetrameric cations, $[(\mu\text{-CH}_3\text{OH})_4(\text{CH}_3\text{OH})_4(\mu\text{-H}_2\text{O})_2\text{Na}_4]^{4+}$ (133)³¹⁸ have been found in the structure of $[(\text{CH}_3\text{OH})_8(\text{H}_2\text{O})_2\text{Na}_4]^{4+}\text{Mo}_8\text{O}_{26}^{4-}$. They consist of four planar Na atoms, two bridging water molecules (240.8pm), four symmetrically bridged methanol molecules (238.0,238.8pm) and four terminal methanol molecules (233.3pm); the octahedral coordination of the cation is completed by eight oxygen atoms from $\text{Mo}_8\text{O}_{26}^{4-}$ anions (240.3,242.1 pm).



Extended array structures are formed by $[(C_4H_8O_2)_2Na]^+AsPh_2^-$ (134)³¹⁹ and $[(Me_2NCOCMe_2CONMe_2)_2Na]^+ClO_4^-$ (135).³²⁰ The diphenylarsenide salt (134) consists of an alternating sequence of bis(dioxane) coordinated Na atoms (230.7, 232.0 pm) and Ph_2As anions which gives rise to infinite Na-As-Na-As chains (293.7, 296.2 pm) parallel to (100). Although nearly linear at arsenic ($NaAsNa = 173.6^\circ$), the chains are bent at sodium ($AsNaAs = 121.5^\circ$) resulting in a distorted tetrahedral Na coordination sphere.³¹⁹ In the perchlorate salt (135), each bidentate $Me_2NCOCMe_2CONMe_2$ molecule bridges two Na atoms by coordination through oxygen (229.7-232.5 pm). The five-fold coordination of the Na atom, which is intermediate between trigonal bipyramidal and square pyramidal, is completed by an oxygen atom of a ClO_4^- anion (237.8 pm).³²⁰

Structural elucidation using single crystal XRD methods have been successfully completed for sodium salts of N-methyliminobis-(methanesulphonic acid) (136),³²¹ the monomethyl ester of fosfomycin (137),³²² 1-(phospho)glucose (138)³²³ and 1-(uridinediphospho)glucose (139).³²⁴ Although six-coordinate Na atoms predominate, five-coordinate Na atoms are found in the fosfomycin and 1-(phospho)glucose salts; coordination geometries are invariably irregular.

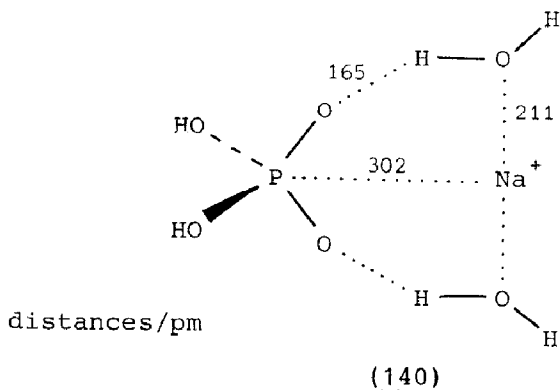
The two symmetry related Na atoms in the sulphonate dihydrate, (136), $2H_2O$ ³²¹ are coordinated by four anion oxygen atoms (242.6-252.3 pm) and two water molecules (236.1, 239.7 pm). The structure



of the fosfomycin salt, (137),³²² contains two crystallographically independent molecules. In both cases, four short Na-O bonds are formed with oxygen atoms of phosphite groups ($r(\text{Na}(1) \dots \text{O}) = 227.5\text{--}240.3$, $r(\text{Na}(2) \dots \text{O}) = 230.1\text{--}236.2\text{pm}$) and a longer Na-O bond involves the epoxy oxygen atom of a fosfomycin molecule ($r(\text{Na}(1) \dots \text{O}) = 266.6$, $r(\text{Na}(2) \dots \text{O}) = 261.2\text{pm}$).

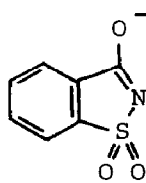
Interactions between phosphate anions and Na^+ ions have been studied both experimentally^{323,324} and theoretically.³²⁶ The structures of two 1-(phospho)glucose derivatives have been determined. Very few details of the cation coordination geometries are given in the paper reporting the structure of the disodium salt of 1-(phospho)glucose hydrate, (138), $3.5\text{H}_2\text{O}$.³²³ It contains three crystallographically distinct Na atoms; two are located on 2-fold axes, the other has no apparent symmetry. Two of the Na atoms are six-coordinate, the other is five-coordinate; their coordination spheres comprise both unidentate phosphate anions and water molecules. The structure of the related disodium salt of 1-(uridinediphospho)glucose dihydrate, (139), $2\text{H}_2\text{O}$,³²⁴ contains two six-coordinate crystallographically distinct Na atoms. Na(1) is surrounded by three oxygen atoms from different anions ($229.9\text{--}235.6\text{pm}$), two water molecules (237.0 , 263.1pm) and a remote oxygen atom of a fourth anion (299.3pm). Na(2) is coordinated by four oxygen atoms from different anions ($230.8\text{--}245.6\text{pm}$), one water molecule (237.9pm) and a remote oxygen atom from one of the four original anions (280.0pm).

Interactions of the phosphate anion with Na^+ ion in the presence of water have also been studied by ab initio MO theory.³²⁶ The results predict that the most stable structures for $\text{H}_2\text{PO}_4^-\cdot\text{Na}^+\cdot 2\text{H}_2\text{O}$ complexes have the water molecules located partially between the anion and cation (140); these bridging water



molecules increase the separation between the ions to optimise the water-ion interactions.

The last of the novel structures to be abstracted for this subsection is that of sodium dipotassium trisaccharinate monohydrate.³²⁵ The coordination polyhedra around the three alkali metal atoms (the two K atoms are crystallographically independent) are highly irregular. The Na atom has a six-fold coordination geometry generated by two water molecules (241.2, 284.1pm) and by three oxygen (229.0-235.3) and one nitrogen (253.8) atom of separate anions (141). The two K atoms adopt eight- and six-fold coordination geometries; K(1) is surrounded by one water molecule (292.8pm), five oxygen (274.9-311.3pm) and



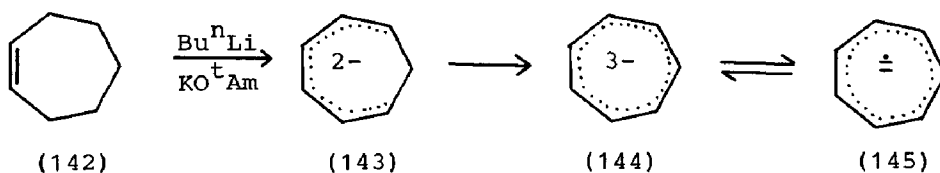
(141)

two nitrogen (288.9, 323.6pm) atoms from different anions, while K(2) interacts with five oxygen (259.9-280.2pm) and one nitrogen (287.8pm) atom provided solely by anions.³²⁵

1.4.11 Potassium, Rubidium and Caesium Derivatives

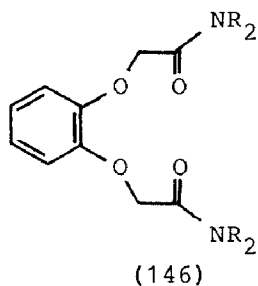
A limited number of papers pertinent to this subsection were found during the literature search; a total of seven were abstracted for potassium,³²⁷⁻³³³ one for rubidium³³⁴ and none for caesium.

The esr spectrum³²⁷ of the cycloheptatrienyl radical dianion (145) which is in equilibrium with the corresponding trianion (144), generated together with the cycloheptadienyl dianion (143), by the reaction of cycloheptane (142) with a 1:1 n-butyllithium - potassium t-amylate mixture is characteristic of the potassium



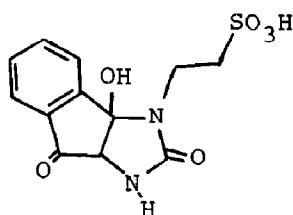
rather than the lithium salt. Although this suggests that potassium salts of hydrocarbon anions are favoured, it may be due to preference of lithium for oxygen containing anions.³²⁷

The chelation ability and coordination modes of a number of 1,2- and 1,3-phenylenedioxydiacetamides for K^+ ion have been systematically studied³²⁸ using i.r. and nmr (1H and ^{13}C) spectroscopy. Only the 1,2-diphenylenedioxydiacetamides (146) function as ligands; they act as tetradentate chelating ligands using all four oxygen atoms to bind the cation.

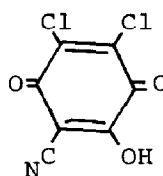


The structures of five potassium derivatives, pertinent to this subsection, have been determined. They fall into two broad classifications; those in which the K atom is surrounded by chelating ligands³²⁹ and those in which the K atom interacts with organic anions and/or solvent (water) molecules.³³⁰⁻³³³ The dimeric cationic moiety in the crystal structure of $[K(phen)_3]_2^{2+}, 2[Cr_2(CO)_{10}(\mu-H)]^{-}$ ³²⁹ is located on an inversion centre and hence contains cubic K atom coordination spheres. All six o-phenanthroline (phen) molecules act as bidentate chelating ligands; two bridge the K atoms (290.7-334.2pm) and four simply chelate them (283.5-311.7pm).³²⁹

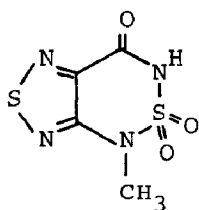
The structures of the monopotassium salts of (147),³³⁰ (148)³³¹ and (149)³³² and of dipotassium 1,3-dithiosquarate dihydrate ($T = 140K$)³³³ contain KO_6 , KO_5N , KO_7 and KO_5S_2 coordination units, respectively. The K-O contacts in the six-coordinate species, $r(K...O) = 265.1-287.8pm$ (KO_6) and $279.8-288.9pm$ (KO_5N) are considerably shorter than those in the KO_7 unit, average $r(K...O) = 291pm$, but similar to those in the KO_5S_2 unit, average $r(K...O) = 279.5pm$. The K-N (282.6pm) and K-S (344.5, 346.9pm) contacts in the KO_5N and KO_5S_2 units are typical of these coordination geometries.



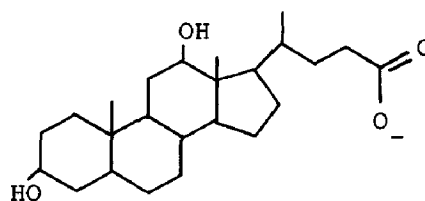
(147)



(148)



(149)



(150)

In the structure of rubidium deoxycholate-water (3/10),³³⁴ the three crystallographically different Rb atoms are surrounded by water molecules and located within the interior of 2₁ helices formed by the anions (150). Rb(1) is linked to six water molecules (294-332pm), the two oxygen atoms of a bidentate carboxylate group (310,337pm) and the oxygen atom of a monodentate carboxylate group (291pm), Rb(2) interacts solely with eight water molecules (291-332pm) and Rb(3) is coordinated by five water molecules (283-333pm), the oxygen atoms of two monodentate carboxylate groups (303,305pm) and the oxygen atom of the hydroxyl group (294pm) of a chelating anion. None of the Rb coordination units have a regular geometry.³³⁴

REFERENCES

- 1 P.Hubberstey, Coord. Chem. Rev., 66(1985)1.
- 2 P.Hubberstey, Coord. Chem. Rev., 66(1985)74.
- 3 F.Kapteijn and J.A.Moulijn, J. Chem. Soc., Chem. Commun., (1984)278.
- 4 F.Kapteijn, A.J.C.Mierop, G.Abbel and J.A.Moulijn, J. Chem. Soc., Chem. Commun., (1984)1085.
- 5 C.C.Addison, "The Chemistry of the Liquid Alkali Metals", John Wiley and Sons, Chichester, 1984.
- 6 Various articles in "Fusion Reactor Materials", Proc. Third Topical Meeting on Fusion Reactor Materials, Albuquerque, 19-22 Sept., 1983, publ. in J. Nucl. Mater., 122 and 123(1984).
- 7 Various articles in "Liquid Metal Engineering and Technology", Proc. Third Int. Conf. on Liquid Metal Engineering and Technology, Oxford, 9-13 Apr. 1984, British Nuclear Energy Society, London, Vols. 1,2(1984), Vol. 3(1985).
- 8 R.O.Bach, Ed., "Lithium - Current Applications in Science, Medicine and Technology", John Wiley and Sons, N.Y., 1985.
- 9 Various articles in J. Electrochem. Soc., 131(1984).
- 10 J.R.Hoenigman and R.G.Keil, Ref. 8, pp.233-255.
- 11 M.P.Gardener and R.E.Altermatt, Ref. 8, pp. 195-206.
- 12 A.B.Ashworth, M.G.Dowling, C.C.Addison and R.J.Pulham, Ref. 7, Vol. 3, pp. 1-6.
- 13 S.P.Awasthi, H.U.Borgstedt and G.Frees, Ref. 7, Vol. 1, pp. 265-269.
- 14 S.R.Babu, G.Periaswami, R.Geetha, T.R.Mahalingam and C.K.Mathews, Ref. 7, Vol. 1, pp. 271-275.
- 15 C.R.Pellettt and R.Thompson, Ref. 7, Vol. 3, pp.43-48.
- 16 S.P.Awasthi and M.Sundaresan, Ref. 7, Vol. 1, pp. 243-248.
- 17 B.R.Grundy, Ref. 7, Vol. 3, pp. 7-14.
- 18 P.Hubberstey and P.R.Bussey, Ref.7, Vol. 3, pp.143-149.
- 19 I.E.Schreinlechner, P.F.Sattler and J.Kozuh, Ref. 8, pp. 207-216.
- 20 R.F.Keough, G.E.Meadows, R.Kolowith, D.L.Baldwin and J.J.McCown, Ref. 7, Vol. 2, pp. 65-70.
- 21 J.Konys, Ref. 7, Vol. 2, pp. 71-76.
- 22 J.DeKeyser, F.Casteels, H.Tas, N.Rumbaut and M.Soenen, Ref. 7, Vol. 3, pp. 163-170.
- 23 M.Bouchacourt, P.Debergh, C.Oberlin and P.St.Paul, Ref. 7, Vol. 1, pp. 45-52.
- 24 L.Mason, N.S.Morrison, C.M.Robertson and E.A.Trevillion, Ref. 7, Vol. 1, pp. 53-59.
- 25 U.Buckmann, J.Jung and H.Runge, Ref. 7, Vol. 1, pp. 61-65.
- 26 H.Nafe, Ref. 7, Vol. 1, pp. 381-386.
- 27 H.Ullmann, H.-J.Lang, W.Richter, F.A.Kozlov, T.A.Vorob'eva, Yu.A.Tsoj and S.A.Davydov, Ref. 7, Vol. 1, pp. 387-392.
- 28 R.C.Asher et. al., Ref. 7, Vol. 1, pp. 393-398.
- 29 G.Periaswami, T.Gnanasekaran, V.Ganesan and C.K.Mathews, Ref. 7, Vol. 1, pp. 399-403.
- 30 V.Ganesan, T.Gnanasekaran, R.Sridharan, G.Periaswami and C.K.Mathews, Ref. 7, Vol. 1, pp. 369-373.
- 31 V.Leonelli, G.Casavola, B.DeLuca, G.Furguele and S.Orsini, Ref. 7, Vol. 3, pp. 111-115.
- 32 H.U.Borgstedt, C.K.Mathews and S.R.Pillai, Ref. 7, Vol. 1, pp. 75-78.
- 33 D.Rettig, K.Teske, H.Ullmann, F.A.Kozlov, Yu.I.Zagoru'lko, Yu.P.Kovalev, Yu.V.Privalov and N.M.Ledovskikh, Ref. 7, Vol. 1, pp. 67-73.
- 34 C.A.Smith and P.A.Simm, Ref. 7, Vol. 3, pp. 103-109.

- 35 M.N.Ivanovskii, V.A.Morosov, A.L.Shimkevich and B.A.Schmatko, Ref. 7, Vol. 3, pp. 15-22.
- 36 P.Hubberstey and A.T.Dadd, J. Nucl. Mater., 122,123(1984)1231.
- 37 P.Hubberstey and P.G.Roberts, J. Nucl. Mater., 120(1984)74.
- 38 P.Hubberstey, Ref. 7, Vol. 2, pp. 85-91.
- 39 H.Migge, J. Nucl. Mater., 122,123(1984)903.
- 40 M.G.Barker, S.A.Frankham and N.J.Moon, Ref. 7, Vol. 2, pp. 77-83.
- 41 H.U.Borgstedt and S.R.Pillai, Ref. 7, Vol. 2, pp. 269-272.
- 42 A.J.Hooper, E.A.Trevillion and A.C.Whittingham, Ref. 7, Vol. 2, pp. 255-260.
- 43 J.H.DeVan and C.Bagnall, Ref. 7, Vol. 3, pp. 65-72.
- 44 O.K.Chopra and P.F.Tortorelli, J. Nucl. Mater., 122,123(1984)1201.
- 45 Y.Suzuki, I.Mutoh, M.Koyama, Y.Ikenaga, Y.Ishida and T.Kobayashi, Ref. 7, Vol. 1, pp. 215-222.
- 46 A.M.Garcia, M.M.Espigares, J.Arroyo and H.U.Borgstedt, Ref. 7, Vol. 1, pp. 223-227.
- 47 T.Hirano, T.Suzuki and R.Watanabe, Ref. 7, Vol. 1, pp. 229-233.
- 48 B.H.Kolster and L.Bos, Ref. 7, Vol. 1, pp. 235-241.
- 49 A.W.Thorley, Ref. 7, Vol. 3, pp. 31-41.
- 50 M.G.Barker and D.R.Moore, Ref. 7, Vol. 2, pp. 249-253.
- 51 S.Casadio, G.D'Alessandro, F.Pierdominici, C.Meloni and M.Vittori, Ref. 7, Vol. 2, pp. 261-267.
- 52 P.J.Jeffcoat and A.W.Thorley, Ref. 7, Vol. 2, pp. 489-496.
- 53 A.W.Thorley, A.Blundell and W.G.Murphy, Ref. 7, Vol. 3, pp. 197-205.
- 54 P.Roy and G.J.Licina, Ref. 7, Vol. 3, pp. 207-211.
- 55 Yu.I.Zagorulko and F.A.Kozlov, Ref. 7, Vol. 3, pp. 213-216.
- 56 M.R.Hobdell, G.Skyrme and E.A.Trevillion, Ref. 7, Vol. 3, pp. 217-224.
- 57 F.Casteels, J.DeKeyser, M.Soenen, H.Tas and J.Dresselaers, Ref. 7, Vol. 3, pp. 73-80.
- 58 P.F.Tortorelli and J.H.DeVan, Ref. 7, Vol. 3, pp. 81-88.
- 59 H.R.Konvicka and P.F.Sattler, Ref. 7, Vol. 3, pp. 89-92.
- 60 H.R.Konvicka and P.A.Sattler, J. Nucl. Mater., 122, 123(1984)1241.
- 61 E.Reudl, V.Coen, T.Sasaki and H.Kolbe, J. Nucl. Mater., 122,123(1984)1247.
- 62 K.Shibata, K.Suzuki, Y.Narita and C.Yamanaka, J. Nucl. Chem., 122,123(1984)1252.
- 63 P.F.Tortorelli and J.H.DeVan, J. Nucl. Chem., 122,123(1984)1258.
- 64 O.K.Chopra and D.Smith, J. Nucl. Mater., 122,123(1984)1219.
- 65 P.F.Tortorelli and J.H.DeVan, J. Nucl. Chem., 122,123(1984)1264.
- 66 V.Coen, A.T.Dadd, H.Kolbe and L.Orecchia, Ref. 7, Vol. 1, pp. 347-354.
- 67 F.D.Schowengerdt, Ref. 8, pp. 217-231.
- 68 Y.C.Chan and E.Veleckis, J. Nucl. Mater., 122,123(1984)935.
- 69 C.H.Wu, J. Nucl. Mater., 122,123(1984)941.
- 70 M.Hoch, J. Nucl. Mater., 120(1984)102.
- 71 W.R.Watson and R.J.Pulham, Ref. 7, Vol. 3, pp. 99-102.
- 72 R.E.Buxbaum, J. Less Common Metals, 97(1984)27.
- 73 M.G.Barker, Ref. 8, pp. 177-185.
- 74 I.Schreinlechner, F.Holub and K.Schwetz, Ref. 7, Vol. 3, pp. 93-97.
- 75 M.A.Mignanelli and P.E.Potter, J. Nucl. Chem., 125(1984)182.

- 76 M.A.Mignanelli and P.E.Potter, Ref. 7, Vol. 2, pp. 117-124.
77 J.Jung and H.Runge, Ref. 7, Vol. 2, pp. 315-320.
78 T.Suzuki, S.Masuda and Y.Tanazawa, J. Nucl. Mater.,
127(1985)113.
79 P.G.Gadd and H.U.Borgstedt, Ref. 7, Vol. 2, pp. 107-111.
80 B.P.Alblas, W. van der Lugt, J.Dijkstra and C. van Dijk,
J. Phys. F: Met. Phys., 14(1984)1995.
81 H.Ruppersberg and W.Schirmacher, J. Phys. F: Met. Phys.,
14(1984)2787.
82 H.Ruppersberg, J. Phys. F: Met. Phys., 14(1984)L197.
83 P.Hubberstey, P.G.Roberts and A.T.Dadd, J. Less Common
Metals, 98(1984)141.
84 T.Itami, S.Takahashi and M.Shimoji, J. Phys. F: Met. Phys.,
14(1984)427.
85 J.Hafner, A.Pasturel and P.Hicter, J. Phys. F: Met. Phys.,
14(1984)1137.
86 J.Hafner, A.Pasturel and P.Hicter, J. Phys. F: Met. Phys.,
14(1984)2279.
87 K.N.Khanna, J. Phys. F: Met. Phys., 14(1984)1827.
88 M.-L.Saboungi and T.P.Corbin, J. Phys. F: Met. Phys.,
14(1984)13.
89 B.P.Alblas, W. van der Lugt, J.Dijkstra, W.Geertsma and
C. van Dijk, J. Phys. F: Met. Phys., 13(1983)2465.
90 P.Hubberstey, Coord. Chem. Rev., 66(1985)7.
91 J.G.Kirkwood and F.P.Buff, J. Chem. Phys., 19(1951)774.
92 J.Evers, G.Oehlinger, G.Sextl and A.Weiss, Angew. Chem.,
Int. Ed. Engl., 23(1984)528.
93 K.A.Tschuntonow, S.P.Yatsenko, Yu.N.Hryn, Ya.P.Yarmolyuk
and A.N.Orlov, J. Less Common Metals, 99(1984)15.
94 W.Geertsma, J.Dijkstra and W. van der Lugt, J. Phys. F:
Met. Phys., 14(1984)1833.
95 R.Teghil, B.Janis and L.Bencivenni, Inorg. Chim. Acta,
88(1984)115.
96 L.Bencivenni, K.A.Gingerich and R.Teghil, Inorg. Chim. Acta,
85(1984)L11.
97 I.R.Beattie and J.E.Parkinson, J. Chem. Soc., Dalton Trans.,
(1984)1363.
98 L.Bencivenni, H.M.Nagarathna, D.W.Wilhite and K.A.Gingerich,
Inorg. Chem., 23(1984)1279.
99 S.A.Arthers, I.R.Beattie and P.J.Jones, J. Chem. Soc.,
Dalton Trans., (1984)711.
100 Z.H.Kafafi, R.H.Hauge, W.E.Billups and J.L.Margrave,
Inorg. Chem., 23(1984)177.
101 S.B.H.Bach and B.S.Ault, Inorg. Chem., 23(1984)4394.
102 N.G.Rambidi, Yu.G.Abashkin and A.I.Dement'ev, Russ. J.
Inorg. Chem., 29(1984)1719.
103 S.P.Konovalov and V.G.Solomonik, Russ. J. Inorg. Chem.,
29(1984)948.
104 A.M.Sapse, J.D.Bunce and D.C.Jain, J. Am. Chem. Soc.,
106(1984)6579.
105 C.J.Marsden, J. Chem. Soc., Dalton Trans., (1984)1279.
106 A.-M.Sapse, E.Kaufman, P. von R.Schleyer and R.Gleiter,
Inorg. Chem., 23(1984)1569.
107 E.Kaufmann, T.Clark and P. von R.Schleyer, J. Am. Chem.
Soc., 106(1984)1856.
108 M.Hodoscek and T.Solmajer, J. Am. Chem. Soc., 106(1984)1854.
109 K.Mizutani, T.Yano, A.Sekiguchi, K.Hayashi and
S.Matsumoto, Bull. Chem. Soc., Japan, 57(1984)3368.
110 V.I.Baranovskii, O.V.Sizova and N.V.Ivanova, Russ. J.
Inorg. Chem., 29(1984)483.

- 111 G.Boche and H.U.Wagner, J. Chem. Soc., Chem. Commun., (1984)1591.
- 112 E.-U.Wurthwein, P. von R.Schleyer and J.A.Pople, J. Am. Chem. Soc., 106(1984)6973.
- 113 J.W.Chinn, J.A.Gurak and R.J.Lagow, Ref. 8, pp. 291-305.
- 114 A.Maercker and M.Theis, Angew. Chem., Int. Ed. Engl., 23(1984)995.
- 115 J.A.Gurak, J.W.Chinn, R.J.Lagow, H.Steinfink and C.S.Yannoni, Inorg. Chem., 23(1984)3717.
- 116 H.Kawa, J.W.Chinn and R.J.Lagow, J. Chem. Soc., Chem. Commun., (1984)1664.
- 117 S.M.Bachrach and A.Streitwieser, J. Am. Chem. Soc., 106(1984)5818.
- 118 P. von R.Schleyer, T.Clark, A.J.Kos, G.W.Spitznagel, C.Rohde, D.Arad, K.N.Houk and N.G.Rondan, J. Am. Chem. Soc., 106(1984)6467.
- 119 R.S.McDowell and A.Streitwieser, J. Am. Chem. Soc., 106(1984)4047.
- 120 J.W.Chinn and R.J.Lagow, J. Am. Chem. Soc., 106(1984)3694.
- 121 A.J.Kos, T.Clark and P. von R.Schleyer, Angew. Chem., Int. Ed. Engl., 23(1984)620.
- 122 R.L.Disch, J.M.Schulman and J.P.Richie, J. Am. Chem. Soc., 106(1984)6246.
- 123 G.Boche, G.Decker, H.Etzrodt, H.Dietrich, W.Mahdi, A.J.Kos and P. von R.Schleyer, J. Chem. Soc., Chem. Commun., (1984)1493.
- 124 P. von R.Schleyer, A.J.Kos, D.Wilhelm, T.Clark, G.Boche, G.Decker, H.Etzrodt, H.Dietrich and W.Mahdi, J. Chem. Soc., Chem. Commun., (1984)1495.
- 125 P.Hubberstey, Coord. Chem. Rev., 56(1984)27.
- 126 C.E.Johnson and G.W.Hollenberg, J. Nucl. Mater., 122,123 (1984)871.
- 127 H.Yoshida, S.Konishi, H.Takeshita, T.Kurusawa, H.Watanabe and Y.Naruse, J. Nucl. Mater., 122,123(1984)934.
- 128 M.Tetenbaum and C.E.Johnson, J. Nucl. Mater., 126(1984)25.
- 129 J.H.Norman and G.R.Hightower, J. Nucl. Mater., 122,123(1984)913.
- 130 H.R.Ihle and C.H.Wu, J. Nucl. Mater., 122,123(1984)901.
- 131 R.J.Pulham, W.R.Watson and J.S.Collinson, J. Nucl. Mater., 122,123(1984)1243.
- 132 J.S.Collinson and R.J.Pulham, Ref. 7, Vol. 1, pp. 355-359.
- 133 C.B.Chan, N.H.Tioh and G.T.Hefter, Polyhedron, 3(1984)845.
- 134 G.G.Birdukovskaya, L.S.Kudin, M.F.Butman and K.S.Krasnov, Russ. J. Inorg. Chem., 29(1984)1726.
- 135 B.Schoch, A.Rabenau, W.Weppner and H.Hahn, Z. Anorg. Allg. Chem., 518(1984)137.
- 136 H.Sabrowsky and A.Thimm, Naturwissenschaften, 71(1984)635.
- 137 H.C.Gaebell and G.Meyer, Z. Anorg. Allg. Chem., 513(1984)15.
- 138 H.T.Evans, J.A.Konnert, I.-M.Chou and L.A.Romankiw, Acta Crystallogr., Sect. B, 40(1984)86.
- 139 P.Pattison, N.K.Hansen and J.R.Schneider, Acta Crystallogr., Sect. B, 40(1984)38.
- 140 S.R.Aghdaee and A.I.M.Rae, Acta Crystallogr., Sect. B, 40(1984)214.
- 141 W.Honle, H.G. von Schnering, A.Schmidpeter and G.Burget, Angew. Chem., Int. Ed. Engl., 23(1984)817.
- 142 K.Mereiter, A.Preisinger, A.Zellner, W.Mikenda and H.Steidl, J. Chem. Soc., Dalton Trans., (1984)1275.

- 143 H.Jacobs, T.Tacke and J.Kockelkorn, *Z. Anorg. Allg. Chem.*, 516(1984)67.
- 144 I.Grund, H.-U.Schuster and P.Muller, *Z. Anorg. Allg. Chem.*, 515(1984)151.
- 145 P.Wenz and H.-U.Schuster, *Z. Naturforsch., Teil B*, 39(1984)1816.
- 146 P.Hubberstey, *Coord. Chem. Rev.*, 66(1985)30.
- 147 R.Werthmann and R.Hoppe, *Z. Anorg. Allg. Chem.*, 509(1984)7.
- 148 R.Luge and R.Hoppe, *Naturwissenschaften*, 71(1984)264.
- 149 W.Losert and R.Hoppe, *Z. Anorg. Allg. Chem.*, 515(1984)87.
- 150 R.Hoppe and R.Baier, *Z. Anorg. Allg. Chem.*, 511(1984)161.
- 151 P.Kroeschell and R.Hoppe, *Z. Anorg. Allg. Chem.*, 509(1984)127.
- 152 R.Werthmann and R.Hoppe, *Z. Anorg. Allg. Chem.*, 519(1984)117.
- 153 K.Kato and E.Takayama, *Acta Crystallogr., Sect. B*, 40(1984)102.
- 154 B.-O.Marinder and M.Sundberg, *Acta Crystallogr., Sect. B*, 40(1984)82.
- 155 G.Brachtel, N.Bukovec and R.Hoppe, *Z. Anorg. Allg. Chem.*, 515(1984)101.
- 156 T.Betz and R.Hoppe, *Z. Anorg. Allg. Chem.*, 512(1984)19.
- 157 R.Luge and R.Hoppe, *Z. Anorg. Allg. Chem.*, 513(1984)141.
- 158 H.J.Orman and P.J.Wiseman, *Acta Crystallogr., Sect. C*, 40(1984)12.
- 159 M.I.Gadzhiev and I.S.Shaplygin, *Russ. J. Inorg. Chem.*, 29(1984)1231.
- 160 W.Losert and R.Hoppe, *Z. Anorg. Allg. Chem.*, 515(1984)95.
- 161 H.Leuken, P.Hannibal and U.Stamm, *Z. Anorg. Allg. Chem.*, 516(1984)107.
- 162 Y.Kera, *Bull. Chem. Soc. Japan*, 57(1984)1478.
- 163 E.V.Proskuryakova, N.V.Porotnikov and N.G.Chaban, *Russ. J. Inorg. Chem.*, 29(1984)780.
- 164 K.O.Klepp and W.Bronger, *J. Less Common Metals*, 98(1984)165.
- 165 V.M.Bazhenov, S.P.Raspopin and Yu.F.Chervinskii, *Russ. J. Inorg. Chem.*, 29(1984)1814;
- 166 V.V.Safonov and V.A.Mireev, *Russ. J. Inorg. Chem.*, 29(1984)1050.
- 167 N.D.Chikanov, *Russ. J. Inorg. Chem.*, 29(1984)1235.
- 168 A.M.Podorozhnyi and V.V.Safonov, *Russ. J. Inorg. Chem.*, 29(1984)1393.
- 169 A.G.Dudareva, O.V.Polyanskaya, N.V.Tenyanko, A.I.Ezhov and A.B.Strekachinskii, *Russ. J. Inorg. Chem.*, 29(1984)1512.
- 170 I.N.Belyaev, D.S.Lesnykh and I.G.Eikhenbaum, *Russ. J. Inorg. Chem.*, 15(1970)430.
- 171 G.Meyer, *Z. Anorg. Allg. Chem.*, 517(1984)191.
- 172 H.-C.Gaebell and G.Meyer, *Z. Anorg. Allg. Chem.*, 515(1984)133.
- 173 S.Ohba and Y.Saito, *Acta Crystallogr., Sect. C*, 40(1984)1639.
- 174 R.E.Schmidt and D.Babel, *Z. Anorg. Allg. Chem.*, 516(1984)187.
- 175 M.Ledesert and J.C.Monier, *Acta Crystallogr., Sect. B*, 40(1984)73.
- 176 G.Meyer, *Z. Anorg. Allg. Chem.*, 511(1984)193.
- 177 B.F.Hoskins, A.Linden, P.C.Mulvaney and T.A.O'Donnell, *Inorg. Chim. Acta*, 88(1984)217.

- 178 G.Meyer, *Z. Anorg. Allg. Chem.*, 515(1984)127.
- 179 G.Meyer, P.Ax, A.Cromm and H.Linzmeier, *J. Less Common Metals*, 98(1984)323.
- 180 K.Koyama, Y.Hashimoto, S.Omori and K.Terawaki, *Bull. Chem. Soc. Japan*, 57(1984)2311.
- 181 D.Altermatt, H.Arend, V.Gramlich, A.Niggli and W.Petter, *Acta Crystallogr., Sec. B*, 40(1984)347.
- 182 A.Bogacz, W.Szczepaniak, J.-P.Bros, Y.Fouque and M.Gaune-Escard, *J. Chem. Soc., Faraday Trans. I*, 80(1984)2935.
- 183 C.-Q.Wu and R.Hoppe, *Z. Anorg. Allg. Chem.*, 514(1984)92.
- 184 Y.S.Hong, K.N.Baker, C.F.Williamson and W.O.J.Boo, *Inorg. Chem.*, 23(1984)2787.
- 185 J.E.Ford, G.Meyer and J.D.Corbett, *Inorg. Chem.*, 23(1984)2094.
- 186 J.D.Smith and J.D.Corbett, *J. Am. Chem. Soc.*, 106(1984)4618.
- 187 U.Kampli and H.U.Gudel, *Inorg. Chem.*, 23(1984)3479.
- 188 K.G.G.Hopkins and P.G.Nelson, *J. Chem. Soc., Dalton Trans.*, (1984)1393.
- 189 P.Hubberstey, *Coord. Chem. Rev.*, 66(1985)41.
- 190 G.E.Pacey, *Ref. 8*, pp. 35-45.
- 191 X.-Y.Xu and J.Smid, *J. Am. Chem. Soc.*, 106(1984)3790.
- 192 G.Weber, F.Hirayama, W.Saenger and G.M.Sheldrick, *Acta Crystallogr., Sec. C*, 40(1984)1570.
- 193 D.L.Hughes and J.N.Wingfield, *J. Chem. Soc., Chem. Commun.*, (1984)408.
- 194 D.L.Hughes and J.N.Wingfield, *J. Chem. Soc., Dalton Trans.*, (1984)1187.
- 195 B.G.Cox, N. van Truong, J.Rzeszotarska and H.Schneider, *J. Chem. Soc., Faraday Trans. I*, 80(1984)3275.
- 196 B.G.Cox, N. van Truong, J.Rzeszotarska and H.Schneider, *J. Am. Chem. Soc.*, 106(1984)5965.
- 197 J.-H.Fuhrhop and U.Liman, *J. Am. Chem. Soc.*, 106(1984)4643.
- 198 D.M.Holton, P.P.Edwards, D.C.Johnson, C.J.Page, W.McFarlane, B.Wood, *J. Chem. Soc., Chem. Commun.*, (1984)740.
- 199 Y.Hasegawa, T.Nakano, Y.Odiri and Y.Ishikawa, *Bull. Chem. Soc. Japan*, 57(1984)8.
- 200 Y.Takeda, T.Namiasaki and S.Fujiwara, *Bull. Chem. Soc. Japan*, 57(1984)1055.
- 201 E.Buncel, H.S.Shin, R.A.B.Bannard and J.G.Purdon, *Canad. J. Chem.*, 62(1984)926.
- 202 E.Makrlik, J.Halova and M.Kyrs, *Coll. Czech. Chem. Commun.*, 49(1984)39.
- 203 Y.Takeda, Y.Ohyagi and S.Akabori, *Bull. Chem. Soc. Japan*, 57(1984)3381.
- 204 T.G.Myasoedova, A.V.Ponomareva, P.A.Zagorets and E.A.Filippov, *Russ. J. Inorg. Chem.*, 29(1984)1109.
- 205 B.R.Bowsher, A.J.Rest and B.G.Main, *J. Chem. Soc., Dalton Trans.*, (1984)1421.
- 206 K.Kimura, E.Hayata and T.Shono, *J. Chem. Soc., Chem. Commun.*, (1984)271.
- 207 H.Dugas, P.Keroack and M.Plak, *Canad. J. Chem.*, 62(1984)489.
- 208 T.M.Fyles and D.M.Whitfield, *Canad. J. Chem.*, 62(1984)507.
- 209 L.M.Dulyea, T.M.Fyles and D.M.Whitfield, *Canad. J. Chem.*, 62(1984)498.
- 210 E.Blasius, R.A.Rausch, G.D.Andreetti and J.Rebizant, *Chem. Ber.*, 117(1984)1113.
- 211 H.Hope, M.M.Olmstead, P.P.Power and X.Xu, *J. Am. Chem. Soc.*, 106(1984)819.

- 212 P.P.Power and X.Xiaojie, *J. Chem. Soc., Chem. Commun.*, (1984)358.
- 213 D.L.Ward, A.I.Popov and N.S.Poonia, *Acta Crystallogr., Sec. C*, 40(1984)238.
- 214 D.L.Ward, A.I.Popov and N.S.Poonia, *Acta Crystallogr., Sec. C*, 40(1984)1183.
- 215 C.M.Means, N.C.Means, S.G.Bott and J.L.Atwood, *J. Am. Chem. Soc.*, 106(1984)7627.
- 216 J.D.Owen, M.R.Truter and J.N.Wingfield, *Acta Crystallogr., Sec. C*, 40(1984)1515.
- 217 J.M.Maud, J.F.Stoddart, H.M.Colquhoun and D.J.Williams, *Polyhedron*, 3(1984)675.
- 218 T.Mashiko, C.A.Reed, K.J.Haller and W.R.Scheidt, *Inorg. Chem.*, 23(1984)3192.
- 219 G.Weber, G.M.Sheldrick, A.Menz and F.Dietl, *Inorg. Chim. Acta*, 90(1984)L1.
- 220 M.Ouchi, Y.Inove, T.Kanzaki and T.Hakushi, *Bull. Chem. Soc. Japan*, 57(1984)887.
- 221 S.Kitazawa, K.Kimura, H.Yano and T.Shono, *J. Am. Chem. Soc.*, 106(1984)6978.
- 222 C.S.Chen, S.J.Wang and S.C.Wu, *Inorg. Chem.*, 23(1984)3901.
- 223 E.M.Holt, G.D.Malpass, R.G.Ghirardelli, R.A.Palmer and B.Rubin, *Acta Crystallogr., Sec. C*, 40(1984)394.
- 224 E.M.Holt, G.D.Malpass, R.G.Ghirardelli, R.A.Palmer and B.Rubin, *Acta Crystallogr., Sec. C*, 40(1984)396.
- 225 G.Shoham, D.W.Christianson, R.A.Bartsch, G.S.Heo, U.Olsher and W.N.Lipscomb, *J. Am. Chem. Soc.*, 106(1984)1280.
- 226 L.Echegoyen, A.Kaifer, H.Durst, R.A.Schultz, D.M.Dishong, D.M.Goli and G.W.Gokel, *J. Am. Chem. Soc.*, 106(1984)5100.
- 227 I.Ikeda, H.Emura and M.Okahara, *Bull. Chem. Soc. Japan*, 57(1984)1612.
- 228 J.F.Koszuk, B.P.Czech, W.Walkowiak, D.A.Babb and R.A.Bartsch., *J. Chem. Soc., Chem. Commun.*, (1984)1504.
- 229 S.Shinkai, M.Ishihara, K.Ueda and O.Manabe, *J. Chem. Soc., Chem. Commun.*, (1984)727.
- 230 H.Bock, B.Hierholzer, F.Vogtle and G.Hollmann, *Angew. Chem. Int. Ed. Engl.*, 23(1984)57.
- 231 F.R.Fronczek, V.J.Gatto, C.Minganti, R.A.Schultz, R.D.Gandour and G.W.Gokel, *J. Am. Chem. Soc.*, 106(1984)7244.
- 232 H.Tsukube, *J. Chem. Soc., Chem. Commun.*, (1984)314.
- 233 V.J.Gatto and G.W.Gokel, *J. Am. Chem. Soc.*, 106(1984)8240.
- 234 S.Shinkai, K.Inuzuka, K.Hara, T.Sone and O.Manabe, *Bull. Chem. Soc. Japan*, 57(1984)2150.
- 235 Y.Nakatsuji, T.Mori and M.Okahara, *J. Chem. Soc., Chem. Commun.*, (1984)1045.
- 236 M.Shiga, H.Nakamura, M.Takayi and K.Ueno, *Bull. Chem. Soc. Japan*, 57(1984)412.
- 237 K.Hiratani and S.Aiba, *Bull. Chem. Soc. Japan*, 57(1984)2657.
- 238 K.Kimura, K.Kumami, S.Kitazawa and T.Shuno, *J. Chem. Soc., Chem. Commun.*, (1984)442.
- 239 T.Izumi, T.Tezuka, S.Yusa and A.Kasahara, *Bull. Chem. Soc. Japan*, 57(1984)2435.
- 240 S.Akabori, Y.Habata and M.Sato, *Bull. Chem. Soc. Japan*, 57(1984)68.
- 241 G.Weber, *Acta Crystallogr., Sec. C*, 40(1984)592.
- 242 J.D.Owen, *Acta Crystallogr., Sec. C*, 40(1984)951.
- 243 J.D.Owen, *Acta Crystallogr., Sec. C*, 40(1984)246.
- 244 G.Casini, F. de Sarlo, D.Donati, A.Guarna and P.Orioli, *J. Chem. Research (S)*, (1984)2.
- 245 A.F.Danil de Namor and L.Ghousseini, *J. Chem. Soc., Faraday Trans. I*, 80(1984)2349.

- 246 B.G.Cox, N. van Truong and H.Schneider, *J. Am. Chem. Soc.*, 106(1984)1273.
- 247 J.M.Bemtgen, M.E.Springer, V.M.Loyola, R.G.Wilkins and R.W.Taylor, *Inorg. Chem.*, 23(1984)3348.
- 248 S.C.Critchlow and J.D.Corbett, *Inorg. Chem.*, 23(1984)770.
- 249 A.R.Kauser, *Inorg. Chim. Acta*, 86(1984)61.
- 250 T.Alfheim, J.Dale, P.Groth and K.D.Krautworst, *J. Chem. Soc., Chem. Commun.*, (1984)1502.
- 251 P.Groth, *Acta Chem. Scand., Ser. A*, 38(1984)183.
- 252 K.B.Yatsimirskii, M.I.Kabachnik, E.I.Sinyavskaya, T.Y.Medved', Y.M.Polikarpov, and B.K.Shcherbakov, *Russ. J. Inorg. Chem.*, 29(1984)510.
- 253 K.B.Yatsimirskii, E.I.Sinyavskaya, L.V.Tsymbal, T.Y.Medved', B.K.Shcherbakov, Y.M.Polikarpov and M.I.Kabachnik, *Russ. J. Inorg. Chem.*, 29(1984)512.
- 254 R.W.Hay and D.M.S.Clark, *Inorg. Chim. Acta*, 83(1984)L23.
- 255 S.Buoen, J.Dale, P.Groth and J.Krane, *J. Chem. Soc., Chem. Commun.*, (1982)1172.
- 256 S.Ogawa, R.Narushima and Y.Arai, *J. Am. Chem. Soc.*, 106(1984)5760.
- 257 T.W.Bell and F.Guzzo, *J. Am. Chem. Soc.*, 106(1984)6111.
- 258 V.A.Bidzilya, L.P.Oleksenko, V.G.Golovaty and V.T.Shabel'nikov, *Russ. J. Inorg. Chem.*, 29(1984)808.
- 259 V.McKee, C.C.Ong and G.A.Rodley, *Inorg. Chem.*, 23(1984)4242.
- 260 X.He and B.Craven, *Acta Crystallogr., Sec. C*, 40(1984)1157.
- 261 I.Ymen, *Acta Crystallogr., Sec. C*, 40(1984)33.
- 262 I.Ymen, *Acta Crystallogr., Sec. C*, 40(1984)241.
- 263 A.Oskersson and I.Ymen, *Acta Crystallogr., Sec. C*, 40(1984)30.
- 264 R.G.Delaplane, R.Tellgren and I.Olovsson, *Acta Crystallogr., Sec. C*, 40(1984)1800.
- 265 G.Olovsson, I.Olovsson and M.S.Lehmann, *Acta Crystallogr., Sec. C*, 40(1984)1521.
- 266 T.Lis and J.Matuszewski, *Acta Crystallogr., Sec. C*, 40(1984)2016.
- 267 T.Lis, *Acta Crystallogr., Sec. C*, 40(1984)376.
- 268 J.D.Oliver, B.L.Barnett and L.C.Strickland, *Acta Crystallogr., Sec. C*, 40(1984)377.
- 269 J.-P.Legros, D.Troy and J.Galy, *Acta Crystallogr., Sec. C*, 40(1984)801.
- 270 J.C.W.Mak, W.-H.Yip, G.Smith, E.J.O'Reilly and C.H.L.Kennard, *Inorg. Chim. Acta*, 88(1984)35.
- 271 R.Faggiani, H.E.Howard-Lock, C.J.L.Lock, M.L.Martins, and P.S.Smalley, *Canad. J. Chem.*, 62(1984)1127.
- 272 R.Mattes and B.Fusser, *Z. Naturforsch., Teil B*, 39(1984)1.
- 273 J.C.Barnes and J.D.Paton, *Acta Crystallogr., Sec. C*, 40(1984)1809.
- 274 B.Schubert and E.Weiss, *Chem. Ber.*, 117(1984)366.
- 275 A.Se bald, B.Wrackmeyer, C.R.Theocharis and W.Jones, *J. Chem. Soc., Dalton Trans.*, (1984)747.
- 276 H.Hope, D.Oram and P.P.Power, *J. Am. Chem. Soc.*, 106(1984)1149.
- 277 G. van Koten, J.T.B.H.Jastrzebski, C.H.Stam and N.C.Niemann, *J. Am. Chem. Soc.*, 106(1984)1880.
- 278 H.Schumann, H.Lauke, E.Hahn and H.Pickardt, *J. Organomet. Chem.*, 263(1984)29.
- 279 S.Gambarotta, M.Mazzanti, C.Floriani and M.Zehnder, *J. Chem. Soc., Chem. Commun.*, (1984)1116.
- 280 S.Gambarotta, F.Corazza, C.Floriani and M.Zehnder, *J. Chem. Soc., Chem. Commun.*, (1984)1305.

- 281 P.Hubberstey, *Coord. Chem. Rev.*, 66(1985)74.
- 282 W.Isenberg, R.Mews and G.M.Sheldrick, *Angew. Chem., Int. Ed. Engl.*, 23(1984)795.
- 283 D.Barr, W.Clegg, R.E.Mulvey and R.Snaith, *J. Chem. Soc., Chem. Commun.*, (1984)226.
- 284 A.L.Spek, A.J.M.Duisenberg, G.W.Klumpp and P.J.A.Geurink, *Acta Crystallogr., Sec. C.*, 40(1984)372.
- 285 D.Barr, W.Clegg, R.E.Mulvey and R.Snaith, *J. Chem. Soc., Chem. Commun.*, (1984)79.
- 286 O.Graalmann, U.Klingebeil, W.Clegg, M.Haase and G.M.Sheldrick, *Angew. Chem., Int. Ed. Engl.*, 23(1984)891.
- 287 L.M.Jackman and L.M.Scarmoutzos, *J. Am. Chem. Soc.*, 106(1984)4627.
- 288 D.Barr, W.Clegg, R.E.Mulvey and R.Snaith, *J. Chem. Soc., Chem. Commun.*, (1984)285.
- 289 D.Barr, W.Clegg, R.E.Mulvey and R.Snaith, *J. Chem. Soc., Chem. Commun.*, (1984)287.
- 290 B.Cetinkaya, P.B.Hitchcock, M.F.Lappert, M.C.Misra and A.J.Thorne, *J. Chem. Soc., Chem. Commun.*, (1984)148.
- 291 A.Schmidpeter, G.Burget, H.G. von Schnering and D.Weber, *Angew. Chem., Int. Ed. Engl.*, 23(1984)816.
- 292 C.P.Rao, A.M.Rao and C.N.R.Rao, *Inorg. Chem.*, 23(1984)2080.
- 293 D.Barr, W.Clegg, R.E.Mulvey and R.Snaith, *J. Chem. Soc., Chem. Commun.*, (1984)974.
- 294 D.Barr, W.Clegg, R.E.Mulvey and R.Snaith, *J. Chem. Soc., Chem. Commun.*, (1984)700.
- 295 D.Seebach, W.Bauer, J.Hansen, T.Laube, W.B.Schweizer and J.D.Dunitz, *J. Chem. Soc., Chem. Commun.*, (1984)853.
- 296 D.Colgan, R.I.Papasergio, C.L.Raston and A.H.White, *J. Chem. Soc., Chem. Commun.*, (1984)1708.
- 297 R.L.Polt, G.Stork, G.B.Carpenter and P.G.Williard, *J. Am. Chem. Soc.*, 106(1984)4276.
- 298 T.Fjeldberg, P.B.Hitchcock, M.F.Lappert and A.J.Thorne, *J. Chem. Soc., Chem. Commun.*, (1984)822.
- 299 T.Fjeldberg, M.F.Lappert and A.J.Thorne, *J. Mol. Struct.*, 125(1984)265.
- 300 P.B.Hitchcock, M.F.Lappert, P.P.Power and S.J.Smith, *J. Chem. Soc., Chem. Commun.*, (1984)1669.
- 301 L.M.Engelhardt, G.E.Jacobsen, C.L.Raston and A.H.White, *J. Chem. Soc., Chem. Commun.*, (1984)220.
- 302 H.H.Karsch and G.Muller, *J. Chem. Soc., Chem. Commun.*, (1984)569.
- 303 H.H.Karsch, L.Weber, D.Wewers, R.Boese and G.Muller, *Z. Naturforsch., Teil B*, 39(1984)1518.
- 304 D.Barr, W.Clegg, R.E.Mulvey and R.Snaith, *J. Chem. Soc., Chem. Commun.*, (1984)469.
- 305 C.Eaborn, M.N.A.El-Kheli, P.B.Hitchcock and J.D.Smith, *J. Chem. Soc., Chem. Commun.*, (1984)1673.
- 306 C.Eaborn, P.B.Hitchcock, J.D.Smith and A.C.Sullivan, *J. Chem. Soc., Chem. Commun.*, (1984)870.
- 307 H.Schumann, I.Albrecht, J.Pickardt and E.Hahn, *J. Organomet. Chem.*, 276(1984)C5.
- 308 W.Clegg, D.A.Brown, S.J.Bryan and K.Wade, *Polyhedron*, 3(1984)307.
- 309 H.H.Karsch, A.Appelt and G.Muller, *J. Chem. Soc., Chem. Commun.*, (1984)1415.
- 310 K.C.Waterman and A.Streitwieser, *J. Am. Chem. Soc.*, 106(1984)3138.
- 311 M.F.Lappert, A.Singh, L.M.Engelhardt and A.H.White, *J. Organomet. Chem.*, 262(1984)271.

- 312 W.-P.Leung, C.L.Raston, B.W.Skelton and A.H.White,
J. Chem. Soc., Dalton Trans., (1984)1801.
- 313 L.M.Engelhardt, W.-P.Leung, C.L.Raston, P.Twiss and A.H.
White, J. Chem. Soc., Dalton Trans., (1984)321.
- 314 L.M.Engelhardt, R.I.Papasergio, C.L.Ralston and A.H.White,
J. Chem. Soc., Dalton Trans., (1984)311.
- 315 H.Dietrich, W.Mahdi, D.Wilhelm, T.Clark and P. von R.
Schleyer, Angew. Chem., Int. Ed. Engl., 23(1984)621.
- 316 D.B.Collum, D.Kahne, S.A.Gut, R.T.DePue, F.Mohamadi,
R.A.Wanat, J.Clardy and G. van Duyne, J. Am. Chem. Soc.,
106(1984)4865.
- 317 J.L.Atwood, T.Fjeldberg, M.F.Lappert, N.T.Luong-Thi,
R.Shakir and A.J.Thorne, J. Chem. Soc., Chem. Commun.,
(1984)1163.
- 318 E.M.McCarron and R.L.Harlow, Acta Crystallogr., Sec. C,
40(1984)1140.
- 319 A.Belforte, F.Calderazzo, A.Morvillo, G.Pelizzi and D.Vitali,
Inorg. Chem., 23(1984)1504.
- 320 S.F.Lincoln, T.W.Hambley, A.M.Hounslow, N.J.Maeji and
M.R.Snow, Austral. J. Chem., 37(1984)1363.
- 321 T.S.Cameron, W.J.Chute and O.Knop, Canad. J. Chem.,
62(1984)540.
- 322 A.Perales, M.Martinez-Ripoll and J.Fayos, Acta
Crystallogr., Sec. C, 40(1984)357.
- 323 N.Narenda, T.P.Seshadri and M.A.Viswamitra, Acta
Crystallogr., Sec. C, 40(1984)1338.
- 324 Y.Sugawara and H.Iwasaki, Acta Crystallogr., Ser. C,
40(1984)389.
- 325 K.M.A.Malik, S.Z.Haider, M.A.Hossain and M.B.Hursthouse,
Acta Crystallogr., Ser. C, 40(1984)1696.
- 326 C.V.Prasad and G.R.Pack, J. Am. Chem. Soc., 106(1984)8079.
- 327 D.Wilhelm, T.Clark, P. von R.Schleyer, J.L.Courtneidge and
A.G.Davies, J. Organomet. Chem., 273(1984)C1.
- 328 W.O.Lin, M.C.B.V. de Souza and H.G.Alt, Z. Naturforsch.,
Teil B, 39(1984)1375.
- 329 G.Bombieri, G.Bruno, M.D.Grillone and G.Polizzotti,
J. Organomet. Chem., 273(1984)69.
- 330 D.D.Bray, D.D.Clarke, N.Chatterjie and B.Sinha, Acta
Crystallogr., Ser. C, 40(1984)348.
- 331 M.Konno, Acta Crystallogr., Sec. C, 40(1984)236.
- 332 C.Esteban-Calderon, M.Martinez-Ripoll and S.Garcia-Blanco,
Acta Crystallogr., Sec. C, 40(1984)80.
- 333 R.Mattes and G.Johann, Acta Crystallogr., Sec. C,
40(1984)740.
- 334 A.R.Campanelli, S.Candeloro de Sanctis, E.Giglio and
S.Petriconi, Acta Crystallogr., Sec. C, 40(1984)631.